HYDROLOGICAL AND HYDRAULIC ANALYSIS OF POST SEISMIC HONGCHUN DEBRIS FLOW, SICHUAN PROVINCE, CHINA

MAMODU ADEGBE

Enschede, The Netherlands, February, 2012

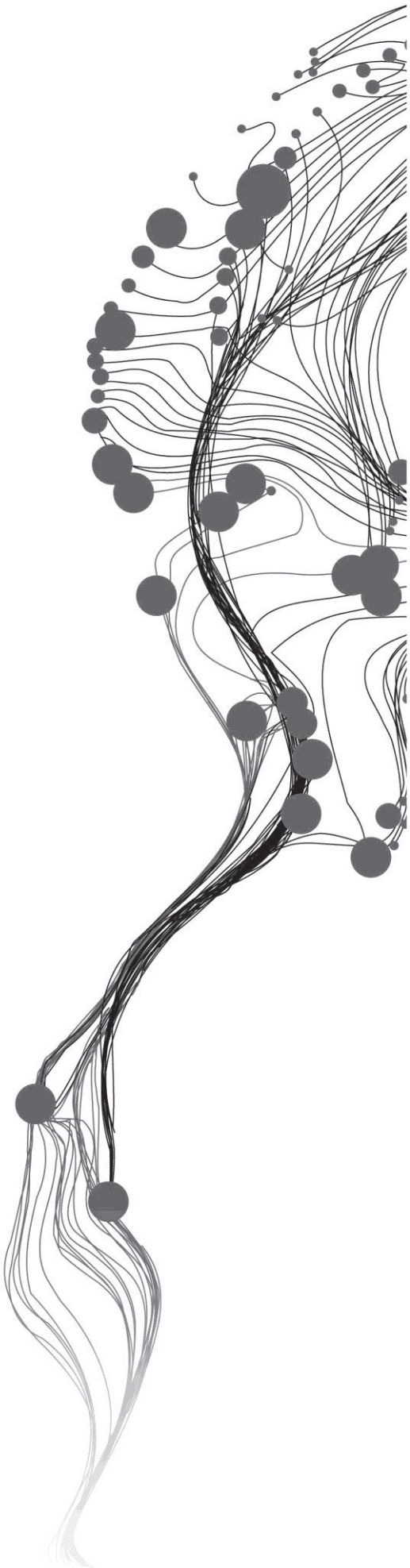

HYDROLOGICAL AND HYDRAULIC ANALYSIS OF POST SEISMIC HONGCHUN DEBRIS FLOW, SICHUAN PROVINCE, CHINA

MAMODU ADEGBE
Enschede, The Netherlands, February, 2012

Thesis submitted to the Faculty of Geo-Information Science and Earth Observation of the University of Twente in partial fulfilment of the requirements for the degree of Master of Science in Geo-information Science and Earth Observation.
Specialization: Geo-Hazards.

SUPERVISORS:
Dr. D. ALKEMA
Prof.V.G. Jetten

THESIS ASSESSMENT BOARD:
Dr .C.Van Westen (Chairman)
Dr. R.Van Beek (External Examiner)
Dr. D.Alkema (First Supervisor)
Prof. V.G. Jetten (Second Supervisor)

Observer:
Harald Van der Werff (Programme Director)

DISCLAIMER

This document describes work undertaken as part of a programme of study at the Faculty of Geo-Information Science and Earth Observation of the University of Twente. All views and opinions expressed therein remain the sole responsibility of the author, and do not necessarily represent those of the Faculty.

ABSTRACT

In many parts of the world debris flows are one of the most dangerous of all mass wasting events. Mountainous areas with high slope instability, high seismic activities and extreme rainfall condition are the main triggering factors (Huang & Li, 2008). The Monday, May 12, 2008, mega-earthquake of magnitude 8.0 that struck the Wenchuan area, Northwestern Sichuan province in China was catastrophic Tang et al (2011)and led to Landslides and subsequent Debris flow in Hongchun catchment which has an area of 5.35 km^2 and a channel length of 3.55 km.

The main objectives of this research is to understand the hydrological and hydraulic analysis of the post seismic Hongchun debris flow, inventorize the landslides as the potential source of debris in the catchment, estimated the volume of debris in the catchment based on field observation and attempt the reconstruction of the August 14th, 2010 debris flow event in the Hongchun catchment.

LISEM was used to model the rainfall-runoff relationship of the catchment and the infiltration patterns. The total Volume, area extent, velocity, depth, specific energy and impact force of the debris flow were obtained using the FLO-2D model.

LISEM simulated one runoff scenario on a whole catchment hydrograph with three peaks corresponding to high discharge but produce very little runoff. The interception (2mm) and infiltration (0n the average was 120mm) were not high.The model reveals almost a uniform infiltration pattern for the catchment. This might be due to the uniform texture and geology of the catchment.

The study found through the intensive field geomorphological mapping of the landslides (inventory), field observation and historical knowledge (through interviews) that the co-seismic landslides are the potential source of debris flows in the Hongchun catchment. 41 landslides were mapped in the catchment and characterized according to their parts (scarp or body), age, and degree of activity and the estimates of their volume were made to 1,675,000 m3.
The 2010, event initiated in two different areas and the FLO-2D modeling were chosen from this two main initiation zone based on susceptibility assessed from Geomorhological field mapping and Tang (2011).

40.3% of the August 14, 2010 debris flow event was reconstructed using FLO-2D model in a manner consistent within the limit of the data available and limit of the researcher expertise with the FLO-2D model. In addition, the model was calibrated (161,350 m3) using a back analysis of the debris flow event of 2010.

Finally, given the available tools, LISEM, FLO-2D, geomorphological mapping, field observation, interviews and data, 40.3% of the debris flow event of 14th August, 2010 was reconstructed. These results are however, preliminary and are guide for future research.

ACKNOWLEDGEMENTS

I am greatly indebted to the following for the progress of this study. The Dutch government, for granted me the coveted NFP fellowship. This gave me a life-time golden opportunity to learn in the ITC faculty of the University of Twente, Enschede. A renowned, world-class institution of international repute. My heartfelt appreciation goes to ITC for the professional and academic development, nurturing and helping me develop a passion for professional ethics, global best practice attitude and consistent hard work.

I was greatly privileged to work under the supervision of Dr. D. Alkema and Prof. V.G. Jetten. Their ideas were critical and crucial to the development that took place through the research phase. My first supervisor Dr. D.Alkema for the unwavering support, wealth of experience and informed guidance who helped me shape and develop ideas. His painstaking effort and thorough reviewing ensured that the research was progressively on track.

My unreserved appreciation goes to Prof.V.G Jetten, for the consistent reviewing and an unequivocal assistance through the research. The staff in the AES who worked with me all time, Dr Cees Van Westen, Drs.N.Kingma, Bart Krol, Rob Hennemann, D.G.Rossiter, J.Ettema , Norman Kerle ,Robert Voskuil, Michiel Damen, Bouldewijn de Smeth for their valuable contributions. The former course director, Drs Tom Loran (Who was like a father to me), the new course director Harald Van der Werff and the course secretary Ceciel Wolters are duely appreciated. I specially appreciate Byron Qaun for giving me tutorial, guides and hands-on experience with FLO-2D software despite his tight schedule.

My special thanks to Prof.Dr Tang Chuan and Prof. Zhu Jing of the Chengdu University of Technology, China for their immense assistance with some data. My special thanks to my field assistants, Cheng lei for his continued support and translations/interpretations in the course of the field work in China. Special thanks to Fan Xuanmei for her consistent assistant during the course of the research and field work. Special thanks to Prof Fu. Xiaomin and Zheng Hai Jun for assisting me at the CDUT laboratory in China. To my new friends in China, Dr Zhao Qin, Scofield Yuan, Ren Yisheng, Luo li, Yue li, Yang Xiao Mei and Joshua Micheal Newson, you will eternally remain my friends.

To all my colleagues in the AES department, geo-hazard programme and in modelling. The team work was great Beatriz Iao Ramos, Rajib Islam, Otgoo and Chengxio Tang. Your support was huge and I express my gratitude to the support rendered. My colleagues in other department who helped me in one way or the other are highly appreciated. Especially, Mosa Mampho Moseme, Nthabi Mohlakoana Kaxulu and Eliasa Keenja.

Special thanks to Dr Fred Achem, Dr Idris Abdullahi, Mr Edward Samuel, Innocent Bello, Nneka Chiedozieudeh, Essien John, Mahmoud. I.Mahmoud, Esther Shupel, Sakirat Adeniyi , Olusola Adefurin, Omeizikam Onouha, Tolulope Adetutu ,Obi Kingsley, Akilapa Femi, Dr Akingbade Adewale, Oluwale Ojukutu, Ajibolade Gregory Tunji, Chief Obasuyi and the rest of the Nigerian community here in the Netherlands and at home (Nigeria) not mention here due to space and time. I appreciate you all for your love, friendship, support and prayers.

I remained eternally grateful and indebted to my parents Mr and Mrs Mamodu Ijekeli, for all their sacrifices, love, care, education and up-bringing in the ways of the lord. Given the chance to choose in another life time, you will still be my parents. To my beloved brothers, Enemadukwu, Enemona, Arome and my adorable sisters (angels) Ajuma and Agwuye (gift). Remember that my life is worth nothing without you all (my family). To my fiancée Ms Ebere Ngozi Ogbonna, who was and is there for me all times, I will always love you with a passion.

DEDICATION

This thesis is dedicated to all the people and the families of those who lost their lives in the August 14th, 2010 debris flow event in the Hongchun catchment, Sichuan province, China.

TABLE OF CONTENTS

Table of Contents

LIST OF FIGURES

LIST OF TABLES

1. INTRODUCTION

1.1. Background.

In many parts of the world debris flows are one of the most dangerous of all mass wasting events. Mountainous areas with high slope instability, high seismic activities and extreme rainfall condition are the main triggering factors (Huang & Li, 2008). Debris flows are also referred to as mudslides, mudflows, debris avalanches, or hyperconcentrated flow(Kowalski, 2008). Debris flow is a common type of landslides that occur generally during intense rainfall on water saturated soil. They can occur suddenly and inundate entire towns in a matter of minutes. Also, the mass can travel long distances over fairly gentle slopes damaging structures and many other elements that lie in their paths(Kowalski, 2008). Different elements at risk such as people, building and infrastructures, whether in urban or rural environments, are either directly or indirectly affected by the occurrence of these events, disturbing their economy, development and sustainability.

The Monday, May 12, 2008, mega-earthquake of magnitude 8.0 that struck the Wenchuan area, Northwestern Sichuan province in China was catastrophic Tang et al (2011). This high intensive earthquake disturbs the slope bedrock and creates an abundance of loose landslide debris on the slopes and gullies and maybe reactivated old landslides. This affects the stability of these slopes for a long period of time. The debris later serves as source material for rainfall induced debris flows as reported by Lin et al,(2006) and Tang et al (2011). The Hongchun catchment was devastated by large debris flow in August 14, 2010 after rainfall events of short duration. The debris flows from Hongchun catchment produced a debris dam (see fig11) which then changed the course of the Minjiang River and resulted in the flooding of the Yinxiu town, including the newly reconstructed settlement. This catastrophic flood event claimed the lives of 56 people. More than 5,500 residents at high risk were forced to evacuate (Tang, et al., 2011) .

The Debris flows were triggered by a combination of three essential factors: sufficient available loose material, surface runoff, and steepness of the drainage channels on the slopes Tang et al, (2011). The Hongchun catchment is located on the left bank of the Minjiang River (see fig7) and has a catchment area of 5.35 km^2 and a channel length of 3.55 km. The upslope elevation of the gully is more than 1,700m asl and the gully mouth is at 880m asl. The highest part of the debris flow source area is at 2,168 m asl. The Yingxiu–Beichuan fault just runs through the Hongchun catchment (Tang, et al., 2011) see fig 9. This makes the study area an active seismic spot and interesting for post seismic debris flow studies. The focal mechanism of the earthquake was successive massive rock fracturing 15 km in depth at the lower part of the catchment was reported by Tang et al, (2011). The epicenter of this strong

earthquake was in the medium to high mountains just west of the Sichuan Basin, where the geological environment is quite fragile, hence numerous geo-hazards were triggered, including slope collapses, debris flows and landslides(Huang & Li, 2008) . Seismic analysis confirms that the major shock occurred on the Beichuan–Yingxiu Fault and that aftershocks rapidly extended in a straight Northeast–Southeast direction. Due to the high seismic intensity of the earthquake, most of the large landslides moved at high speed and for considerable distances (Huang & Li, 2008). Four types of seismically triggered geohazards occurred as a result—rock avalanches and landslides, landslide-dammed lakes (''earthquake lakes'') and debris flows hit most of the area affected by the quake Cui et al (2009). The Debris flow hazard is considered in this work. The core of this research is based on the hydrological and hydraulic analysis of the Hongchun catchment and attempting the reconstruction of the August 14, 2010 debris flow using FLO-2D Software.

It can be anticipated that post-seismic geohazards, particularly for debris flows, will continue for 5–10 years and even for as long as 20 years (Cui, et al., 2009). It should be noted that identification of the areas that might be inundated by future debris flows and estimates of flow volume/area extent are required to quantify debris flow hazard. It is important to note that, many pre-existing alluvial fans are being utilised or considered as settlement areas, the risk due to debris flows has dramatically increase (Tang, et al., 2011). For physical planning, reconstruction, prevention, debris flow mitigation, risk assessment and risk management reasons, there is the need for a detailed hydrological and hydraulic analysis of the post seismic debris flow in the Hongchun catchment. This will help in gaining a better understanding of hydrologic and hydraulics processes and debris flow propagation in the Hongchun catchment, Sichuan Province, China.

1.2. Problem statement

Debris flows are common in mountainous areas and present a severe hazard due to their high mobility and impact energy. In addition to causing significant morphological changes along rivers and mountain slopes, these flows are frequently reported to have brought about extensive property damage and loss of life(Cesca & D'Agostino, 2006). Therefore, accurate prediction of run-out distances and velocities can reduce these losses by providing a means to delineate hazard areas, to estimate hazard intensity for input into risk studies and to provide parameters for the design of protective measures(Cesca & D'Agostino, 2006).

Debris flows are increasingly a concern in China. As a result, different studies have been conducted since the menace of the Wenchuan 8.0 magnitude (Richter scale) Earthquake Disaster on May 12, 2008 which led to other induced secondary geohazards like Debris flow. Most of the researches done were concentrated on the earthquakes, Landslide, damage estimations and building evaluation ((Tang, et al., 2011), (Cui, et al., 2009) with a little or nothing documented on the hydrological and hydraulics analysis of the Debris flow. Hence, this research was targeted at

attempting the reconstruction of the August 14, 2010 debris flows in the Hongchun catchment so as to generate past and may be predict future debris flow scenarios. The estimation of the dynamic characteristics of debris flows is in fact needed by administrators, decision makers, planners and practitioners who have to protect the life, the property and the economic activities of people who live in debris flows prone areas.(Petrascheck & Kienholz, 2003).

Modeling debris flow as a complete phenomenon is complicated. The present research is focused on only the initiation conditions that are causative to the debris flow and attempt to reconstruct the August 14th, 2010 debris flow event. There are different factors that determine the reach of Debris flows and the associated hazards. The initial mass, the friction component during the flow and the amount of material entrained or picked up during the flow (scouring). Debris flows are very viscous, hyperconcentrated sediment flows and are also referred to as mud flows. Mudflows are non-homogeneous, non-Newtonian, transient flood events whose fluid properties change significantly as they flow down steep watershed channels or across alluvial fans(FLO-2D manual, 2007). Mudflow behaviour is a function of the fluid matrix properties, channel geometry, slope and roughness. The fluid matrix consists of water and fine sediments. At sufficiently high concentrations, the fine sediments alter the properties of the fluid including density, viscosity and yield stress(FLO-2D manual, 2007) . In addition, the DEM is a crucial input to the Model and will determine to a large extent, where the flow will occur and in how far it will be confined to natural or artificial channel that are found in the landscape. Therefore, the quality of the DEM is important in the debris flow mechanics (behaviour).

Spatial relations and distribution on how debris flow behave in response to a triggering factor have been analyzed by many researchers such as Tang et al (2011), Chigira et al (2003), Keefer (1984), Khazai & Sitar (2004), in which they have stated out that debris flow are related to geo-environmental precursors but even more to seismic parameters such as fault type, displacement, earthquake depth and magnitude. Thus, it is important to model and study in detail the relationship of the Hongchun catchment hydrology and hydraulic processes and debris flow propagation to topography, geology and rainfall-runoff. An area where earthquakes induced landslides occurred is better but areas with such occasions are relatively rare. That is why the Hongchun catchment offers opportunity to model a recent very large debris flow event (2010) and maybe generate future scenarios. For mitigation of debris flows risk, apart from engineering measures, also non-engineering measures are required such as land-use zoning to regulate and restrict the use of hazardous areas and relocation to safer places of people currently living in areas susceptible to debris flows and related flooding.(Tang, et al., 2011) .

Despite the existing Debris flow hazards, people have decided to settle in the lower part of the Hongchun catchment instead of considering the option of relocation to another area as was done by other affected areas of the province, because it offers several opportunities for improved livelihoods, due to its tourism, mining activities, industry and

fertility of soils(Tang, et al., 2011). Debris flow hazards have affected Hongchun catchment several times and recent event took place in July 2011 with negatives impacts such as injuries, loss of lives, increased disease incident, loss of crops, damage to infrastructure, loss of land and water shortages and also, damages to the newly reconstructed town. This, pose a great threat and challenges to both the local community and Chinese Government. Due to all these negatives developments and impacts, it has been deemed necessary to identify and model the debris flows in an attempt to reconstruct the August 14th, 2010 debris flow events in the Hongchun catchment. In other to determine the spatial run out volume, initiation area, and entrainment zone and characterization of different debris flows Zonation.

1.3. Main Research Objective

The main objective of this research is to gain better understanding of hydrologic and hydraulic processes and debris flow propagation in the Hongchun catchment, Sichuan Province, China.

1.4. Specific Objectives

The specific objectives of this research are outlined below

1. To understand the catchment hydrological processes.
2. To inventorize landslides bodies as potential sources of Debris flow.
3. To estimate the volume of debris materials.
4. Attempt to reconstruct the 2010 debris flow events.

1.5. Research questions

1. What are the hydrological parameters?
2. Are the landslides bodies the potential source of debris flow?
3. Can the volume of debris material be estimated?
4. Can the 2010 debris flow events be reconstructed?

1.6. Hypothesis

1. The reconstruction of the 2010 debris flow events start with a good understanding of the catchment hydrological and hydraulic processes.

2. Prolong long rainfall may increase the soil saturation, making more water available to be absorbed by the loosed post seismic landslide bodies (debris) lowering the cohesion in the process and increased pore pressure. This process is further catalyzed by the steep nature of the slope, hence remobilizing the materials.

3. The FLO-2D models can be suitable for hydrological and hydraulic analysis.

4. Strong earthquakes not only trigger serious, co-seismic landslides but can also lead to increased post-seismic slope instability like debris flow for a long period of time.

5. The Wenchuan earthquake led to an abundance of loose landslide debris being present on the slopes and in the gullies. The debris later served as source material for rainfall-induced debris flows.

1.7. Research conceptual framework

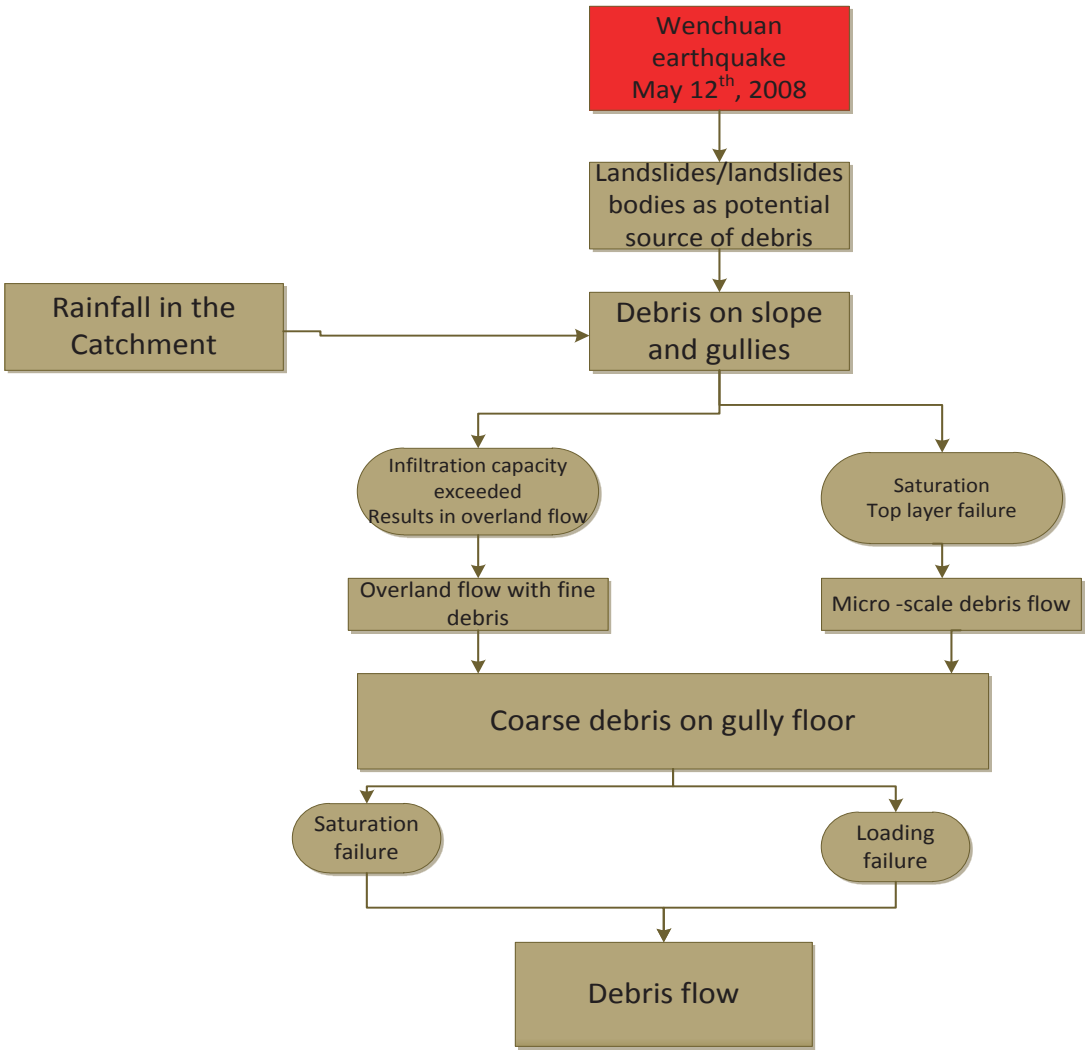

Figure 1: modification of the initiation of debris flow according to Blijenberg (1998) in(Naldini, 2004).

The modified initiation of debris flow in fig1 is used as the conceptual framework to explain the Hongchun debris flow event of August 14th, 2010. This concept relates the hydrological and hydraulic processes with the post seismic activities in the catchment being the epicenter of the Wenchuan earthquake(Tang, et al., 2011). The Wenchuan earthquake in May, 2008 triggered landslides in the Sichuan province. These landslides bodies became potential sources of debris and indirect threat at the upper Hongchun catchment. During the high intensity rainfall, micro debris flow or high velocity overland flow transporting the fine materials occurs in slopes. This muddy flow has higher viscosity and density when compared to water. This viscous mud as it flows downstream, entrained particle of different sizes, shapes, sorting including tree roots thus overloading them. This entire materials then continues to

move downstream as debris flow. Which dammed the Mianjing River and eventually led to the flooding of Ying xiu town as the river was forced to change course/direction of channel flow.

1.8. Thesis structure

This report consists of six chapters in addition to the list of references:

Chapter 1: outlines the framework of the thesis, the problem, objectives and their related questions. The research hypothesis and the conceptual framework are also included in this chapter.

Chapter 2: outlines the literature reviewed in the thesis. It explore the processes and links between Debris flow phenomenon, debris flow component, debris flow casual factors, debris flow initiation, concept of debris flow hazard, Risk and debris flow modelling.

Chapter 3: Introduces the reader to the study area and its suitability in determining the objectives of the study and previous debris flow event in the catchment

Chapter 4: outlines the Research materials, Methodology, introduction to LISEM and FLO-2D software, pre-fieldwork inventory, fieldwork and post fieldwork

Chapter 5: shows the modelling and results, sensitivity analysis and calibration

Chapter 6: present the discussion, conclusion and recommendations from the study.

2. LITERATURE REVIEW

2.1. Debris flow phenomenon

The terminology of debris flows is wide-ranging and has been updated over the years by researchers studying the phenomenon. Debris is defined as a mixture of unsorted materials which can contain everything from clays to cobbles, boulders and organic materials. It is described as having a low plasticity and is produced by mass wasting processes Hungr et al ,(2001). The definition of debris flow by Varnes (1978), which is part of a landslides classification, is commonly used by researchers and states that "flows are rapid movements of materials as a viscous mass where inter-granular movements predominate over shear surface movements. These can be debris flows, mudflows or rock avalanches depending upon the nature of the materials involved in the movements".(Hungr, et al., 2001) however, proposed what they call "more precise terms" for the classification of flow type landslides and defined debris flow as "a very rapid to extremely rapid flow of saturated non-plastic in a steep channel. Plasticity index is less than 5% in sand and finer fractions". Plasticity is the ability of a material to retain its shape attained by pressure deformation. The classification further describes debris flows as being confined to well established channels where the water content increases as the flows descends downstream.

2.2. Debris flow component

A debris flow system theoretically has three components: initiation, transportation and deposition (see fig 2). All the three components are largely controlled by the supply of water to the system. Ellen (1988) identifies 4 sequential phases towards the development of soil slip/debris flow, they are; (1) movement of water to the site of failure, (2) failure of the soil mantle by sliding, (3) mobilization of the soil slip as a debris flow and (4) travel of the debris flow(Ellen, 1988) . The present study limits its scope to understanding the hydrological and hydraulic process of the debris flow.

2.3. Debris flow casual factors

To discern the actual factors that initiate debris flow events is often difficult as observed by Crozier (1986) in (Van Beek, 2002), the intrinsic factors change most of the times only gradually over time and can be considered as preparatory factors whereas the extrinsic factors are transient and can be regarded as triggers, that is, the disturbance that initiates slope instability or failure. The LISEM model was also used to map the infiltration pattern see fig54. This was done in order to see the spatial infiltration pattern across the catchment since it may reveal areas with high water intake and subsequently give an idea of areas that might be unstable (high chance of soil failure). The model reveals almost a uniform infiltration pattern for the catchment. This might be due to the uniform texture and geology of the catchment. However, it was observed that the infiltration tends to be a little more in along the slope and the upper part of the catchment that were mapped geomorphologically as the source areas for the debris. Varnes (1978) provides a list of the major contributing factors that influence landslide activity (see table 1).

Table 8 Basic factors considered as the contributing to landslides

Factor	Element	Examples
Geologic	1.Landform 2.Composition 3.Structure	1. Geomorphic History: stage of development 2. Lithology, stratigraphy, weathering products 3. Spacing and attitude of faults, joints, foliation and bedding surfaces

Environmental	1.Climate and hydrology 2.Catastrophes	1. Rainfall, stream, current and wave action: Groundwater flow; slope exposure; wetting and drying; frost action 2.Earthquakes; volcanic eruptions; hurricane; typhoons and Tsunamis; Flooding and subsidence
Human	Human activities	Construction; Quarrying and mining; Stripping of surface cover; over loading, vibrations
Temporal	Common to all categories	

(Adopted from(Varnes, 1978)

Factors controlling the occurrence and distribution of shallow landslides (debris flow initiations) can be divided into two categories viz: the almost static variables and the dynamic variables.

Table 9 Factors controlling the occurrence and distribution of debris flow initiation

Static Variables	Soil properties(Thickness, Permeability and Material Cohesion, Seepage in the bed rock, Topography (Elevation, Slope, Areas of Convergence and Divergence)
Dynamic Variables	Degree of saturation of soil, cohesion due to the presence of roots and/or partial saturation, Landuse/Landcover

Climatic, hydrological processes and human activities control dynamic variables. They also characterise the temporal pattern of landslides (Crosta & Frattini, 2003). Shallow landslides develop in soils of 1 to 2m depth and the water balance in these soils are characterised by quick response of soil moisture content to the alteration of wet and dry periods during which percolation and evapotranspiration cause a vertical redistribution of soil water Van Asch et al, (1999).

2.4. Debris flow initiation

To understand the interactions happening within complex natural phenomena, it is not only required to know the various elements involved but also to know the relationships. The time lag between the occurrence of a landslide and the removal of its deposit by the generation of debris flow depend on the water supply. However, it sometimes could be so short that one hardly recognize the transition between the phenomena (Takahashi, 1981). To derive a separation between debris flow and deep landslides, deeper landslides (5-20m depth) are in most cases triggered by positive pore pressure on the slip plane induced by rising groundwater level, whereas failure conditions for shallow landslides can occur when, at critical depth which is determined by the cohesion of the soil material and the slope angle, the moisture content in the soil become close to saturation, resulting in considerable reduction of soil strength (Van Asch, et al., 1999). Slow moving landslides like creeps and fast moving persistent erosional processes may advance into debris flow depending on the amount of water supplied to the system Malet et al,(2004).

Several authors assert that it is very crucial to identify the mobilisation mechanism of debris flow. A process largely controlled by the supply of water to the system. Mobilization is the process by which a debris flow develops from an initial static, apparently rigid mass of water- laden soil, sediment or rock. Mobilization requires failure of mass, sufficient water to saturate the mass and sufficient conversion of gravitational potential energy to initial kinetic energy (Inverion, 1997) .Depending on the type of material and other constituents of the slope property, researchers have identified two means of debris flow initiation:

1. During an intense torrential storm, a soil saturation front develops from the top to the bottom. The process of such mobilization can be divided into five steps

a. The tension fractures in the detritic materials and the high pore pressure caused by the conductivity contrast between bedrock and the soil induce the beginning of sliding
b. Internal shear surface in the debris body turn down the shear resistance and induce plastic deformation
c. The shear stress causes dilatancy, while the fluid is drained through the fractures.
d. The mass move downslope, incorporating more materials
e. As the slope gradient decreases, the material accumulates.

2. The second describes the initiation of a debris flow as a sudden failure of coarse debris in a high altitude channel or gully bed Takahashi (1981). The mechanism description of Takahashi (1981) was further modified by Postma (1998) and Blijenberg (1998) in(Naldini, 2004) . The reader is referred to chapter 1.7 of this thesis for detailed explanation and figure1.

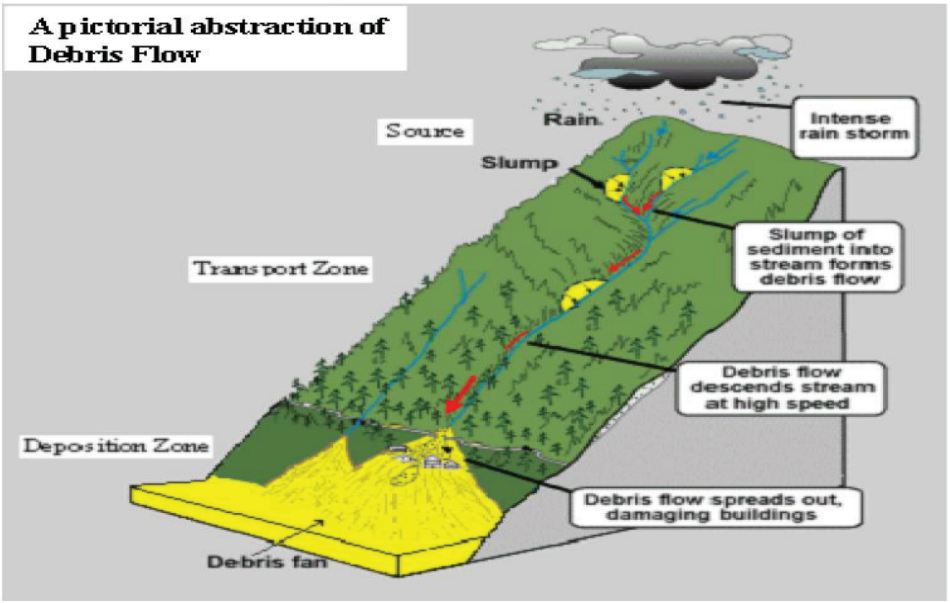

Figure 2 ***Morphology of debris flow*** **(Adopted from (CCI and AD, 2003) and modified)**

2.5. Hydrological effects

According to Van Beek (2002), Landuse has a strong influence on soil moisture availability and thus on the activity of rainfall induced landslides. The effect of vegetation cover on the hydrological processes of shallow landslide (debris flow) can be divided into the loss of precipitation by interception and the removal of soil moisture by evapotranspiration. Three main components of canopy interception can identified (see fig3). These are the interception loss, water retained by the crown surface and later evaporated; throughfall, water falling through and from leaves to the ground and stemflow, water that trickles along twigs and branches and finally down to the ground surface through the main trunk. Interception loss is a primary water loss since it represents water that never enters

the soil. The amount depends on the ability of the forest to collect and retain rainfall, strorm size, intensity and the rate of evaporation. The height and density of the canopy will affect interception capacity (Oyebande, 1998).
Changes in infiltration rate have adverse hydrological effect on vegetation. When rainwater reaches the ground surface underneath vegetation, it stands a high chance of being infiltrated compared to unvegetated soil (Styczen & Morgan, 1995).

The most important effect of vegetation on debris flow initiation is the combined process of the removal of moisture from the soil by evaporation and transpiration from the vegetation cover.
Evaporation is the process whereby liquid water is converted to water vapour and removed from the evaporating surface while transpiration consists of the vaporization of liquid water contained in the plant tissue and the vapour removal to the atmosphere. The process plays a crucial role in reducing the net amount of water retained in the soil column contributing to the pore pressure especially when the water is contributed through distributed rainfall events over a day. The contribution from this process may be of little importance in the case of where high intensity rainfall from few minutes or hours results in increased pore pressure. The soil moisture content is modified since the vegetation cover affects the frequency at which the soil become saturated, hence, controlling the likelihood of run-off generation or mass soil failure (Styczen & Morgan, 1995)

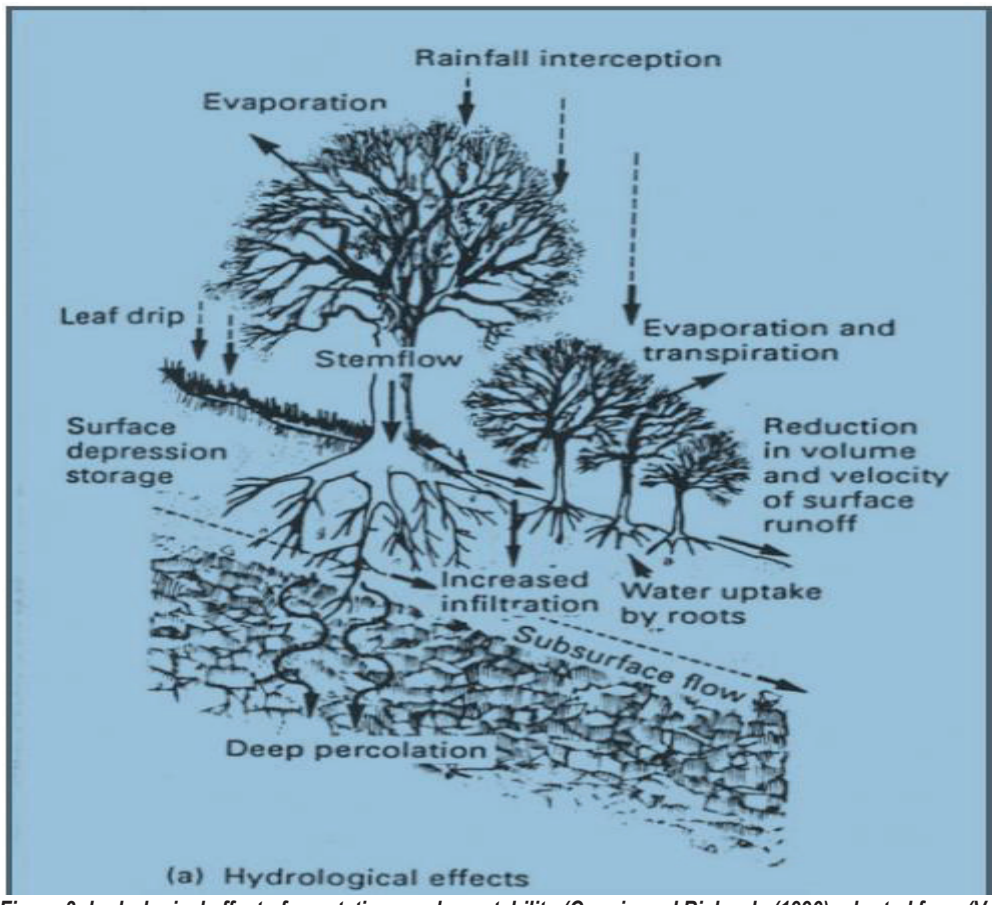

Figure 3: hydrological effect of vegetation on slope stability (Coppin and Richards (1990) adopted from (Van Beek, 2005)

2.6. Concepts of Debris flow hazard and risk

The assessment of the risk to mass movement see fig 5 including debris flows is critical for the prediction of future hazard events in order to protect people, their property and to estimate any future losses or damages. Furthermore, it forms the basis for risk management which comprises of the prevention, preparedness, relief and recovery of people and property from the hazards (Van Westen, 2010). Determining mitigation and prevention methods are needed to reduce the risk of debris flows (see fig 4)

Risk is defined as "the probability of losses" of elements (people or property) vulnerable to hazards and is quantitatively expressed by the following equation (Van Westen, 2010) :

Risk= Hazard * Vulnerability * elements at risk (Eq.1)

When the conditional probability of landslides risk is taken into account, equation 1 can be re-written as follows(Van Westen, 2010) :

RS= (PT * PS * PR) * V *A (Eq.2)

Where RS is the specific annual risk expressed in monetary values of an element at risk vulnerable to a landslide, PT is the temporal probability of the landslide occurrence, PS is the spatial probability of the landslide occurrence, PR is the conditional probability of run-out with a landslides having a specific type and volume, V is the physical vulnerability of the element at risk to the landslide event and A is the monetary value of the element at risk. (PT * PS * PR) can be described as the hazard component of risk or simply the debris flow hazard. Thus, the debris flow hazard has a time component and a magnitude component. The time component is the probability or likelihood of debris flow occurring at s specific time in the future and is expressed as an annual probability or the chance of an event occurring within a specific return periods like 5, 10 , 50 or 100 years.

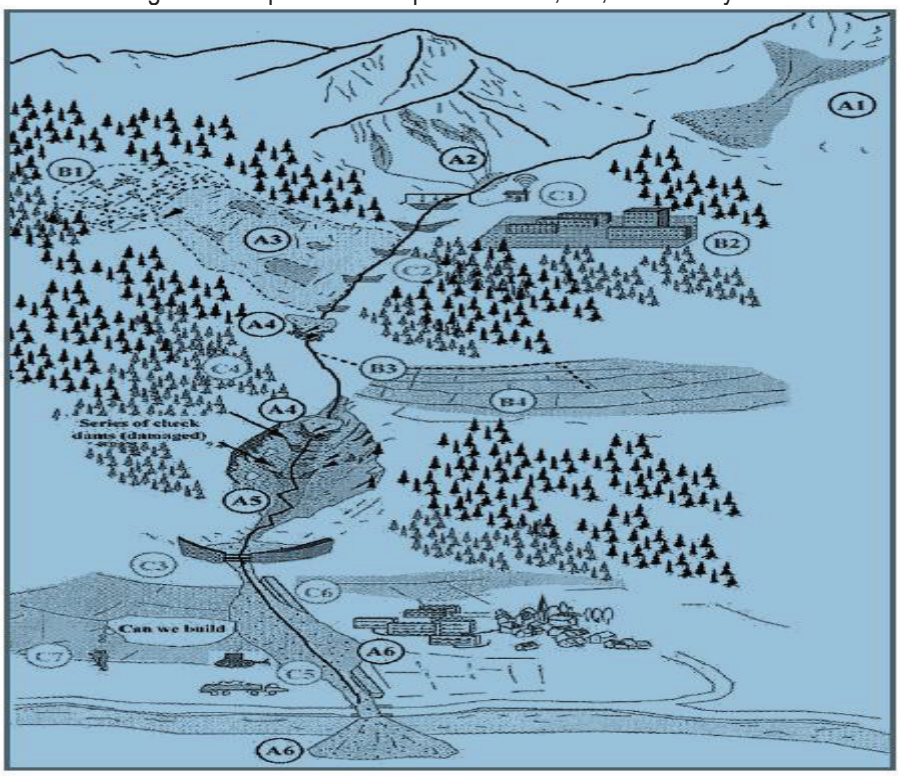

Figure 4: Aspect of debris flow risk.

(A) Processes determining debris flow hazards; (A1) Landslide initiation, (A2) Erosion; (A3) shallow slides, (A4) natural dams, (A5) incision and bank erosion, (A6) overflow onto the debris fan. (B) Impact of human activities to debris flow hazards: (B1) deforestation, (B2) urbanization, (B3) drainage routing, (B4) land cultivation and degradation. (C) Mitigation: (C1) early warnings, (C2) check dams, (C3) storage basins, (C4) reforestation, (C5)

clearing storage systems and channels, (C6) deflection walls, (C7) land use planning (after: (Remaitre & Malet, 2010))

The magnitude component of the debris flow can be expressed in run-out distance, peak discharge or volume (Jacob, 2005). The run-out distance is the distance from the point of initiation until the point of complete deposition and stoppage of flow. The peak discharge is the maximum cross-sectional area multiplied by the debris flow velocity at specific time interval when the flow occurs at the maximum cross-sectional area. The impact pressure is also considered a magnitude component if it is used in relating it to the vulnerability of a house or other elements at risk to the actual force applied by the incoming debris flow(Van Westen, 2010)

Debris flow hazard magnitude can further be determined by the hazard intensity. Debris flow hazard intensity parameters are: velocity, flow depth, maximum deposit thickness, impact force and the debris flow run-out onto elements at risk (Jacob, 2005)

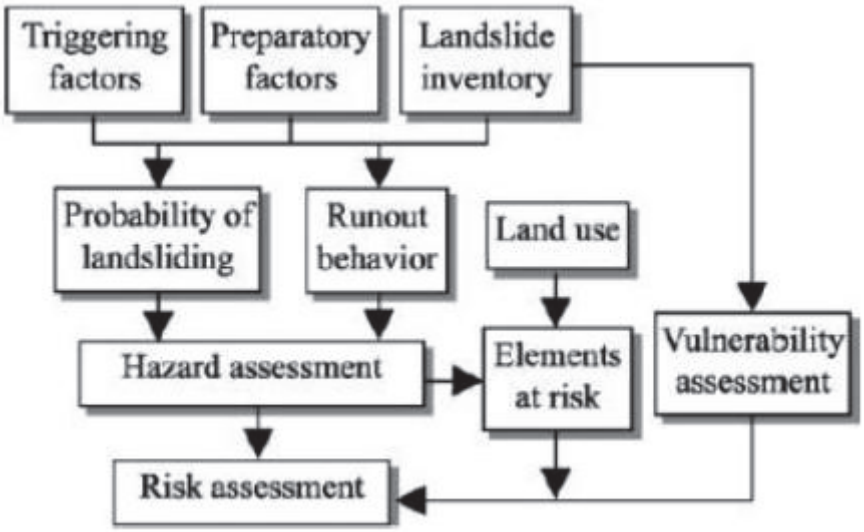

Figure 5 Framework summarizing the steps in a Landslide risk assessment (adapted from: Dial et al,(2002)

2.7. Debris flow modelling

Modeling plays an important role in hydrological and hydraulic analysis of rainfall-runoff, floods and debris flow propagation by enhancing knowledge and understanding (Moradkhami & Sorooshian, 2009) . They have high destructive power combined with incredible speed, thereby making them sudden events and unpredictable (Bashir, 2009). In modeling, several considerations have to be addressed. While there are many models, they differ essentially in structure and treatment of the hydrological and hydraulic processes as well as the assumptions they hold. Abulohom et al,(2001) emphasized that, there is no universal model and as such, the data availability, type of hydrologic quantity to be modeled, scale of operation, accuracy required, availability, computing facilities, political and economic considerations are important in the choice of model for a particular work.

Storms are important for initiating run off and triggering of debris flow. In order to gain a better understanding of the hydrological and hydraulic conditions, and the rainfall-runoff in the Hongchun catchment, a tool capable of modeling these phenomenons will be required. A stepwise approach combining 1D and 2D models proposed by Alkema,(2007) was found appropriate for this study.

Brunsden (1999) describes various modeling approaches that are widely used by geomorphologists in the application of landslides studies. He lists them under various subtitles such as slope stability models, Rheological models and hydrological landslides models. They are not mutually exclusive but are complimentary; one can be used as an input to other most especially in a dynamic environment.

Slope stability models are generally of two types; namely static models and dynamic process model. Static models consider landslides in their stable state and seek to determine the factors that cause the instability in the slope (Broomhead, 1996). Dynamic models are capable to run with time, using rules of cause and effect to simulate temporal changes in the landscape(Karssenberg, 2002). Both static and dynamic are mathematical models.

Dynamic model can be spatial or non-spatial. A spatial model addresses the spatial temporal variation of a phenomenon such as debris flow initiation, while a non-spatial model may be temporal simulation of a cancer growth in an organ. Dynamic models are also classified as deterministic and stochastic models(Karssenberg, 2002). Deterministic models have state variables which have a single value for each location in space and time and in moment in time. Stochastic models are those that deal with chances; if non-spatial, the state variables in the model will be random variables having a certain probability distribution and if spatial, will be random fields. A dynamic model becomes stochastic model when its inputs are stochastic.

Researchers overtime have approach debris flow initiation modeling in several ways.(Aleotti, 2004) uses threshold based warning system for debris flow prediction. The method results in identifying rainfall events, which are potentially capable of initiating debris flow. Glade et al, (2000) uses antecedent rainfall daily rainfall model to calculate the regional landslides triggering rainfall thresholds in this model. First, introduced by, triggering rainfall conditions are represented by a combination of rainfall occurring in period before the event (antecedent rainfall) and rainfall on the day after the events.

Debris flow have also been modelled using the RAMMS (Rapid mass movements) dynamic numerical software package which was originally designed to model snow avalanche Christen et al,(2010c). But has been applied in the past to model other types of mass movements like lahars(Quan Luna, 2007) and debris flows(Cesca & D'Agostino, 2006) ;(Kowalski, 2008). The dynamic RAMMS model is based on the Voellmy-Salm model which assumes that the total basal friction of the flow can be categorized into two, namely: a velocity independent dry-coulomb friction coefficient μ and a velocity dependent turbulent coefficient ξ ().

The Rheological parameters can determine to a large extend the run-out distance. Hence the so-called Voellmy friction parameters are very pertinent in run-out distance modeling and the associated hazard.
Pack et al, (1998) uses a coupled model approach towards addressing slope instability. They use a model by name SINMAP, a short form for stability index mapping and top model. They state a promising approach to modeling the spatial distribution of shallow debris slides combines a mechanistic infinite slope stability model with a steady state hydrology model. A steady state hydrology model attempts to assess scenarios assuming a constant water level and thus a constant pore pressure condition, while a dynamic hydrology model simulates the changes in slope to changing water levels (and thus pore pressure conditions), based on the rainfall received. Pack et al(1998) observe that the SINMAP approach applies to shallow landslides controlled by the convergence of shallow ground water flows, but do not apply to deep-seated instability including deep earth flows and rotational slump.

FLO-2D model was built by FLO-2D software Inc in the United States.FLO-2D is based on a finite difference solution of the 2-D Saint Venant equations for non-Newtonian fluids. FLO-2D is commercially available software capable of simulating debris flow and mudflows whose behavior differs from water because they are very viscous, hyperconcentrated sediment flow. Mudflows are non-homogeneous, non-Newtonian, transient flood events whose fluid properties change significantly as they flow down steep watershed channels or across alluvial fans. Mudflow behavior is a function of the fluid matrix properties, channel geometry, slope and roughness. The fluid matrix consists of water and fine sediments. At sufficiently high concentrations, the fine sediments alter the properties of the fluid including density, viscosity and yield stress. Hyperconcentrated sediments flow is simulated by FLO-2D model using quadratic rheological models that include viscous stress, yield stress, turbulence and dispersive stress terms as a function of sediments concentration (FLO-2D manual, 2007) this software will also be used in this research(see details in chapter 4.).

Hyperconcentrated sediment flow involves the complex interaction of fluid and sediments processes including turbulence, viscous shear, fluid-sediment particle momentum exchange, and sediment particle collision (FLO-2D manual, 2007). Sediment particles can collide, grind and rotate in their movement past each other. Fine sediment cohesion controls the Newtonian behavior of the fluid matrix. This cohesion contributes to the yield stress which must be exceeded by an applied stress in order to initiate fluid motion. By combining the yield stress and viscous components, the well known Bingham rheological model is prescribed. (FLO-2D manual, 2007).

There are several important sediment concentration relationships that help to define the nature of hyperconcentrated sediment flow. These relationships relate the sediment concentration by volume, sediment concentration by weight, the sediment density, the mudflow mixture density and the bulking factor. (FLO-2D manual, 2007) When examining parameters related to debris flow, it is therefore important to identify the sediment concentration either as a measure of weight or volume. For the purpose of this research, the sediment concentration by volume was used. The sediment concentration by volume C_V is given by:

C_V= volume of the sediment/volume of water plus sediment

C_v is related to the sediment concentration by weight C_w by:

$$C_v = C_w\gamma / \{\gamma_s - C_w(\gamma_s - \gamma)\}$$

Where y=specific weight of the water and ys=specific weight of the sediment.

The full range of sediment flows span from water flooding to mud floods, mudflows and landslides. The distinction between these events depends on the sediment concentration measured either by weight or volume (see figure 6).

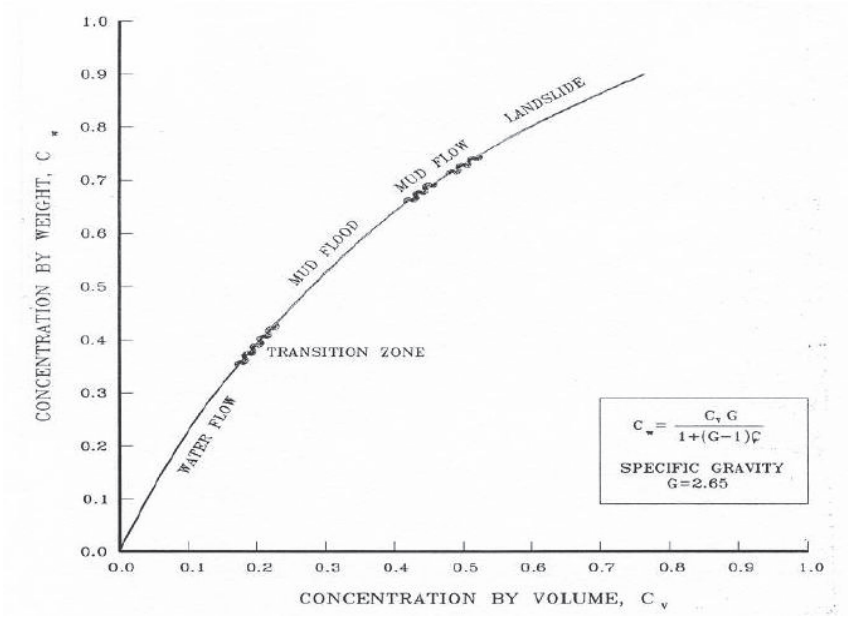

Figure 6 Classification of hyperconcentrated sediments flow (adopted from: FLO-2D manual, 2007)

Sediment concentration by volume expressed as a percentage is the most commonly used measure (FLO-2D manual, 2007). Therefore, the sediment concentration by volume was also used in the sensitivity analysis of this research. Table 3 lists the four different categories of hyperconcentrated sediment flows and their dominant flow characteristics

Table 10: Debris flow behaviour as a function of sediment concentration

	Sediment Concentration		Flow Characteristics
	by Volume	by Weight	
Landslide	0.65 - 0.80	0.83 - 0.91	Will not flow; failure by block sliding
	0.55 - 0.65	0.76 - 0.83	Block sliding failure with internal deformation during the slide; slow creep prior to failure
Mudflow	0.48 - 0.55	0.72 - 0.76	Flow evident; slow creep sustained mudflow; plastic deformation under its own weight; cohesive; will not spread on level surface
	0.45 - 0.48	0.69 - 0.72	Flow spreading on level surface; cohesive flow; some mixing
Mud Flood	0.40 - 0.45	0.65 - 0.69	Flow mixes easily; shows fluid properties in deformation; spreads on horizontal surface but maintains an inclined fluid surface; large particle (boulder) setting; waves appear but dissipate rapidly
	0.35 - 0.40	0.59 - 0.65	Marked settling of gravels and cobbles; spreading nearly complete on horizontal surface; liquid surface with two fluid phases appears; waves travel on surface
	0.30 - 0.35	0.54 - 0.59	Separation of water on surface; waves travel easily; most sand and gravel has settled out and moves as bedload
	0.20 - 0.30	0.41 - 0.54	Distinct wave action; fluid surface; all particles resting on bed in quiescent fluid condition
Water Flood	< 0.20	< 0.41	Water flood with conventional suspended load and bedload

3. STUDY AREA

3.1. Location

The Hongchun catchment is located in the Sichuan province, (see fig 7) Southwest China. The catchment has an area of 5.35 km^2 with a length of 3.55 km. It lies on latitude 31 03'32"N and longitude 103 29'41"E and also, the epicentre and one of the single worst hit areas of the 2008 Sichuan Earthquake. 80% of the town was destroyed by the earthquake. (Tang, et al., 2011).

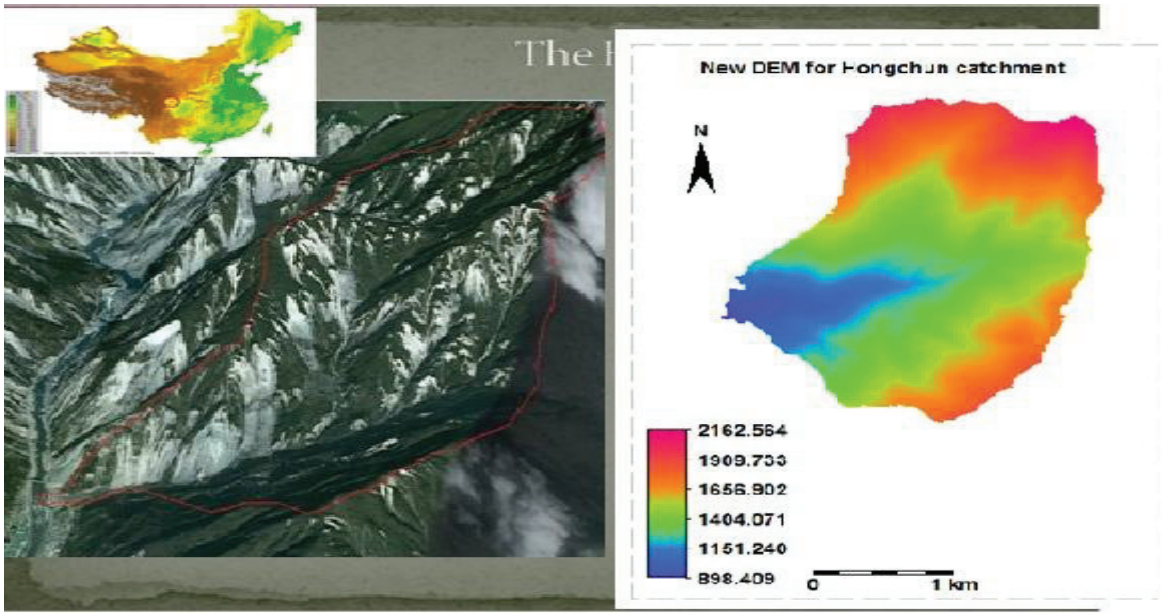

Figure 7: shows the study area and catchment (the DEM unit is metres)

3.2. Geology of the study area

The study area is underlain by Granitic rocks (see fig 8) and was mapped during the fieldwork. All bedrock is deeply fractured (see fig 8) and highly weathered, and covered with a layer of weathered material (Tang, et al., 2011). Joints are well developed in the more competent lithologies. When combined with active faulting and bedding, produces many potential failure surfaces in the rock slopes. The geological main structure and the strike of the rock strata in the study area show a NE–SW orientation (Tang, et al., 2011). Tang et al (20011) reported that, the Yingxiu-Beichuan faults (see fig9), which ruptured during the Wenchuan earthquake, runs through the Hongchun catchment in the study area. The overflow eroded the gully on large landslide deposits in the Hongchun gully. In the source area (see fig 36) mainly granitic rocks are exposed, which are deeply fractured and highly weathered, and massive coseismic landslides were developed on the slope (Tang et al, 2011).

Figure 8: shows exposed massive granitic rocks in the Hongchun catchment with deep fractures

(Source: fieldwork)

3.3 Climate and Rainfall

The study area is situated in the typical humid subtropical, monsoon climate zone with an annual average temperature of 12.9°C. The annual average precipitation over a period of 30 years is 1,253 mm,
With a highest recorded annual precipitation of 1,688 mm in 1964.The maximum recorded rainfall intensity was 269.8mm/day in 1964. (Tang, et al., 2011) .The rainfall is largely concentrated in the period from June to September. On average, 70% of the annual precipitation falls during this period. A total of accumulated rainfall of 162.1mm in 33 hour was recorded from 17:00 P.M. on 12 August, until 02:00 A.M. on 14 August (see fig39). The rainfall intensity that induced the debris flows occurred between 02:00 and 03:00 A.M.; 16.4 mm/h was recorded during that time period (Tang, et al., 2011). The intensity of rainfall necessary to initiate debris flows in the Hongchun catchment is poorly known and also was not the main interest of this research. Previous studies in the Longmenshan area Tan and Hen(1992) have reported rainfall that initiates debris flows to have intensities greater than 30–50 mm/h with a total rainfall of at least 80–100 mm. Lan et al, (2003) examined rainfall amount 110 mm/day as the rainfall thresholds for the occurrence of past landslide events in the Xiaojiang watershed, southwestern China. Comparing the characteristics of the triggering rainfall with these thresholds reported for China in the literature, the August 14 event indicated that post-earthquake debris flows in the Hongchun catchment can be triggered by longer duration, lower intensity rainfall was reported by Tang et al,(2011).

3.3. Drainage

The main river in the study area, the Minjiang River, originates in the northwestern mountainous area. Its annual mean discharge is 452m3/s and peak stream discharges averaged 2,790m3/s in 1958. (Tang et al, 2011). The river in the Hongchun catchment has two main tributaries at the upper part of the catchment. (See fig 9 a and b).
The aerial photograph taken in August 14, 2010 shows the drainage system in the Hongchun catchment as seen in fig 9a.

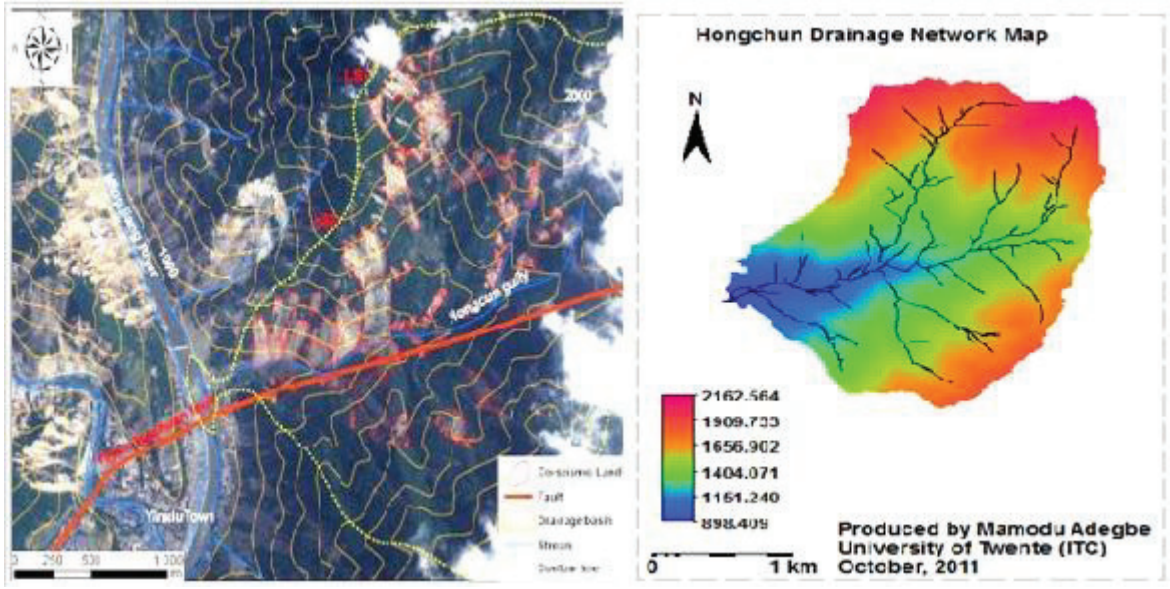

Figure 9: a and b shows drainage/network for the catchment.

3.4. Topography

The Hongchun catchment has a very steep slope and rugged terrain. (See fig 10)The highest point on the catchment is over 2000m asl high while the lowest point at the valley floor is above 800m asl. Topography has a uniform vegetation cover except for area where the landslides have distorted the vegetation. This can be seen on the aerial photograph because they are fresh surfaces with sharp contrast with respect to the background.

Figure 10 ***show rugged topography and uniform vegetation in the catchment (source: fieldwork)***

3.5. Previous debris flow in the catchment

The Hongchun catchment was devastated by large debris flow in August 14, 2010 after rainfall events of short duration see fig 11. The Monday, May 12, 2008, mega-earthquake of magnitude 8.0 that struck the Wenchuan area, Northwestern Sichuan province in China was catastrophic Tang et al (2011). This high intensive earthquake disturbs

the slope bedrock and creates an abundance of loose landslide debris on the slopes and gullies and maybe reactivated old landslides. This affects the stability of these slopes for a long period of time. The debris later serves as source material for rainfall induced debris flows (Lin et al,(2006); (Tang, et al., 2011)). The debris flows from Hongchun catchment produced a debris dam see fig 11, which then changed the course of the Minjiang River and resulted in the flooding of the Ying xiu town, including the newly reconstructed settlement. This catastrophic flood event claimed the lives of 56 people. More than 5,500 residents at high risk were forced to evacuate(Tang, et al., 2011) . The most recent debris flow events in Hongchun catchment were in July 3rd and August 21st, 2011 which indicates that the risk of debris flow in the catchment may still be high. Considering the threats to the newly reconstructed town and the fact that the lower catchment is still being used for re-settlement.

Figure 11 *aerial photo showing the August 14 debris flow activities (Tang et al, 2011)*

4. MATERIALS AND METHODOLOGY

4.1. Overview and flowchart of methodology

Storms are important in initiating flash flood and also triggering debris flow as literature review (chapter 2) demonstrated. A tool capable to model this problem at a catchment scale was therefore necessary hence the applicability of the LISEM model coupled with FLO-2D. Despite the complex nature of the terrain, LISEM was used to model the rainfall-runoff relationship of the catchment and the infiltration patterns. The FLO-2D was important to understand the debris flow propagation and extent. A stepwise approach combining 1D and 2D models proposed by Alkema (2004) was found appropriate for this study. Modelling was an appropriate tool to answer the research questions 1 and 4 posed in chapter 1 pertaining the hydrological and the hydraulic processes and the debris flow reconstruction in the catchment. However, modelling data –needs for the research was met through the process outline in the flowchart below (see fig12). Specific data –needs were met through primary and secondary data collection.

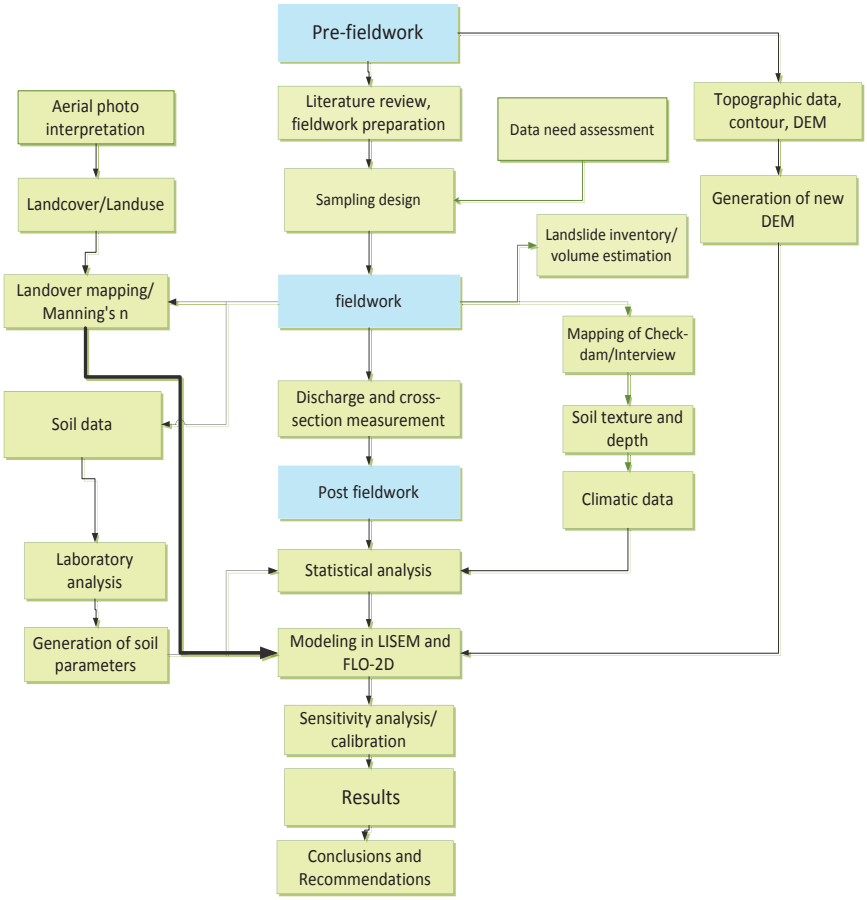

Figure 12 shows flowchart of the research methodology

4.2. LISEM input data

The model structure of LISEM outlining important model parameter is shown on figure 13

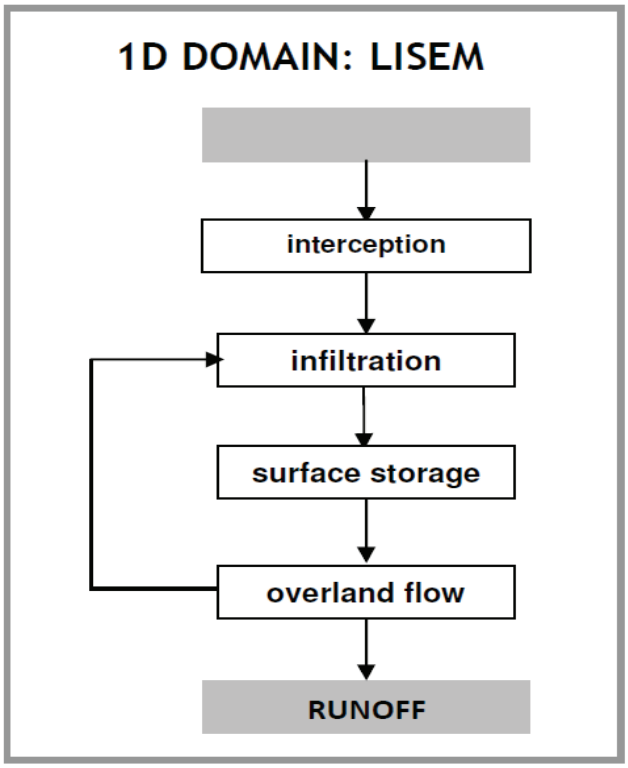

Figure 13 LISEM rainfall-runoff model (Source: Jetten 2002)

Figure 13 shows the rainfall-runoff module for LISEM with the erosion option switch off. LISEM is a data intensive model, requiring at least 24 maps for runoff simulation. However, using PCRaster script that derived parameter maps from five basic maps (DEM, landcover, soil, channel and road) in conjunction with a table of soil physical properties (measured during filed work and laboratory analysis) see table 11. The database for LISEM was created. The data requirement for LISEM are listed on table 4 and some maps are on Appendix 3

Table 11: input parameters for LISEM rainfall-runoff modelling

PARAMETER	NAME	METHOD	RANGE/Units
Catchment data			
Local drain direction	LDD.map	DEM derivative	1-9 (-)
Catchment boundary	Area.map	DEM derivative	1 (-)
Slope direction	GRAD.map	DEM derivative	>0&<=1 (-)
Rain-guage area	ID.map	Field observation	1-n (-)
Outlets	OUTLET.map	DEM derivative	1 (-)
Outpoints	OUTPOINTS.map	DEM derivative	1 (-)
Rainfall data	ASCII table	From Prof Tang	1-n (mm)
Vegetation			
Leaf area index	LAI.map	From PER.map	0-12 (m2/m2)
Vegetation cover	PER.map	Field observation	0-1 (-)
Vegetation height	CH.map	Field observation	0-30 (m)
Soil surface			
Manning's n	N.map	From Literature	0.001-10 (-)

Random roughness	RR.map	From literature	0.05-20 (cm)
Width of road	ROADWIDT.map	From field observation	0-cellwidth (m)
Hardsurface	HARDSURF.map	From field observation	0 or 1 (-)
Infiltration (Green & Ampt: 1layer)			
Saturated hydraulic conductivity	KSAT1.map	Laboratory analysis	0-1000 (mm/h)
Saturated volumetric soil moisture content	THETAS1.map	Laboratory analysis	0-1 (cm3/cm3)
Initial volumetric soil moisture contnent	THETAI1.map	Laboratory analysis	0-1 (cm3/cm3)
Soil water tension at wetting front	PSI1.map	From literature	0-1000 (cm)
Soil depth	SOILDEP1.map	Field observation	0-1000 (mm)
Channels			
Local drain direction of channel network	LDDCHAN.map	From LDD.map	1-9 (-)
Channel gradient	CHANGRAD.map	From GRAD.map	0.0001-10 6 (-)
Mannings's n for channel	CHANMAN.map	From literature	0.001-0.6
Width of channel	CHANWIDT.map	Field observation	0-cellwidth (m)
Channel cross section shape	CHANSIDE.map	Field observation	0-10 (-)

LISEM has four important sub-models that are simultaneously simulated using rainfall input to give runoff output. Rainfall data (input) is the storm event as a time series. Interception loss is modeled using vegetation parameters, infiltration (soil storage) loss by Green and Ampt model while surface storage is based on random roughness parameter. Overland flow is routed using the solution of the kinematic wave (Jetten, 2002) and Manning's equation. The channel parameters are useful as the runoff is directed to the outlet.

4.3. FLO-2D and input data

4.3.1. Introduction to FLO-2D

The FLO-2D model is a commercial code in widespread practical use, is a finite difference debris and mud flow simulation program based on a quadratic rheological law O'Brien et al, (1993). It is an integrated river and floodplain model. A complete flood routing hydrologic and hydraulic model with many urban detail features, sediment transport, mudflow and groundwater modelling. The first version of the FLO-2D model was called MUDFLOW. It was initiated in 1988 to conduct a Federal Emergency Management Agency (FEMA) flood insurance study (FIS) of an urbanized alluvial fan in Colorado (FLO-2D manual, 2007).

FLO-2D is a physical process model that routes rainfall-runoff and flood hydrographs over unconfined flow surfaces or in channels using the dynamic wave approximation to the momentum equation. It has a number of components to simulate street flow, buildings and obstructions, sediment transport, spatially variable rainfall and infiltration, floodways and many other flooding details. Predicted flow depth and velocity between the grid elements represent

average hydraulic flow conditions computed for a small time-step . Typical applications have grid elements that range from 25 ft to 500 ft on a side and while number of grid elements is unlimited, the user is cautioned to avoid extremely large models. FLO-2D has been used on countless projects in over 30 countries. (FLO-2D manual, 2007).

4.3.2. Modeling the hydrologic system with FLO-2D

To model the hydrologic system, FLO-2D consists of a series of components and processor programs that break up a flood simulation into a number of discretized small units. The Grid Developer System (GDS) generates a grid system that represents the topography as a series of small tiles. The FLO-2D model has components for rainfall, channel flow, overland flow, street flow, infiltration, levees and other physical features. All the physical processes simulated by FLO-2D are shown in fig 14

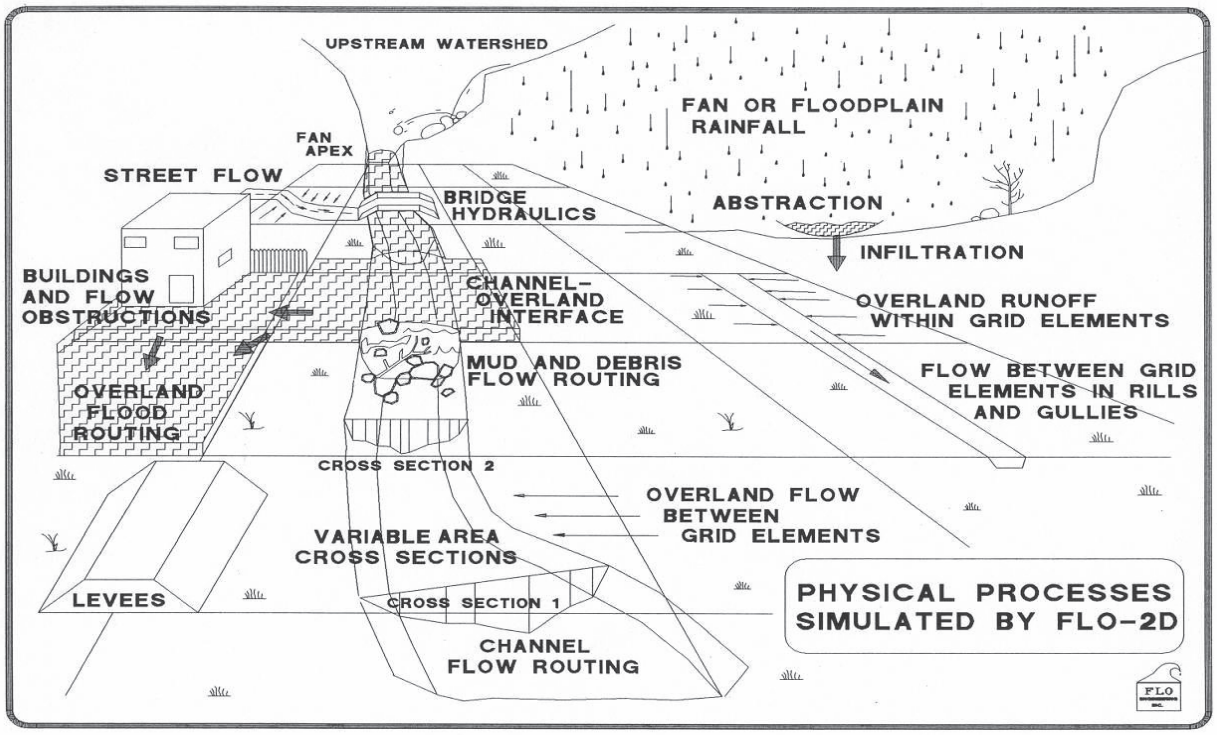

Figure 14 Physical processes simulated by FLO-2D

(Source: FLO-2D manual, 2007)

4.3.3. FLO-2D model theory

FLO-2D is a simple volume conservation model. The model describes the routing behavior of a bulked inflow hydrograph as a homogeneous, one-phase material over a rigid bed (Cesca & D'Agostino, 2006); it moves the flood volume around on a series of tiles for overland flow or through stream segments for channel routing. Floodwave progression over the flow domain is controlled by topography and resistance to flow (FLO-2D manual, 2007). Flood routing in two dimensions is accomplished through a numerical integration of the equations of motion and the conservation of fluid volume for either a water flood or a hyperconcentrated sediment flow. FLO-2D is a flood-routing model, which uses a dynamic-wave momentum equation and a finite-difference routing scheme (FLO-2D manual, 2007). Its formulation is based on the depth-averaged open channel flow equations of continuity and momentum for unsteady conditions developed on an Eulerian framework. The adopted numerical analysis technique is a non-linear explicit difference method.(Cesca & D'Agostino, 2006).

4.3.4. Governing equation

The general constitutive fluid equations include the continuity equation, and the equation of motion (dynamic wave momentum equation): FLO-2D assumes the following constitutive equation (quadratic model):

$$\tau = \tau_c + \mu_N(du/dy) + C(du/dy)^2 \qquad (1)$$

Where τ is the total shear stress (Pa), τc the yield stress (Pa), μN the dynamic viscosity (Pa s), du/dy the shear rate (s-1) and C the inertial stress coefficient. Unless a rheological analysis of the mudflow site materials is available, the following empirical relationships can be used to compute viscosity and yield stress

$$\tau_y = \alpha_2 \quad e^{\beta_2 C_v} \quad \text{and} \quad \eta = \alpha_1 \quad e^{\beta_1 C_v}$$

Where αi and βi are empirical coefficient defined by laboratory experiment (O'Brien and Julien, 1998).
The viscosity (poises) and yield stress (dynes/cm^2) are shown to be function of the volumetric sediment concentration c_v of silts, clay and in some cases, fine sands and do not include larger clastic material rafted along with the flow.
See table 5

.

Table 12 yield stress and viscosity as a function of sediment concentration (adopted from the FLO-2D manual, 2007).

Source	$\tau_y = \alpha e^{\beta Cv}$ (dynes/cm^2)		$\eta = \alpha e^{\beta Cv}$ (poises)	
	α	β	α	β
Field Data				
Aspen Pit 1	0.181	25.7	0.0360	22.1
Aspen Pit 2	2.72	10.4	0.0538	14.5
Aspen Natural Soil	0.152	18.7	0.00136	28.4
Aspen Mine Fill	0.0473	21.1	0.128	12.0
Aspen Watershed	0.0383	19.6	0.000495	27.1
Aspen Mine Source Area	0.291	14.3	0.000201	33.1
Glenwood 1	0.0345	20.1	0.00283	23.0
Glenwood 2	0.0765	16.9	0.0648	6.20
Glenwood 3	0.000707	29.8	0.00632	19.9
Glenwood 4	0.00172	29.5	0.000602	33.1
Relationships Available from the Literature				
Iida (1938)*	-	-	0.0000373	36.6
Dai et al. (1980)	2.60	17.48	0.00750	14.39
Kang and Zhang (1980)	1.75	7.82	0.0405	8.29
Qian et al. (1980)	0.00136	21.2	-	-
	0.050	15.48	-	-
Chien and Ma (1958)	0.0588	19.1-32.7	-	-
Fei (1981)	0.166	25.6	-	-
	0.00470	22.2	-	-

*See O'Brien (1986) for the references.

Conversion: Shear Stress: 1 Pascal (PA) = 10 dynes/cm^2
Viscosity: 1 PAs = 10 dynes-sec/cm^2 = 10 poises

The momentum equation is solved by computing the average flow velocity across a grid element boundary one direction at a time. There are eight potential flow directions, the four compass directions (North, East, South and West) and the four diagonal directions (northeast, southeast, southwest and northwest). Each velocity computation is essentially one-dimensional in nature and is solved independently of the other seven directions.

4.3.5. FLO-2D data requirement

The general data requirements are below, (see table 6) the FLO-2D data input consists of a series of ASCII files organized by model components. These FLO-2D components are initiated through on-off Switches found in the control data file (CONT.DAT)

Table 13 Input data for FLO-2D hydrologic and hydraulic modelling

PARAMETER	NAME	METHOD	FORMAT
2D SPATIAL DATA			
Elevation	DEM	Contour interpolation	asc
Roughness	Friction map	Land use + literature	asc
1D spatial data			
River	Cross section	Field measurement	(numeric)

Temporal data			
Rainfall/discharge	Rainfall/discharge table	From station/ field measurement	txt
Land use/landcover	Land use map	Field observation	asc

4.3.6. FLO-2D Model outputs

The main FLO-2D model outputs viewed in the Mapper are:

- The total or maximum area of inundation of the debris flow (or flood as the case may be).
- The maximum flow depth
- The maximum velocity
- The specific energy
- The impact force
- Hazard maps
- Total volume

The reader should note that FLO-2D does not do entrainment and initiated volume like the RAMMS model.

4.3.7 Model Building

The first step to create hydrological and hydraulic simulation in FLO-2D is building the model. In this step, the user defined the project area, defined the grid size and adds the modeling component like channel, hydraulics structure, hydrograph etc. The elevation data such as the DEM is imported to FLO-2D either as ASCII file format or in a shape file format. Once the elevation data is imported, the grid element size can be determined. The grid size is an important factor in FLO-2D modeling because it indicates how detailed the DEM represents the surface relief. The grid element size also plays an important role for the computation time of the simulations. It will control how fast the Flo-2D debris flow simulation will run. A high flood discharge combined with small grid element can result in long simulations times.

4.4 pre-fieldwork inventories

From the detailed data requirements outlined in this chapter, the inventory of data needs was created on basis of available and needed data as shown in table 7

Table 14 Inventory of data

Available	Resolution	Type	source	unavailable
Elevation	10m	DEM	Prof Tang	River cross sections Discharge Landuse/landcover present) Soil depth Soil physical properties Surface Roughness Rainfall data
	20m	contour	Prof Tang	
	1m	Contour(catchment floor/valley)	Prof Tang	
Aerial photo(18/5/08)	0.5m	image		
Google (02/08/2006)	0.5m	Image (3 bands)		

In order to meet the data requirement for the FLO-2D model outlined in this chapter, a field campaign to collect unavailable data was undertaken from the 21st of September through the 22nd of October, 2011 in the study area. The data collection process is outlined in the following section.

4.5 Fieldwork

The data collection included land use/landcover observations, mapping of the Landslides in the catchment, mapping the check-dams, interviews, soil sampling, measurement of discharge, channel cross-sectional area/ geometry. Observation of soil depth at road cut. The spatial data was captured using a Garmin E-Trex 12 channel. The process is outlined below

4.5.1 Reconnaissance survey

A 1 day field reconnaissance survey of the catchment was carried out so as to get an overview of the landscape, features/landforms, geology and to determine the areas where sampling will be done. The area where discharge will be measured was also determined at this stage. This facilitated the planning/execution of other field observation and activities.

4.5.2 Mapping Landuse /Landcover

Land use type and land cover characteristics were observed and recorded at every point in the catchment. It was observed that the only land use at present time in the catchment is an office where the HUADI construction site is situated close to the outlet of the catchment. The absent of farming activities and other landuse type in the catchment may be due to the May, 2008 earthquake event of magnitude 8.0 and the post earthquake landslides that eventually led to debris flow and flooding of the town. This makes the catchment a high risk zone and was immediately abandoned by farmers for safety reasons. This was also confirmed during an interview held on the 30th of September, 2011 with Mr Wang (the chief supervisor of the Huadi construction company). During the mapping of the catchment, not even traces of old farming activities were found present in the catchment. After a very detailed mapping of the catchment, nine Landover classes were obtained and the Landcover map was generated accordingly in line with field observation (see fig15) The areas covered with with 100 % of grass is classified as grass, shrub and tree consist of about 60% shrub and 40% tree, in each of the classifications, the dominant within the class comes first followed by the next in that class. Tree with shrub consist of 60% percent tree and 40% shrub, others include, bare with grass (60% bare and 40% grass), shrub and

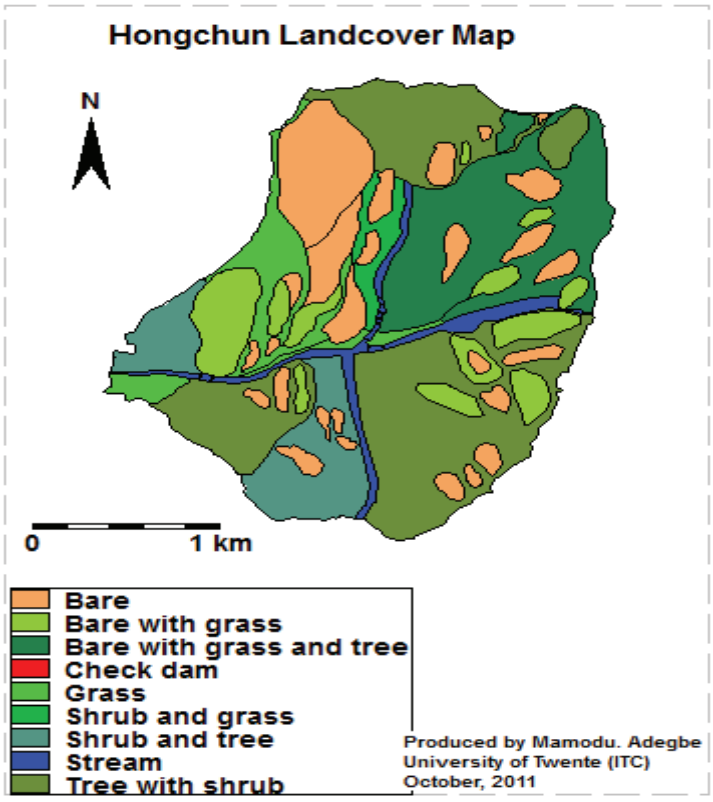

Figure 15 Hongchun catchment landcover classes

grass (60% shrub and 40% grass), bare with grass and tree (60% bare, 20% grass and 20% tree , streams and the check-dams. It was also observed in the field that all the area classified as bare are mainly due to landslides activities in the catchment. However, some grass have grown on the landslide bodies and resulted in the class; bare with grass. It was observed that the trees were not fruit trees or economic trees like bamboo etc but the density of the trees were not thick enough to be classified as forest.

The main water bodies in the catchment are the two streams. They flow from the upper part of the catchment into the valley floor respectively. There is a confluence of the two main streams in the catchment. However, they are signs of dried streams in the catchment. (This may be seasonal streams). Vegetation height, percentage covered were observed and recorded.

4.5.3 Mapping landslides (inventory) in the catchment

In order to answer the research question if the landslides bodies are the potential source of debris responsible for the debris flow in the catchment? an intensive mapping of landslides inventory was carried out in the catchment based on visual image interpretation/inspection. A total of 41 landslides were mapped in the catchment see fig 18, the scarp or body (see fig 20 and appendix 4) of the landslides were also mapped, the degree of activity whether active, dormant or re-activated were noted and mapped (see fig 21 and appendix 4). Also, the landslides age (appendix 4) were mapped as new (see fig16) and old landslides (see fig 17) depending on how fresh the surfaces are. The new landslides were easily mapped in the catchment because of their fresh surfaces and fresh deposits of debris while the old ones have been overgrowned or have vegetation growing in them.

An attempt was made to estimate the landslides deposit volume at each location mapped (see fig19). This was to give a very rough idea of the volume of the debris still left in the catchment and also as an indicator for potential future hazard assessment. The evaluation of the landslides volume was based on field observation of the deposit volume, detachment area, deposit height, deposit base, morphology and geometry. The landslides volume (see fig 19 and appendix 4) were then classified based on threshold determine during reconnaissance survey of the catchment as follows; landslides volume is characterized as (a) small if the estimated volume is less than 10,000 cubic meters, (b) medium if the estimated volume lies within 10,000-50,000 cubic meters and (c) large if the estimated deposit volume is greater than 50,000 cubic meters. Out of the 41 landslides mapped in the Hongchun catchment, 14 of the landslides fall into the thin category with a total estimated volume of 100,000 cubic meters; 10 of the landslides were categorized as medium with a total volume estimate of 375,000 cubic meters and 17 of the landslides fall within the thick category with a total estimate of 1,200,000 cubic meters. The resulting total estimates of all the three categories of the landslides volume is 1,675,000 cubic meters. These give a very rough idea of the total volume of debris from the landslides in the catchment.

The total estimated volume of the landslides volume from the field observation did not agree with the figure gotten from the field interview with Mr Wang the chief supervisor of the HUADI Construction Company at the Hongchun catchment site(according to him, 2.25 million cubic meters of debris is still left in the catchment). This difference of 675,000 cubic meters obviously, was due to differences in approach and the method used in the estimation of the landslides deposit volume. However, the approach used in this research was prompted by lack of good DEM after the earthquake but was fairly good in giving a rough idea of the volume of debris resulting from the earthquake induced landslides. In a data drought environment it may be very useful. Field estimations of landslides volume is not entirely a new concept, (Cardinali et al., 2002) estimated landslides volume on field observation based on landslides type, intensity and expected velocity.

Figure 16 new landslide (source: fieldwork)

figure17 Old landslide (source: fieldwork)

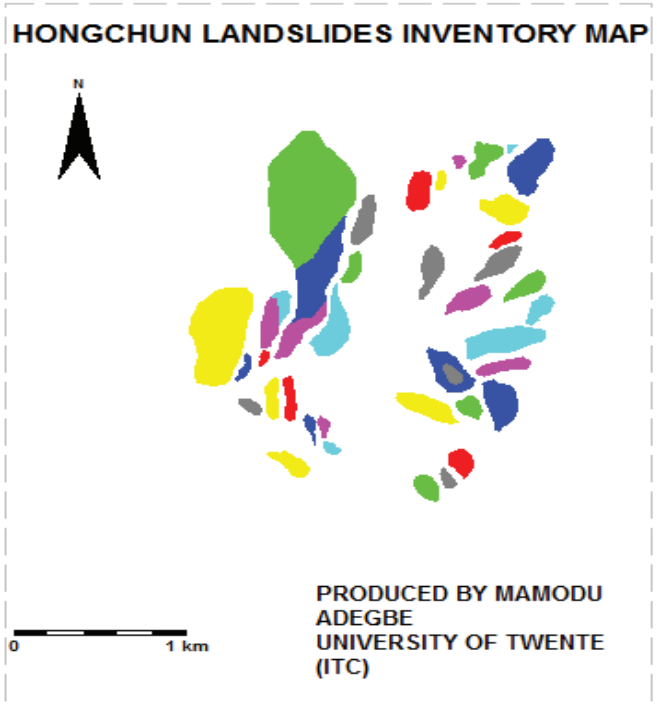

Figure 18 landslide inventory map

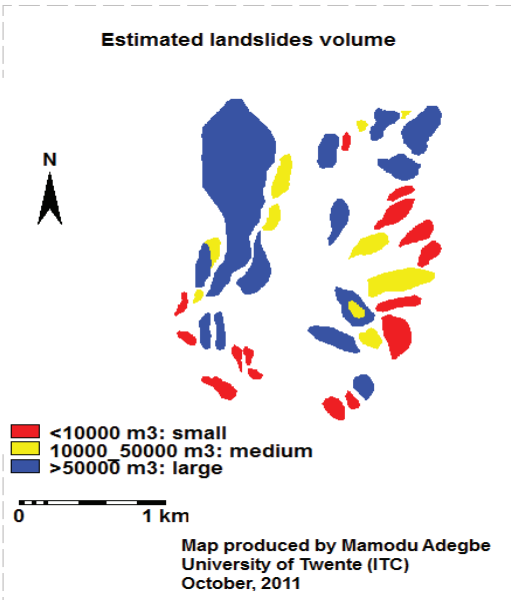

Figure 19 landslides volume estimates

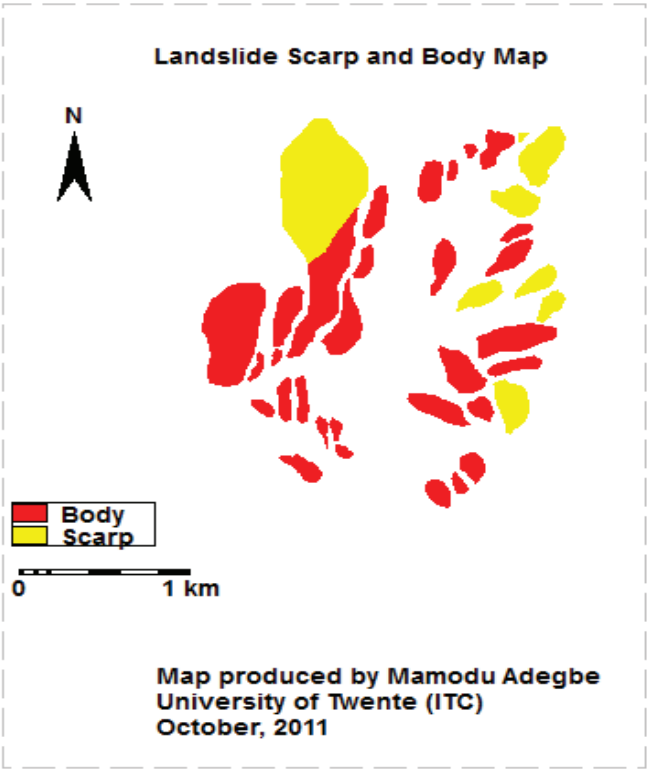

Figure 20 Landslides part map

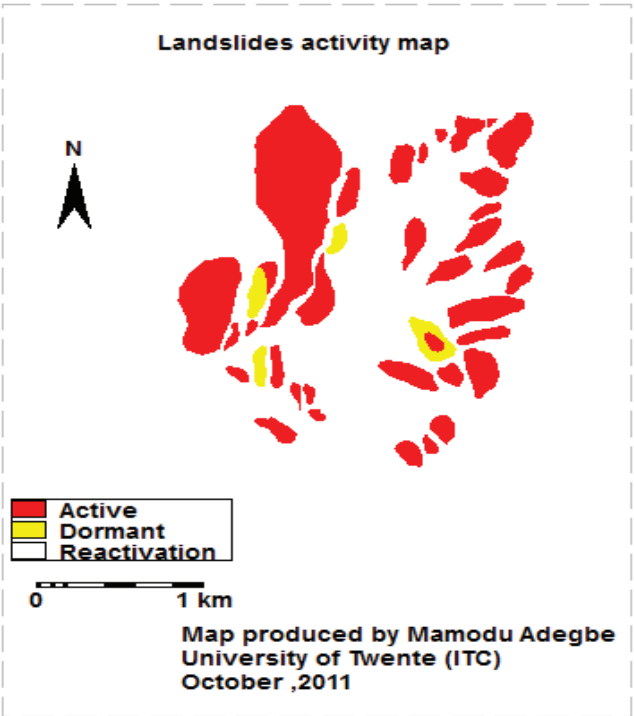

figure 21 Landslides activity map

4.5.4 Mapping check-dams and embankments

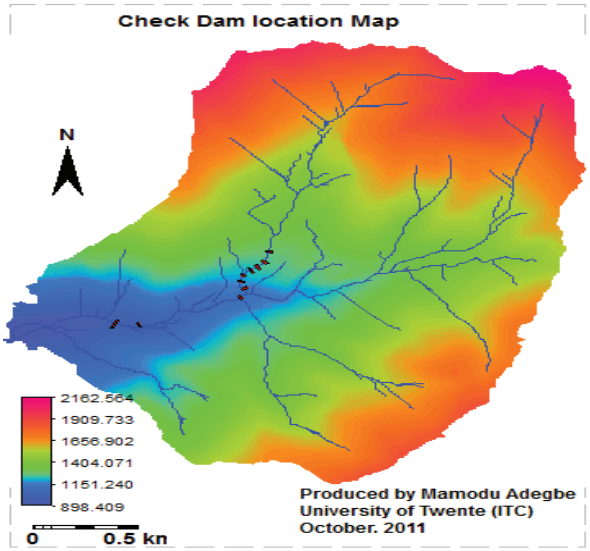

Figure 22 map of check dam locations

The check-dams in the Hongchun catchment serves as a prevention and a control measure to the landslides and debris flow events in the catchment and also for the highway. However, it was revealed during an interview sections that prior to the May 12, 2008 earthquake of magnitude 8.0 that hit the province and the subsequent secondary hazards, there was no check-dam in the hongchun catchment. Immediately after the August 14, 2010 debris flow in the hongchun catchment, the need for protection of life and property of the people living in the lower part of the catchment led to the construction of 20 check-dams across the catchment channel bed see fig 22. The cost of the project was 27 million US dollars as revealed during the course of interview held on the 30th of September, 2011. Also, it was revealed that, the check-dams were completed in April 25th, 2011. Three months later, on the 3rd of July, 2011 a debris flow event of 200 000 cubic meter occurred after a rainfall of 130mm. This was also followed by debris flow event of 50,000 cubic meters on the 21st of August, 2011 after a rainfall of 150mm.

During the fieldwork, some of the check-dams were mapped, their height, were measured see fig 23.The capacity of the 20 check-dams is 260,000. The capacity of the first dam in the catchment which is also the biggest of all the check-dam is 140,000 cubic meters. Its height is 21m and the length is 114m see fig 23.
All the check-dams are constructed with cement, iron and concrete and they all have pile foundation which makes them strong. They were designed to -withstand earthquake higher than 8.0 magnitude. (from interview)

Figure 23 the biggest check-dam in the catchment

figure24 measuring the width of check-dam (source: fieldwork)

The check-dam has an extra protection wall against under-cutting action of run-off, erosion or debris flow events see fig 24.

.

Besides the embankment at each of the check-dams, they are several stand alone embankments in strategic locations in the catchment to prevent the re- mobilizations of debris materials see fig25 and fig 26.
Despite the novelty of this embankments, in some locations in the catchment, they are either broken down by the over powering force of the debris or toppled with debris therefore reducing its effectiveness. See fig 25 and fig 26

Figure 25 shows over-toppled embankment

figure 26 shows a broken embankment

At outlet of the catchment, they are artificial terraces that are designed to slow down or reduce the viscosity of the debris thereby reducing the intensity of the debris flow see fig10.
Due to the recent debris flow events of 3rd July and 21st August, 2011 respectively, there are lots of debris materials on the terraces as seen in fig10.

4.5.5 Interviews

In Order to understand the past debris flow event in the catchment from a historical perspective, a 3 hour interview was conducted from 1.30pm to 4.30pm (Chinese time) on the 27 September, 2011. From the interview, translated accordingly by my field assistant, some historical information about the debris flow event in the catchment was revealed. Prior to the May 12th, 2008 earthquake of magnitude 8.0, the Hongchun catchment was not known for debris flow activities. Also, farming was the main Land use of the catchment. These information were confirmed by further interviews by 15 randomly selected adults (both male and female) on the street.

On the 14th of August, 2010, a debris flow estimated at 400,000 cubic meters was initiated in the catchment; it dammed the Mianjing River, changed the flow direction and caused massive flooding of the Ying xiu town, destroying lives and property. It was after the August 14, 2010 event that the construction of the 20 checks-dams across the entire length of the catchment at strategic position started. This was completed on the 25th of April, 2011.

Figure 27 more debris waiting to be mobilized in the catchment

4.5.6 Soil Sampling and failed attempts

A total of 24 undisturbed soil samples were taken (see fig28) using the sampling strategy described in this section with PF rings based on accessibility and safety because of the rugged and steep nature of the catchment. In addition, large outcrops, boulders, debris, cobles and gravel are characteristics of the catchment. A 50mm diameter core sampling ring was inserted into the holder, gently hammered into the top soil layer. It was then dug out using a spade and sliced button of the ring with the sample in an upside down position first to ensure that the soil lumped remained intact. Plastic caps were inserted after slicing the edges. The same procedure as outlined in the Panchansri (2007) was followed. The visually estimated stoniness for all the soil samples ranges from 30-50%. All the soil samples were

taken at the most accessable locations with reasonable soil depth. The samples were numbered accordingly and the corresponding number of the ring was also recorded. The soil samples are generally dark-gray color, sandy-loam soil mixed with lots of gravel which makes it the soil very loosed. The soil in the catchment are so loosed that samples could not be taken to carry out direct shear test in order to determine the cohesion and angle of internal friction but it was okay to determine other physical properties like initial moisture content, porosity, bulk density and saturated hydraulic conductivity.

Even within the very few locations where good samples could be taken in the catchment; they were 13 different locations were these attempts to sample failed (see fig 30). This is because of the high stoniness of such locations estimated to over 50%. The location and height of the failed attempt were recorded with the GPS.

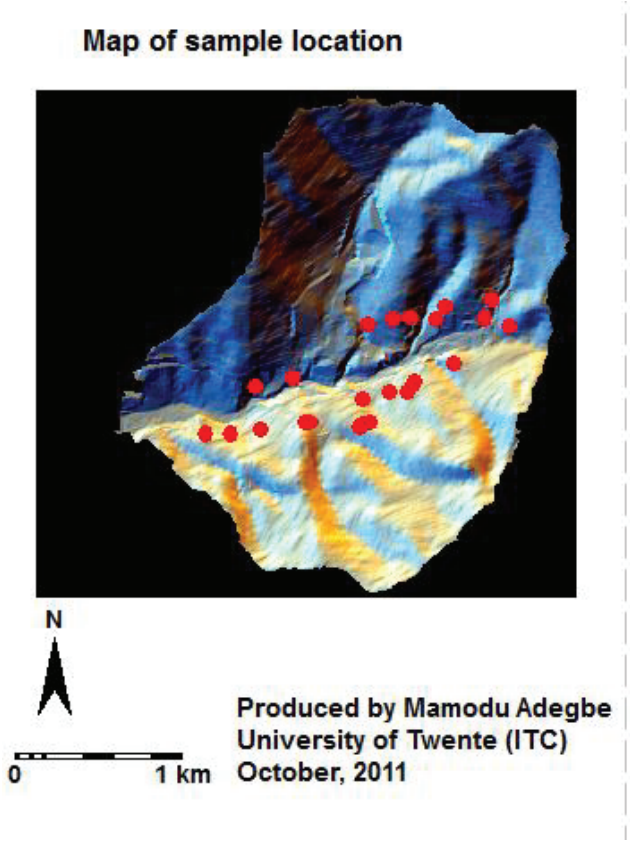

Figure 28 soil sampling locations

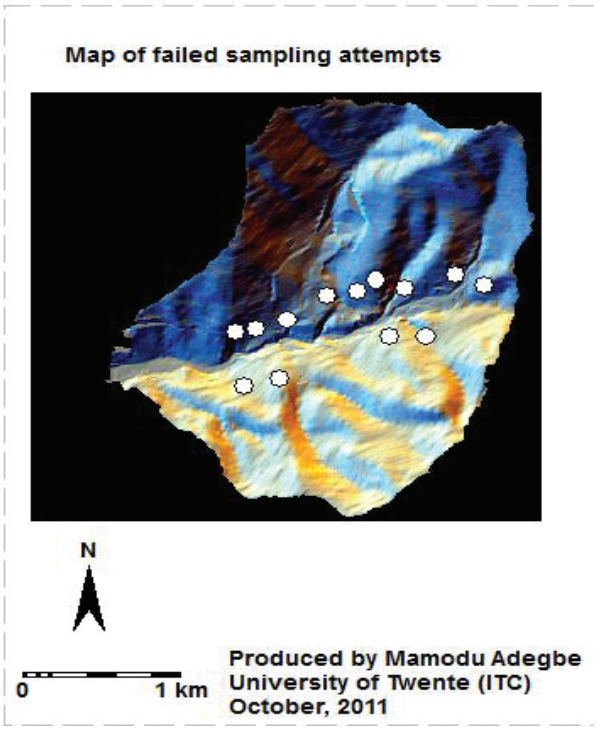

figure 29 failed soil sampling locations

Figure30 show where soil sampling failed due to stony nature of the soil

4.5.7 Soil depth

Soil depth in the Hongchun catchment was mapped based on field observation and measurement (see fig 33) mainly along the valley floor, points where soil samples were taken, Landover verification points and the landslides exposed area (see fig31) this criteria were used because there were no road cuts in the catchment to observed the soil depth and also due to the rugged nature and exposed granitic rock unit underlying the catchment which made augering extremely difficult. It was observed that they soil depth varies widely across the catchment with the thickest point along the valley floor and the shallowest point along the upper part of the slope. Some areas in the catchment have no soil depth mainly the bare area maybe as a result of removal by landslides or removal of the soil by surface run-off in the catchment. It was observed generally in the catchment that the soil depth in the catchment is very small to acts as a good storage. Soil depth (thickness) map was one of the most important inputs in the LISEM model. The soil depth and slope relationship see fig 34 indicates that they are moderately correlation.

Based on the field observation and the measurement, different extrapolation techniques; nearest neighborhood, Kriging by moving average ordinary Kriging etc were carried out (see fig 32) but none of the extrapolation techniques adequately represent the catchment reality**.** Thus, the produced soil depth (see fig 31) was used in the model.

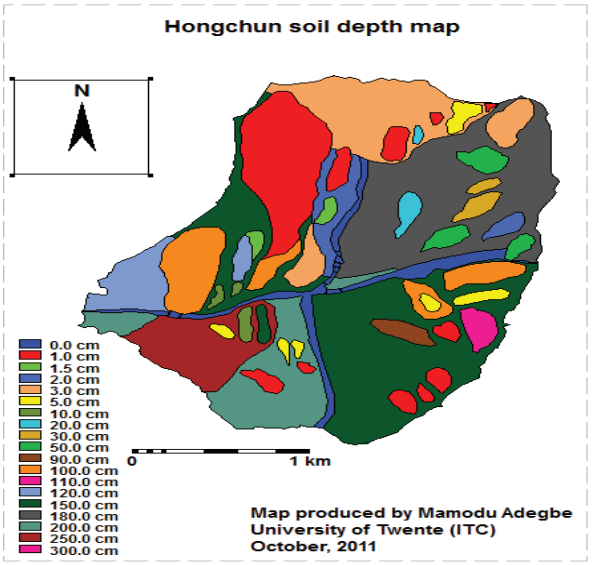

Figure 31 shows soil depth

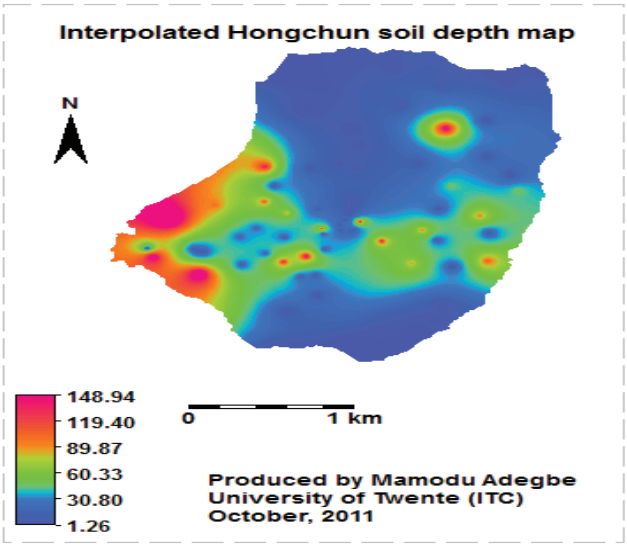

Figure 32 shows interpolated soil depth

Figure 33 soil depth measurements

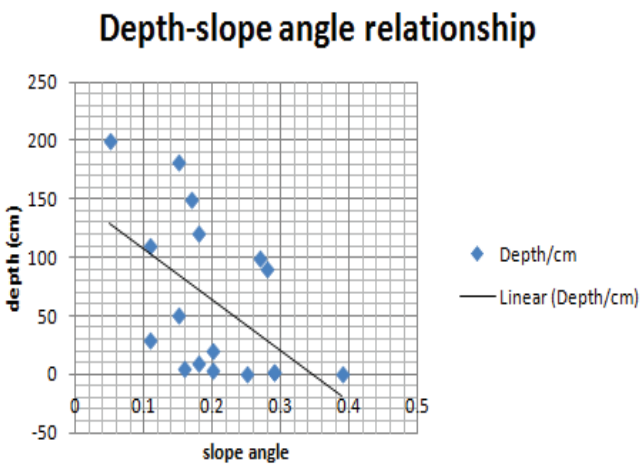

Figure 34 shows depth-slope angle relationship

Several authors Derose et al (1991); Odeh et al (1991) have reported that soil depth is highly correlated to slope and/or landforms characteristics and subsequently slope of the region . In conditions were data is deficient, given few estimates of soil depths, it is plausible to derive a soil depth map from with a known relationship for a similar terrain elsewhere, reported by researchers.

4.5.8 Soil texture

The Hongchun soil textures were mapped based on field observation and inspection very similar to the soil depth approach as explained in chapter 4.4.7. The soil textures in the catchment were classified into four classes based on field observation of the color and texture (see fig 35) namely loamy gravelly, sandy loamy gravelly sandy clay loam gravelly and sandy silt. The common features of all the three out of four texture classes were the gravel content (stoniness). Irrespective of the texture class in the catchment, there were high levels of stoniness ranging from 30-50 percent based on field observed estimate. The sandy silt textures were observed mainly along the stream beds in the catchment. Out of the three texture classes with gravel, the least occurring class is the sandy clay loam gravelly which were found in few locations in the catchment, while the dominant class is the sandy loamy gravelly. The presence of the gravel in the three texture classes maybe due to the underlying basement rock or due to the previous landslides deposit bodies in the catchment.

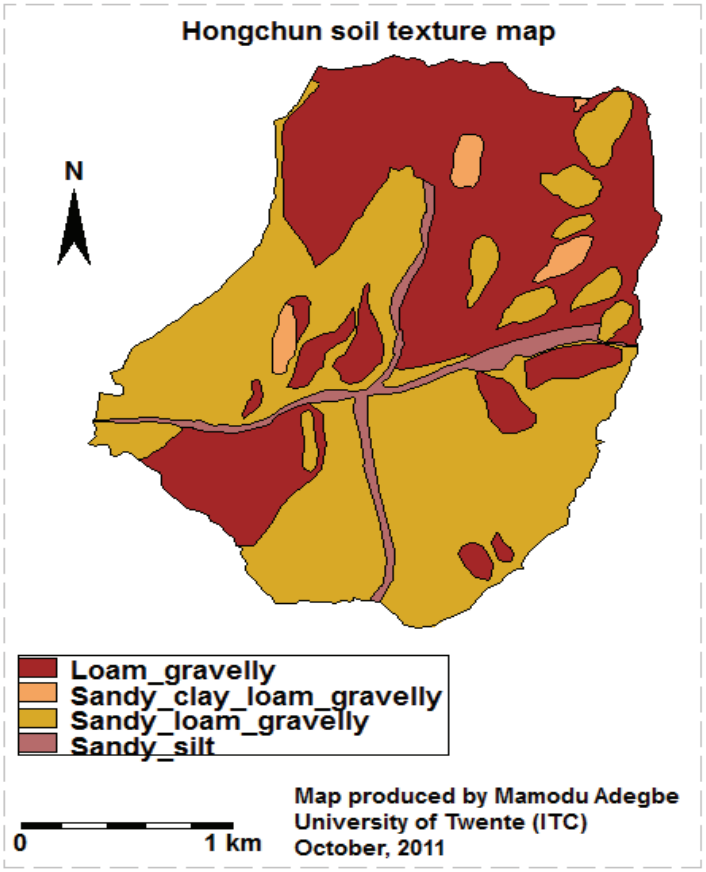

Figure 35 shows Hongchun soil texture

4.5.9 Measurement of cross-sectional area

The cross-sectional area of the catchment was measured at the outlets where the water from the two main streams seems to be concentrated along the artificial terraces with a 50m fiber measuring tape (GWF-5005).
The location and height of the outlet point where the cross-sectional area was measured with GPS and tape respectively. Since the outlet is rectangular, the length and breadth was measured and the area determined by length multiplied by the breadth. The length was measured to be 26.6m and the breadth (depth) was measured to be 2.32m Therefore, the cross-sectional area of the outlets is 61.712 m^2.

4.6 Debris flow initiation area

After the debris flow events of 2010, Tang (2011) identified one main source area contrary to the findings of this research during the geomorphological mapping, two main source area/initiation zones were identified (see fig 36 and fig 37). Tang (2011) further studied the occurrence of debris flows in the Hongchun catchment and one of the conclusions of his work was outlining the area that was most susceptible to future debris flow initiations.

Figure 36 Tang (2011) old initiation area

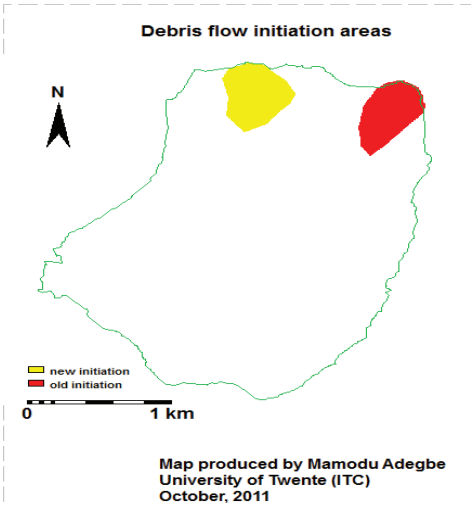

Figure 37 Debris flow initiation areas

Tang (2011) pointed out that the overflow eroded the gully on large landslide deposits in the Hongchun gully. This was also confirmed during the fieldwork carried out by the researcher in addition to the identification of another (new) source area of debris flow initiation in the hongchun catchment.
These two identified (see fig 36 and fig 37) areas of debris flow initiation were marked as the most susceptible to future debris flow initiations based on (Tang et al, 2011), expert evaluation, field observations and geomorphological analysis.
These susceptible areas are on the western part (halve) of the catchment. The location of the check dams only along these areas of the catchment further confirms the field observations and geomorphological analysis of the susceptible areas of future debris flow events and shows the most activity.

With respect to this information on susceptibility, the two initiation zones were defined and used in the FLO-2D model. However, volume of the initiations was not known.

4.7 Measurement of Discharge

The discharge of the catchment was measured at the catchment outlet by multiplying the wet-cross-sectional area of the chosen outlet point by the velocity of water at that point (Q= A * V). Where Q is the calculated water discharge in m^3/s, A is the area of the wet cross-section in m^2 and V is the velocity of the flowing water in m/s. The variables used in calculating the discharge was measured twice daily (morning and afternoon) for ten days consecutively. At each day of the measurement, remarks were made to note the condition of before or during the measurement (whether there was a little rain prior to measurement or no rain).

The variables measured to determine the area of the wet cross-section are depth of the water represented by d and wet surface represented by w . Note that d and w are has their units in meters respectively. The area of the wet cross section A is calculated using the formula; A=1/2*d*w this is because of the triangular nature of the water front.
The velocity of water in m/s was calculated by dividing a specific distance in meters over which the water flows by the time in seconds it took a small leaf from plant (of insignificant weight) to cover that distance. The specific (constant) distance measured with the tape is 2.35m. This was constant for all the measurement made and the time taken by the small leaf to cover this distance was noted by a stop-watch. For each time measured, the average of three different measurement of the time is used to avoid over-estimation or under-estimation (avoid inaccuracy in timing).

After calculating the area of the wet cross section and the velocity of the water, then the discharge was determined for each time of the day by multiplying the area of the wet cross-section by the velocity of water.

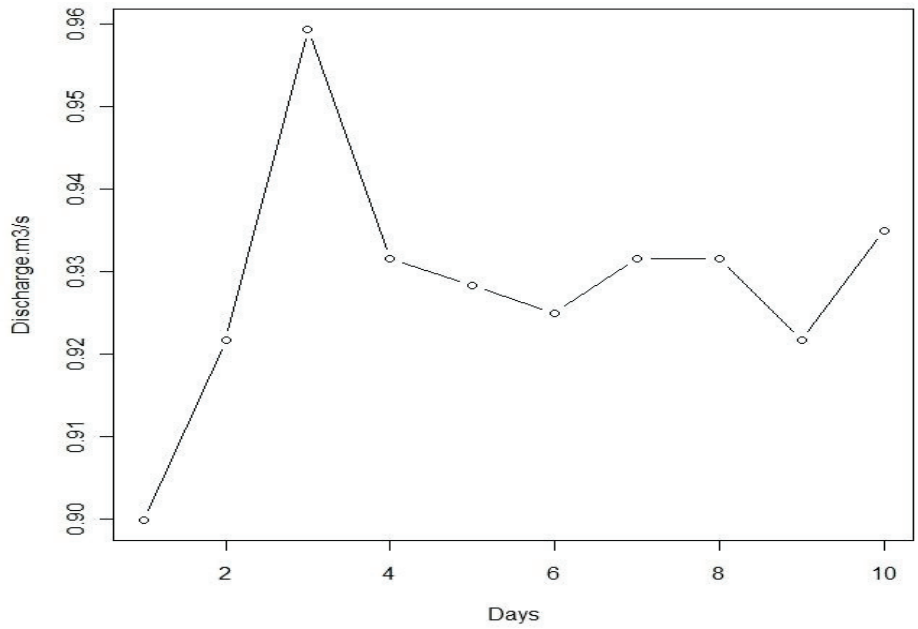

Figure 38 discharge measurement

The discharge for each of the day's shows similar value except for the 3rd day where there was a little rain but still indicates no peak discharge. (See fig 38). Since there was no major peak in the discharge measured as a result of lack of rainfall during the period of measurement, it reflects the base flow or groundwater flow for the catchment. This is because the groundwater flow is discharged at the surface through the river channels.

4.8 Secondary data (Rainfall data)

The only successful rainfall data collected is outlined in table 8. The bar-charts showing the rainfall and the accumulated rainfall are presented on fig 39.

Table 8 Rainfall for study area

Resolution	Period	Number	Name of station
Hourly	12-14 August, 2010	1	Chengdu University of Technology

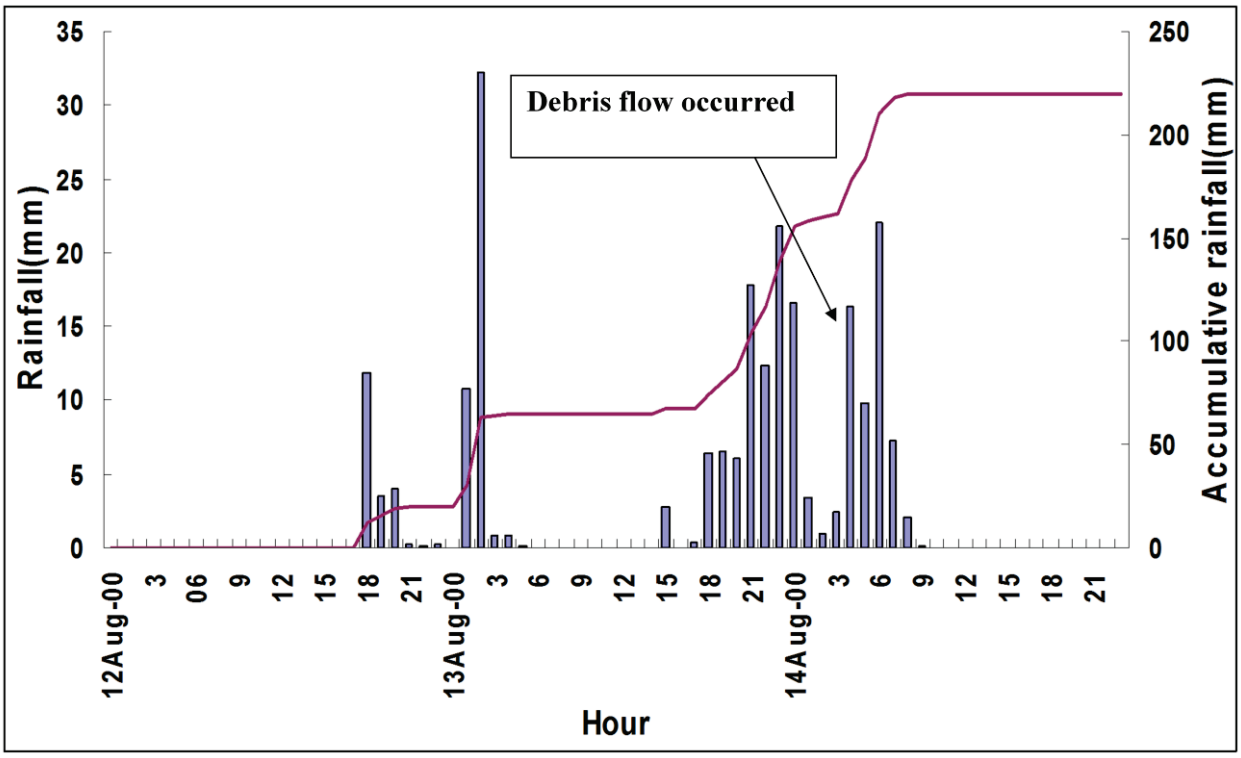

Figure 39 Distribution of hourly and accumulated precipitation between Aug. 12 and Aug. 14, 2010.

All attempts to collect rainfall data were unsuccessful because of the classified information of the Chinese Government.

On the 4th of October, 2011. We were at the Ying xiu rain station which is the only one for the study area to collect rainfall data for atleast 2 years Period but were refused for reasons mentioned above. Although, we have reasons to believe that the data were available they were simply not given to us. Effort was also made to collect rainfall data from Chengdu meteorological station which is 60km away from the study area but was not successful for the same reason mentioned earlier. The only rainfall data we got was from the Chengdu University of Technology courtesy Prof Tang see table 8 which was translated from Chinese to English by Cheng Lei an MSc student with the University who was also my field assistant.

4.9 Post Fieldwork

4.9.1 Soil physical properties

Post field work involved the laboratory analysis of soil samples to determine soil physical parameters to use in the LISEM and the FLO-2D model. Saturated hydraulic conductivity (Ksat), porosity, initial moisture content, field capacity and bulk density were determined as outlined below (see appendix1).12 out of the 24 soil samples taken in the field were analyzed in the State Key Laboratory of Geohazard Prevention and Geoenvironmental Protection of

the Chengdu University of Technology and the remaining 12 soil samples were analyzed in ITC Laboratory. The Laboratory set up for the experiment is shown in appendix 1.

The outlined steps below were followed in the laboratory in order to determine the soil physical properties mentioned in chapter 4.8.1. See appendix 4.1

Ksat = Q/A * (L/ (L+dH))

Where Q is the constant percolation rate, A is surface area of the ring, L is height of the ring and dH is the depth of the constant head.

The resulting soil physical properties assessed from the soil samples in the two laboratories mentioned above are Ksat, porosity, field moisture content, bulk density and initial moisture. A summary of the statistics of measure of central tendency and dispersion is presented on table 9 and fig 40, fig 41; fig42 and fig43 shows the histogram of the soil physical properties (Ksat, Porosity, bulk density and moisture content respectively).

The boxplot of the soil physical properties were plotted against the texture class see fig44 (Ksat by texture class), fig 45 (density by texture class), fig 46 (porosity by texture class) and fig 47 (moisture content by texture class).

The result reveals that the Ksat did not vary in each of the classes because the boxplots for each of the Ksat in the texture class overlapped significantly (see fig 44). In addition, a t-test was carried out in order to compare the two mean valus of the Ksat in each of the texture classes and revealed a similar mean. This is an indication of similarity of texture class with respect to the Ksat. It can be inferred that, the classification carried out in the field by field observation primarily was based on the soil colour and field knowledge but the statistical analysis reveals that the color of soil and general knowledge is not enough to classify the texture of soil as none of these affects the soil physical properties. Therefore, for the hongchun catchment, the texture class of the soil can be taken as uniform (one unit), which is the sandy loamy-gravelly because.

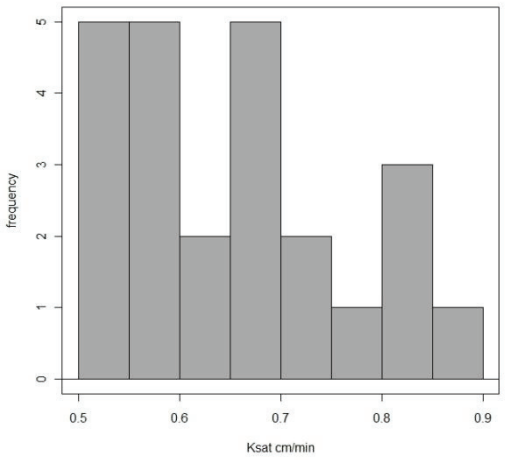

Figure 40 histogram of Ksat

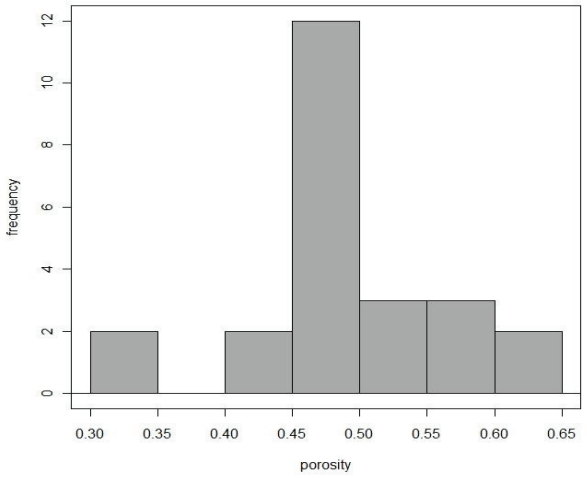

Figure 41 histogram of porosity

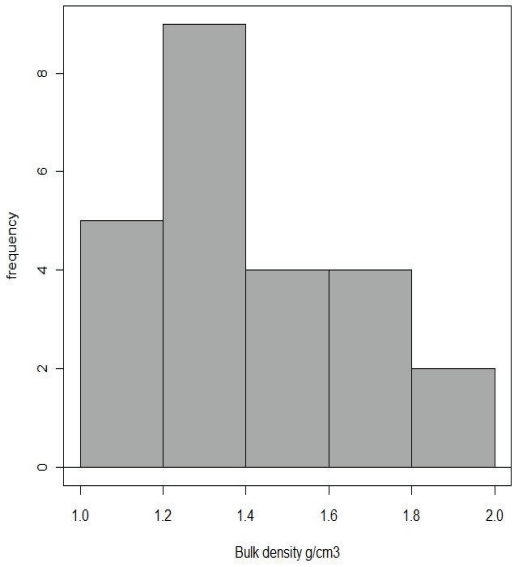

Figure 42 histogram of bulk density

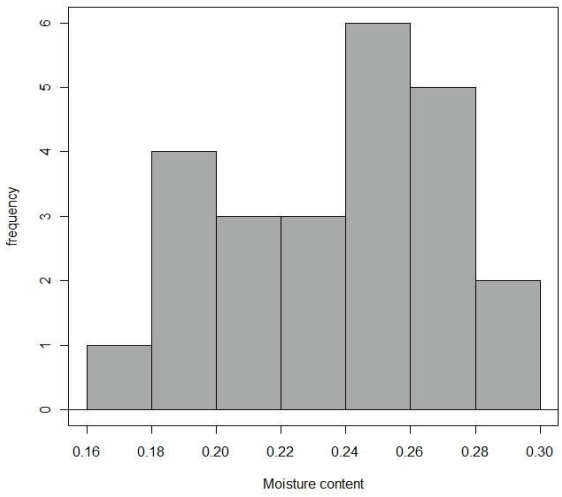

Figure 43 histogram of moisture content

The average of the Ksat was used used for the catchment in the modeling.

Table 9 summary statistics of soil physical properties

Physical properties	Mean	SD	Median	n
Bulk density g/ cm3	1.42	0.24	1.36	24
Field capacity	0.35	0.09	0.36	24
Ksat (cm/min)	0.66	0.11	0.64	24
Moisture cont.	0.24	0.03	0.24	24
Porosity %	49.25	7	49	24

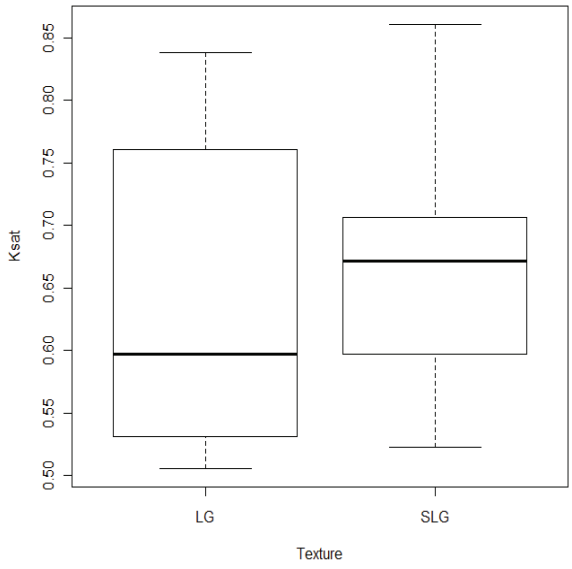

Figure 44 Ksat by texture class

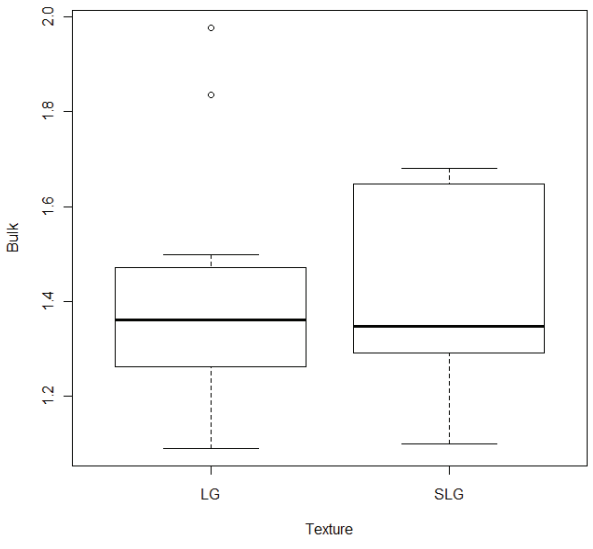

Figure 45 Bulk density by texture class

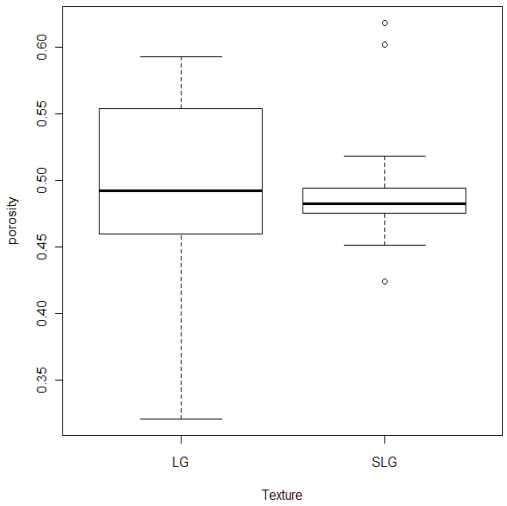

Figure 46 Porosity by texture class

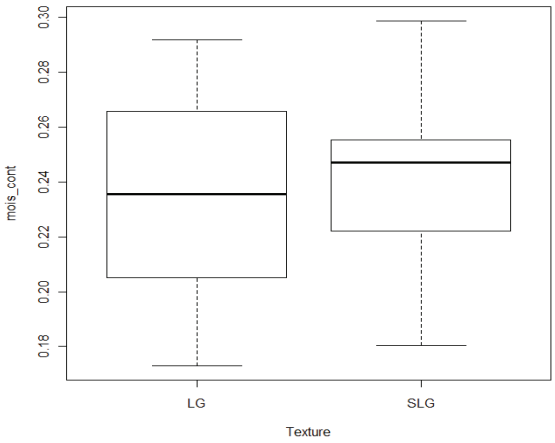

Figure 47 moisture content by texture class

Following the boxplot of fig 44 which shows no significant variation of Ksat in the two texture classes Sampled, t-test (independent sample t-test) was carried out on the Ksat mean value for the two texture class at 95% confidence level. The results revealed a similar mean value of Ksat for the two texture class as shown below. Data: Ksat by Texture. t = -0.4461, df = 22, p-value = 0.6599
Alternative hypothesis: true difference in means is not equal to 0
95 percent confidence interval:
-0.11929927 0.07705938
Sample estimates:
Mean in group LG mean in group SLG
0.6435962 0.6647162

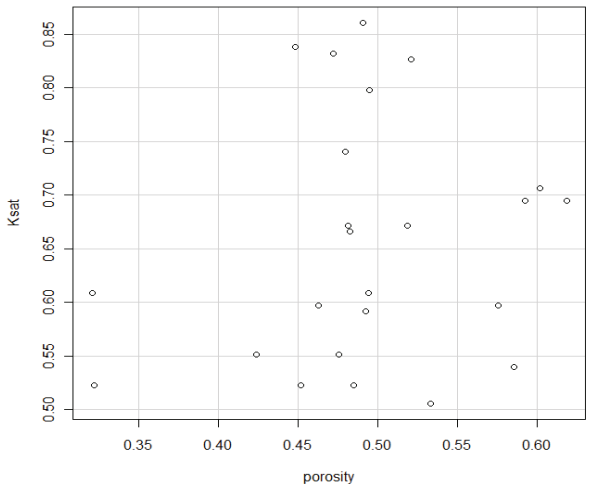

Figure 48 scatter plot of ksat and porosity

The scatter plot see fig 48 as can be seen from the figure above did not reveal significant correlation of the soil physical properties. This indicates the some similarities in the soil physical properties.

4.9.2 Generation of new DEM

The DEM is a crucial input to the Model and will determine to a large extent, where the flow will occur and in how far it will be confined to natural or artificial channel that are found in the landscape. Therefore, the quality/Resolution of the DEM is important in the debris flow mechanics (behavior). Despite the availability of the 10m resolution DEM, the drive to have a higher resolution closed to Lidar DEM led to the production of a new DEM of 5m resolution. The new 5m DEM was produced by combining the 20 m contour lines of the study with 1m contour lines (a very high resolution) of the catchment valley/channel floor.

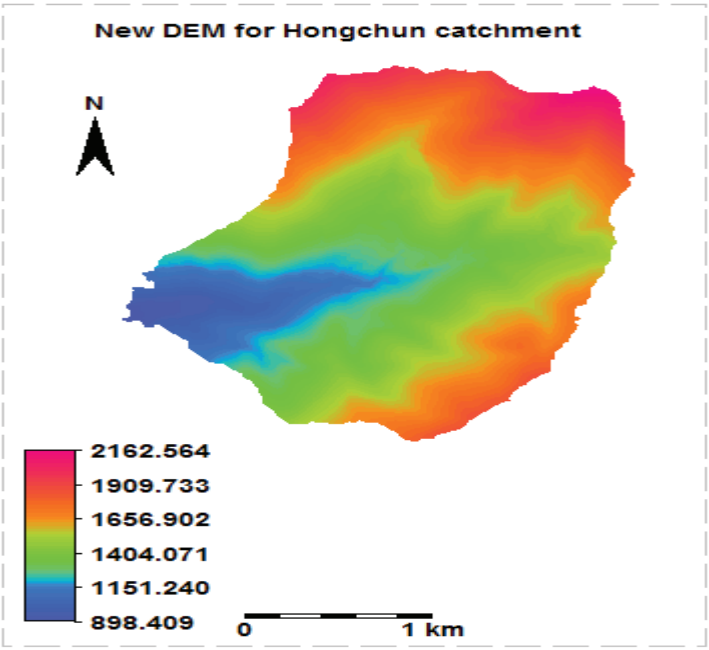

Figure 49 new 5m resolution DEM for the catchment

The 20m contour and the 1m contour were converted into points/resample into 5m resolution respectively in ILWIS and the portion corresponding to the valley floor was removed from the 20m contour and was replaced with the 1m contour. This will ensure a higher resolution and mapping of the valley where the debris flow occurs. The combine contour where later interpolated by Kriging in ILWIS and the new DEM of 5m resolution was produced. See fig 49

4.9.3 Surface Roughness

The respective landcover and surface roughness (see fig 50) also varied in spatial extents. Surface roughness is also characterized as manning's n or friction is an indication of the resistance the surface imposes on the flowing water/debris flow. It is either derived from

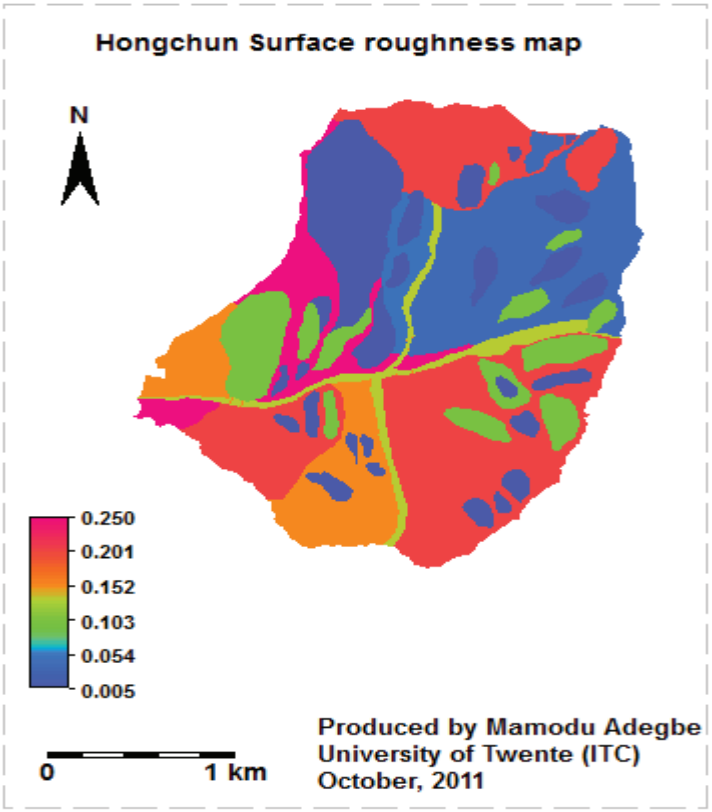

Figure 50 Hongchun catchment surface roughness map.

Landuse or landcover map. Roughness values were obtained from lookup table from literature (Alkema, 2007).

Table 10: the Landover based manning's n values used in the modeling.

Land cover	Manning's n
Bare soil	0.005
Dam/hard surface	0.15*
Trees and shrub	0.20*
Grass and shrub	0.05
Grass	0.25*
Bare with grass and tree	0.04*
Stream	0.13*
Bare with grass	0.10*
Shrub and tree	0.15*

(Source; adapted from Alkema, 2007 with own adjustments *)

The respective Landover and roughness maps were generated based on the roughness values on table 10

,

5.MODELING AND RESULTS

5.1 Introduction

The data collected and processed in Chapter 4 was then used in rainfall-runoff modeling and Debris flow simulation in this chapter. For runoff model using LISEM while the Debris flow area extent/volume, velocity depth, impact force and specific energy were modeled using FLO-2D. The results of the two models are presented in this chapter.

5.2 LISEM Modeling Scenarios

All the spatial data requirements for LISEM were created in PCRaster software using script that derived catchment map from the DEM, vegetation and infiltration maps from the landcover, soil depth from Fieldwork and channels and road maps using attributes as defined on table 11.
PCRaster is software compatible with LISEM(Jetten, 2002).

Table 11 Measured and observed soil physical properties

	Ksat	Thetas	Theta1	Psi	RR	N	per	ch	Lai
Bare soil	396	0.49	0.24	4.0	0.03	0.05	0.05	0.1	2.0
Dam/hardsurf	396	0.49	0.24	4.0	0.60	0.15	0.05	0.01	2.0
Tree and shrub	396	0.49	0.24	3.0	0.90	0.20	0.80	10	9.0
Grass and shrub	396	0.49	0.24	3.0	0.50	0.05	0.70	0.5	8.0
Grass	396	0.49	0.24	2.0	1.0	0.25	0.75	0.7	6.0
Bare with grass & tree	396	0.49	0.24	3.5	0.40	0.04	0.50	1.2	0.4
Stream/water	396	0.49	0.24	0.1	0.01	0.13	0.01	0.01	0.1
Bare with grass	396	0.49	0.24	3.2	0.30	0.10	0.40	0.4	5
Shrub and tree	396	0.49	0.24	3	0.80	0.15	0.60	0.5	7

Table 11 used to generate the landcover parameters maps and unit respectively are: saturated hydraulic conductivity (**Ksat/mm/h),** Porosity (**Thetas, cm3/cm3),** suction at wetting front (**Psi, cm),** initial soil moisture (**Theta1, cm3/cm3),** random roughness (**RR, cm),** mannings's coefficient (**N**), percentage plant cover (**per),** crop height (**ch, M),** and leaf area index **(Lai, m2/m2).**

The soil physical property (table 11) shows that the saturated hydraulic conductivity is very high this was due to the sandy/gravelly nature of the soil and its texture. The mean value for the Ksat was used as explained earlier in chapter 4. However, there was no influence on the Ksat by soil texture as the Boxplots and T-test reveals which contradict the texture classified based on field observations. The initial moisture content and porosity are moderately high respectively.

The LISEM modeling environment has a user interface that allows the modeler to upload input parameters, linking model to respective maps and rainfall directories, enabling automatic creation of run file. Simulation time allows

setting of start, end and time- step while model options enable the modeler to switch on/off runoff, erosion, snow, channels and storage. Infiltration model options allowing the choice from six of the infiltration including the Green and Amp. The output options allow for specifying results directory and formats for the time series data outputs and map series.

All the spatial data was input into the model using the 'basics map' menu bar, inputs outputs options using the Input/output menu bar and once loading and definition of the data was complete, the run file was saved and then using the simulation menu bar, the modeling was initiated. The output time step was set at 30minutes.

While the simulation is in progress, the 'time' and 'water' is shown and the summary of the simulation progress shown. The latest development in the model ('Display') allows visualization of the development of nine results parameters including runoff, water height, velocity, infiltration and soil loss related outputs (switched off in this study),

The model interface and rainfall event used in the simulation are shown on figure51

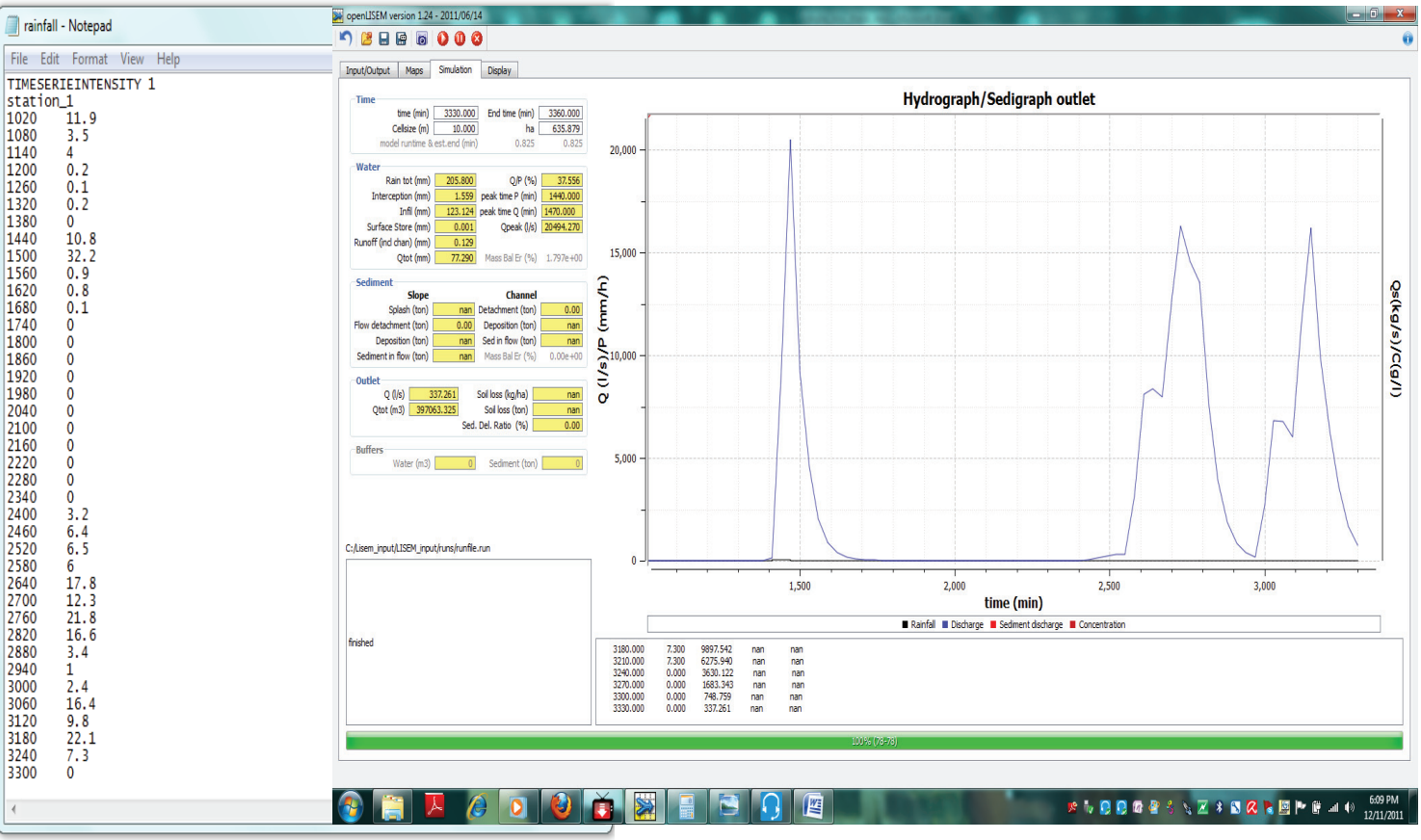

Figure 51 the rainfall event and the model interface

5.2.1 Whole catchment scenario.

The first scenario was simulated using the entire catchment. The spatial data covered the whole catchment the rainfall used remained the same.

5.2.2 Sensitivity analysis

The sensitivity analysis was carried out for Ksat .The Ksat sensitivity analysis is as shown on table 12.
Infiltration was important parameters in sensitivity analysis of the LISEM model as it significantly changed the value of water available for the surface runoff.

Table 12: Results of Ksat sensitivity to the rainfall-runoff model

Ksat (mm/h)	0	25	50	100	200
Rainfall (mm)	205	205	205	205	205
Runoff (mm)	203	189	178	159	127
Infiltration (mm)	0	14.2	25.2	44.5	76.1
Discharge/rainfall (%)	98.7	91.9	86.7	77.4	62.1
Peak Discharge(l/s)	38821	37156	36027	33871	29774
Tot Volume (m3)	1043841	945802	888671	795713	647426

The values resulting from the sensitivity analysis of Ksat are presented on table 12 shows an inverse relationship with peak discharge, total volume and runoff output. Rainfall, interception and mass balance error remained constant. There seems to be a limiting threshold for the Ksat parameter. The lowering of Ksat follows after a study by Hessels et al (2003) who highlighted that field measurements of Ksat tends to be higher than those the model uses for calculations hence the emphasis on reducing Ksat. At 0 Ksat, the result shows zero infiltration which means almost all the water was available for runoff see fig 53.

5.3 Lisem Simulation

The simulation was initiated using a time step of 30 minutes reporting every 60 timesteps, starting from 1020 minutes to 3360 minutes time. Figure 53 shows the simulation tab screen capture with the summary of simulation and the respective hydrograph from the model. As shown on figure 53 the total discharge from the catchment was 397063m3 from the storm event used (August 12-14th, 2010). All the other modeling results and settings including the catchment characteristics are also shown on this. However, due to the repeated model failure to cope with the same time step in the whole catchment scenario, a time step of 30 minutes was used.

5.4 LISEM results

The results from the simulation are shown on a tab (see fig 52) that summaries the catchment and pixel size, modeling time definitions, losses and discharge amounts, outlet quantities, ratios and errors and the hydrograph which is presented

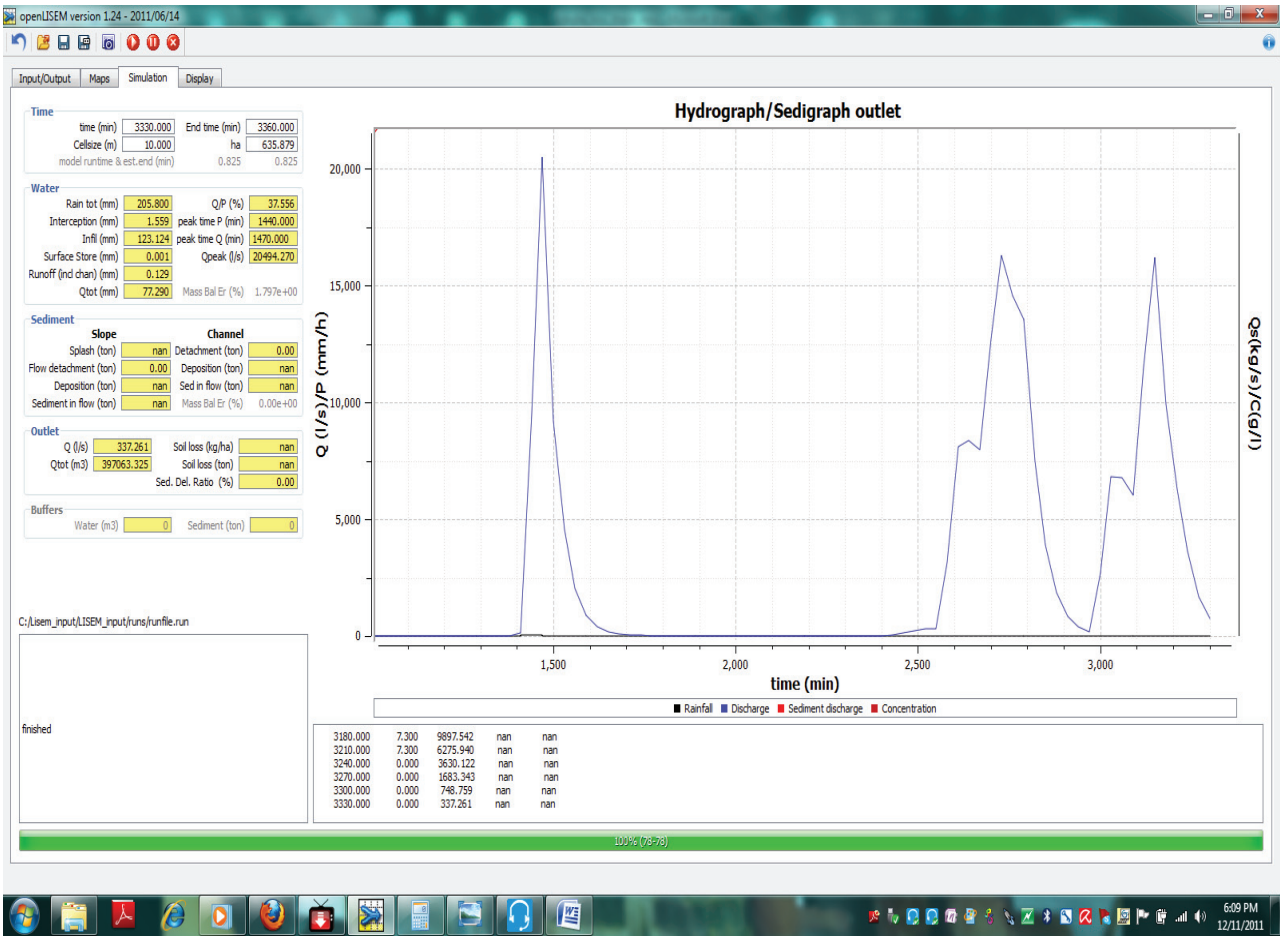

Figure 52 a screen shot of LISEM result.

The hydrograph on fig 52 show 3 peaks which corresponds to high discharge of the 3 days rainfall respectively. It also revealed low discharge during low rainfall. This is usually as expected in a catchment with uniform texture with a very high Ksat. It was observed that using high Ksat 396 mm/h in the runoff modeling has effect on the shape and peaks of the hydrograph (see fig 52) compared to 0 Ksat used in the runoff modeling (see fig 53). This obviously, implies that, a relationship may exist between Ksat values and the shape of the hydrograph. This relationship may be worth exploring in future research.

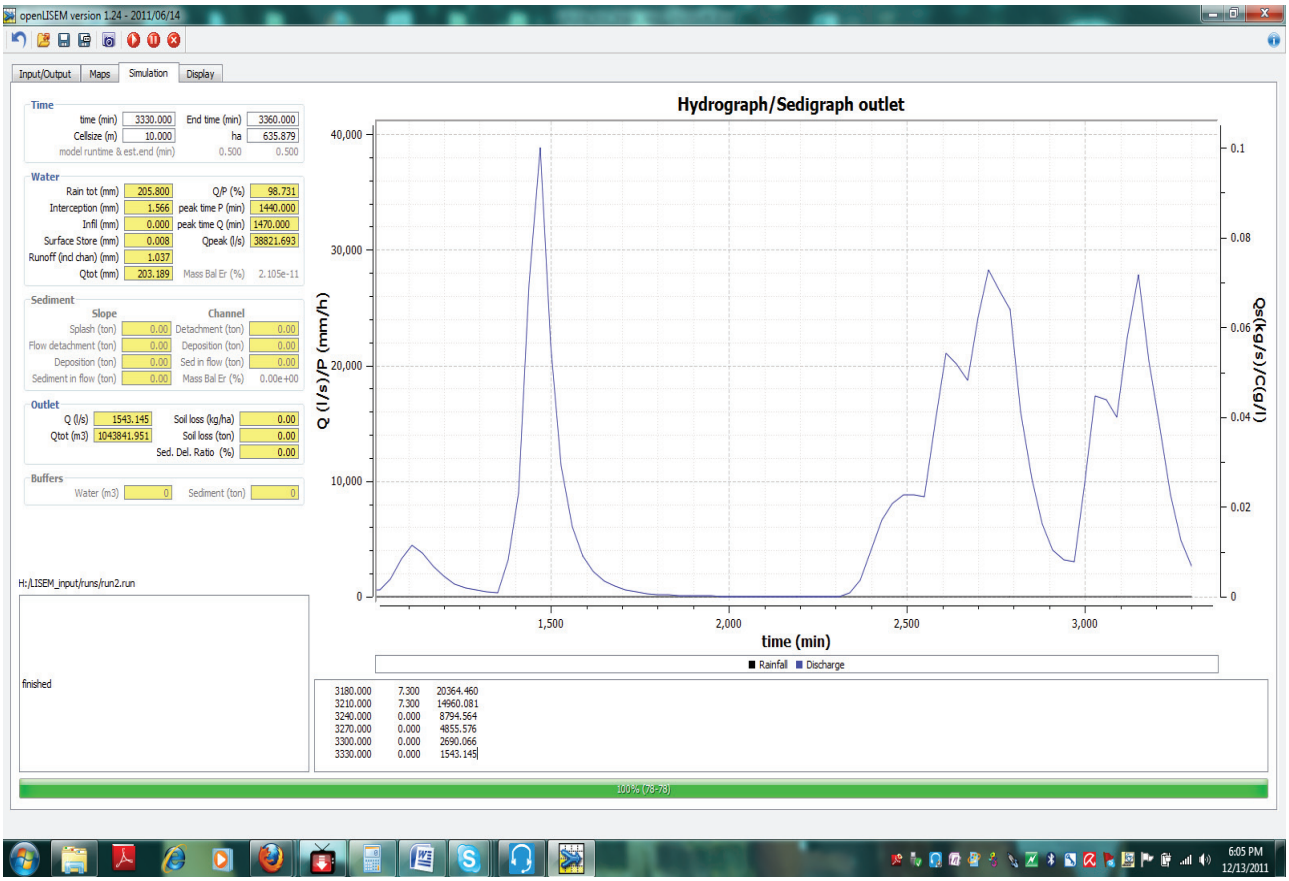

Figure 53 Ksat=0 almost all the water are available for runoff

5.4.1 Runoff coefficient

Runoff coefficient in the study was modeled between 0.4 and 0.8 which is reasonably lower than the Tone River in Japan case study that had 200mm rainfall depth in a predominantly forest and rice land use(Kinosita, 1983) that ranged 0.6 to 0.8. It is worth noting that the referred study had a rainfall depth of 200mm similar to the one used in this study which was 205mm. However, in the same study Kinosita (1983) also revealed a 0.2 to 0.3 runoff coefficient for Pampanga River with also similar rainfall and land use conditions in Philippines, thereby highlighting an important fact that runoff coefficient differs from one catchment to another.

5.4.2Calibration

The model was calibrated based on the runoff coefficient due to lack of the real flood discharge data.

5.4.3 Infiltration pattern

The LISEM model was also used to map the infiltration pattern see fig 54. This was done in order to see the spatial infiltration pattern across the catchment since they might reveal areas with high water intake and subsequently give an idea of areas that might be unstable (high chance of slope/ soil failure). The model reveals almost a uniform infiltration pattern for the catchment. This might be due to the uniform texture and geology of the catchment. However, it was observed that the infiltration tends to be a little more in the slope and the upper part of the catchment that were mapped geomorphologically as the source areas for the debris.

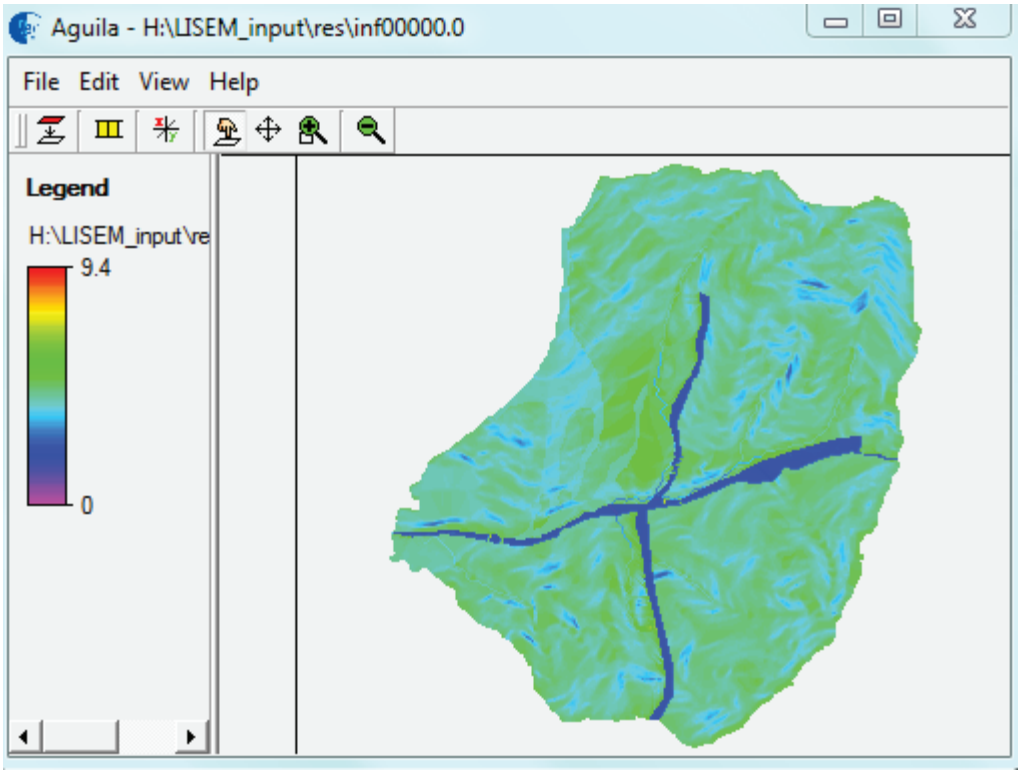

Figure 54 shows cumulative infiltration pattern

In summary, I understood from the Lisem analysis that the 3 days rainfall produce little runoff. The interception loss and infiltration were very small. This may be due to the landcover and soil depth/texture respectively. However, from the sensitivity analysis, the infiltration tends to increase considerably with higher Ksat values. This implies that, for the Hongchun catchment, the soil texture plays a very important role in the infiltration. It was also generally observed that the varing the values of the Ksat from 396 to 0 affected the peak and shape of the hydrograph. This might be due to the availability of water for runoff because at 0 Ksat, almost all the water will be available for runoff mostly in a saturated condition.

5.5 FLO-2D modeling scenarios

5.5.1 Rainfall –runoff modeling

FLO-2D being a lumped hydrology and hydraulic model was used in modeling the rainfall-runoff. A detail description of how to build the model was given in section 4.3.5 and 4.3.6. For this research, the following procedures were followed.

First, a database containing all the input data was build. The model can be run from the FLO-2D GUI main window using the GDS command in the pre-processor menu. The 10m DEM (asc) was imported into the model as ASCII grid files (where the elevation points are simply given as a table of space or comma). The 10m DEM prior to being used in the FLO-2D was converted from Arcgis shape file (raster) to ASCII grid files. A fill sink operation was also carried out on the 10m DEM (asc). This operation was necessary in order to remove pits (local depression) that would acts as artifact and local accumulation that would interrupt the flow and guide it to sinkholes which are not very convenient.

The grid size was defined as 30. So as to manage effectively the model runs time. 10m grid size was not used as expected because it took more than more than 3days to run and the model was still running for such a small catchment. Also, considering the loss of time to studying the workability of the model and the short time left for the research, Selecting smaller grid size does not necessarily increase the model resolution but increases the computational time (FLO-2D manual, 2007).

Another important part of the FLO-2D model is the computational area or boundary because outside this boundary, the model will not compute anything. The computational area which is a reflection of the study area or area of interest can defined by drawing a polygon round the study area by clicking on the each vertex as you move along the desired boundary. The polygon is completed by double clicking on the last polygon. The FLO-2D model requires that each grid element be assigned a representative elevation this is done by interpolation, because a set of DEM points may be randomly distributed in the flow domain and some grid elements may have many points while other might not. However, the default interpolation technique was used in this research.

The Rain.dat switch in the graphical user interface (GUI) is put on and the cumulative rainfall for the August 12 -14th, 2010 was entered in as percentage of total rainfall expressed between 0 to 1. This is because the rainfall distribution has to be related to the overall flood simulation time. The rainfall may occur for only a portion of the total flood simulation and may start later than the flood simulation represents. In this study area where the rainfall and simulation time are not correlation, the recommended(FLO-2D manuals,2007) 0.0 cumulative rainfall at the beginning of the flood simulation for a period of time and similarly 1.0 (100%) cumulative rainfall near the end of the simulation was used.

From the LISEM result, it shows a very small runoff for the catchment which might not generate enough runoff to cause debris flow. Therefore in the Flo-2D model, a zero infiltration was assumed for the catchment (antecedent rainfall might have saturated the soil coupled with the shallow nature of the soil depth) and this assumption was used throughout the FLO-2D model in this research. This assumption was supported by (Professor Vanasch and Cees Van Westen in a personal communication).

The result of the rainfall-runoff, presenting the maximum velocity and time to reach the maximum depth are presented in figure 55 and figure 56

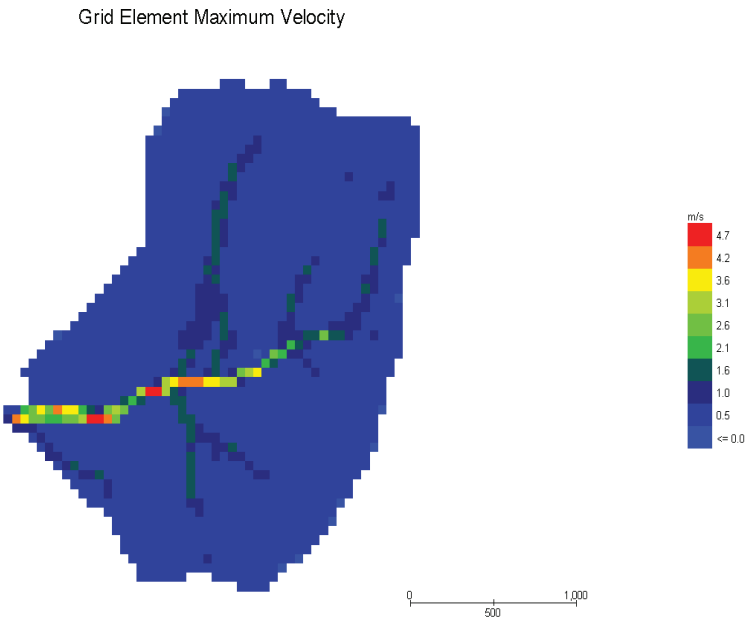

Figure 55 maximum velocity

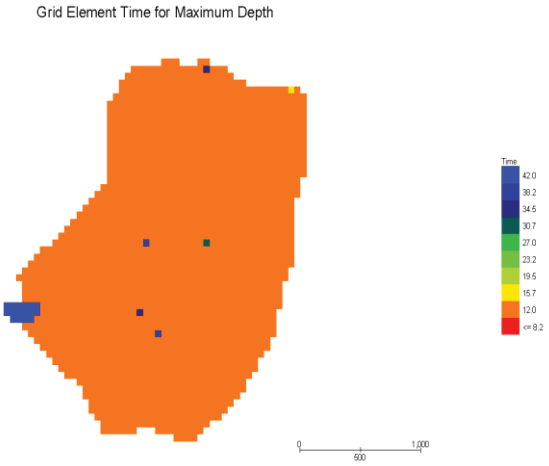

Figure 56 time to reach maximum depth

5.5.2 Debris flow modeling

Debris flow modeling using FLO-2D model is described in details in chapter 2.7 of the thesis and also building the FLO-2D model is also described in the chapter 5.6.1 of the thesis. FLO-2D also requires the modeler to define the area/point (s) where the debris flow initiation starts (source area) which represents the susceptible areas (unstable point) .Refer to chapter 4.5 for details.

For this research, the initiation areas represent the unstable area and were determined from the geomorphological mapping of the catchment. Two main areas of the catchment top were mapped as the source area contrary to Tang (2011) who identifies only one source area for the same catchment. These areas also tally with two big landslides scarp as mapped in the field (see fig 20). Also they were evidences of tree falling forward in those areas signifying instability. The falling of the trees or leaning forward was not due to the response of the tree towards light absorption because the stems were not folded or bended.

A constant sediment concentration 0.5 by volume was used. This was mainly due to lack sediment concentration data for the catchment. Also, the assumption to use the constant value for the sediment concentration was supported by Prof Vanasch, Cees Van Westen and B. Luna in a joint personal communication.
Due to lack data, the hyperconcentrated sediments flow parameters, that is, the viscosity and yield stress were determined from the literature (FLO-2D manual, 2007). The sediment specific gravity was set at 2.65(default throughout the research) while the 'K' laminar flow resistance was set at 24.

5.5.3 Debris flow results

The debris flow result showing the maximum flow velocity (see fig 57), maximum depth (see fig 58), the impact force (see fig 60) and specific energy (see fig 59) is shown below. The FLO-2D results were viewed in the Mapper which is in the post processor menu in the GUI and the boundary used in the thesis was imported as a shape file into the Mapper. However, there are several ways of displaying results in the Mapper. This could be either in grid, contours or shaded contour. The maximum area of inundation of the debris flow is 955000 SQ. METERS

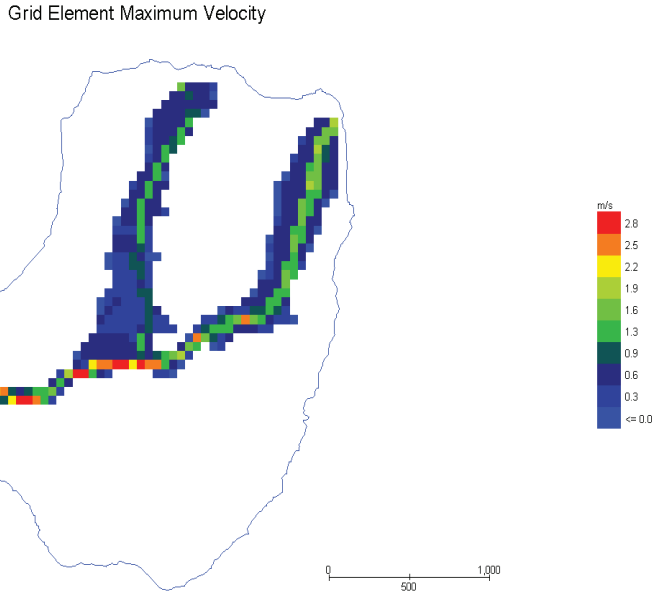

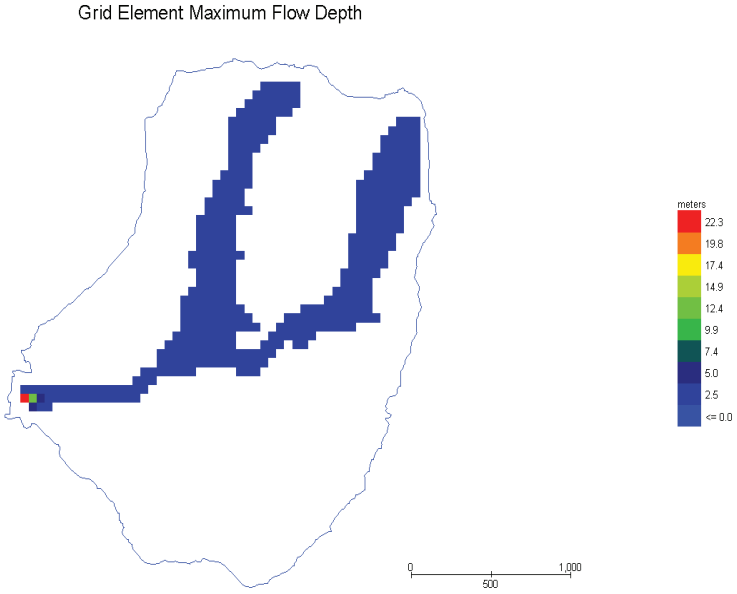

Figure 57 shows debris flow maximum velocity *figure 58 shows debris flow maximum depth*

The velocity of the debris flow varies across the catchment as seen in fig 57, this is partly due to the volume of materials entrained along as the debris moves and the basal friction component of the flow at various point. They velocity is small at initiation but becomes higher at the confluence of flow in the channel due to higher impact or collision of the material and the fluid matrix at the point of convergence. However, the flow depth remains fairly constant.

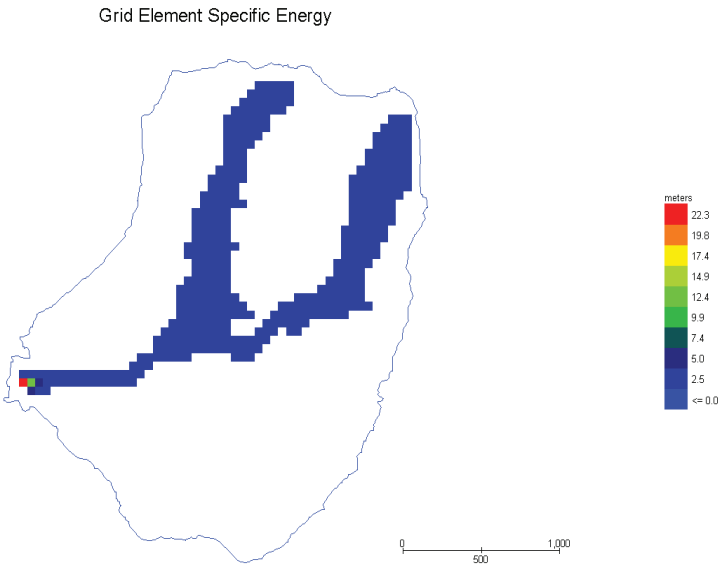

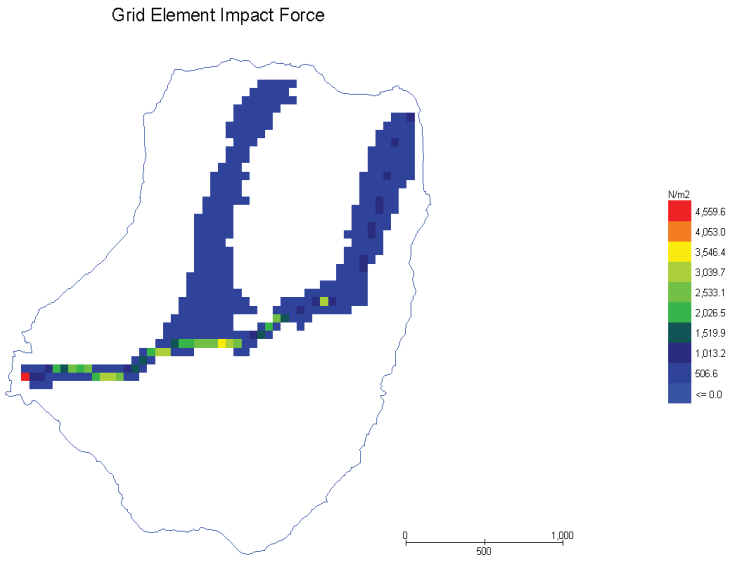

Figure 59 debris flow specific energy *figure 60 debris flow impact force*

The impact force at the initiation point is low this may be due to the fact that the debris flow has not entrained materials so much to affect the impact force (see fig 60). The velocity changes as the debris moves through the channel due to channel narrowing.

5.6 sensitivity analysis

A sensitivity analysis quantifies the variation in a model output due to variations in the model inputs. It shows how sensitive the output of the model is to change in the input and gives an indication which inputs parameter weighs more on the model. The sensitivity analysis was carried out on four inputs parameters. These parameters are:

- Sediment concentration
- Viscosity (viscosity coefficient and exponent)
- Yield stress (yield stress coefficient and exponent)
- Manning's n (friction coefficient).

However, the sediment specific gravity and "k" laminar flow resistance were kept constant at 2.65 and 24 respectively throughout this research.

Each single input parameter was increased or decreased by certain literature value, while the other input parameters were kept constant in order not to affect the sensitivity of the parameter being tested. Table 13 gives the ranges used in the sensitivity analysis for each input parameters based on value ranges obtained from the literature (table 3)

Table 13 the ranges used in the sensitivity analysis

Input parameter	Ranges
Sediment concentration	0.3 to 0.7

Viscosity (coefficient and exponent) poise	α =0.0648	β=6.20
	α =0.00283	**β =23.0**
	α =0.00136	β =28.4
	α =0.0538	β =15.5
Yield stress (coefficient and exponent) dyne/cm2	α =0.0765	β =16.9
	α =0.0345	β =20.1
	α =0.152	β =18.7
	α =2.72	β=10.4
Manning's n (friction coefficient)	0.005 to 0.250	

5.6.1 Sensitivity to changes in sediment concentration

Sediment concentration is a basic important factor when analyzing debris flow simulations (FLO-2D manual, 2007). Most debris flow studies require the estimation of the sediment concentration by volume since this is very important in describing the magnitude of an event. It is also important to note that the sediment concentration determines the classification of flows into water flood, mud flood, debris flows and landsides. (FLO-2D manual, 2007). See figure 6. For this reasons, the sediment concentration by volume ranging from 0.3, 0.4, 0.5, 0.6 and 0.7 was tested while keeping other parameters constant see result in table 14.

Table 14: Result of sensitivity to sediment concentration by volume

	0.3	0.4	**0.5**	0.6	0.7
Total volume (m3)	150,100	155,491	**161,350**	167,749	174,754
Max velocity(m/s)	2.9	2.9	**2.8**	2.6	2.6
Average depth (m)	10.1	11.0	**11.2**	11.3	11.4
Average specific energy(m)	10.1	11.0	**11.2**	11.3	11.4
Max impact force (N/m2)	3,554	4,007	**4,559**	5,355	5,597
Max area of inundation (m2)	945000	947500	**950000**	955500	975000

A, for sediment concentration of 0.3, the maximum velocity (see fig61), the depth (see fig 62), the specific energy (see fig 63) and the impact force (see fig 64) the results are shown below:

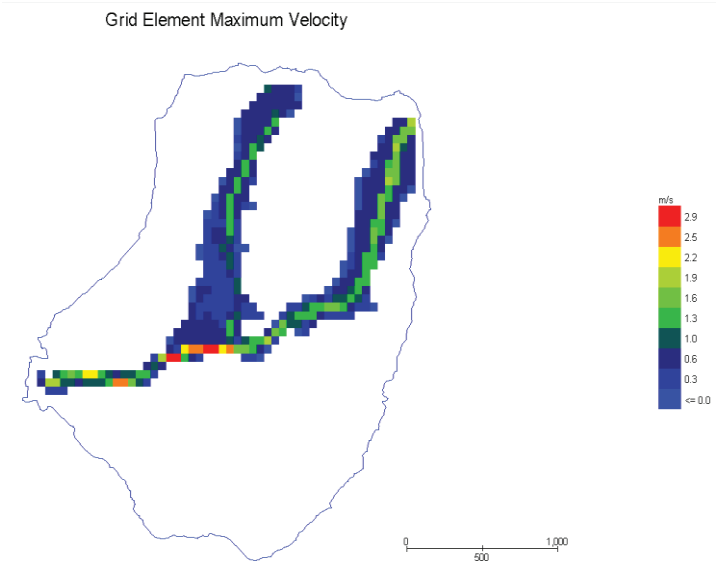

Figure 61 debris flow maximum velocity

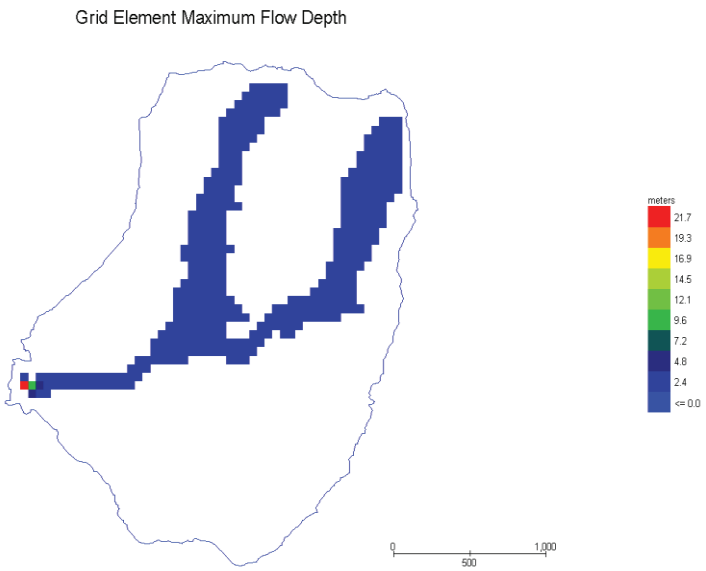

figure 62 debris flow depth

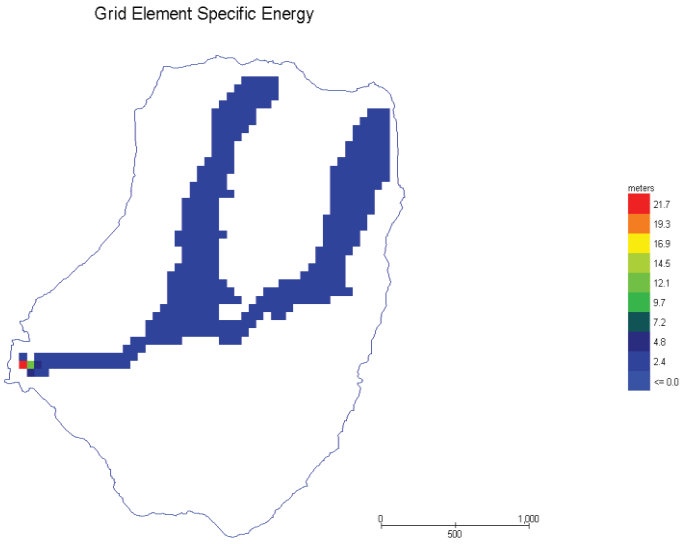

Figure 63 debris flow specific energy

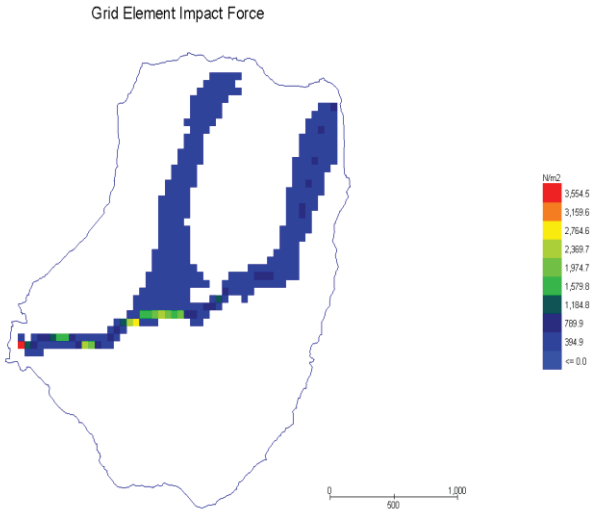

figure 64 debris flow impact force

B, for sediment concentration of 0.4, the maximum velocity (see fig 65), the depth (see fig 66), the specific energy (see fig 67) and the impact force (see fig 68) results are shown below:

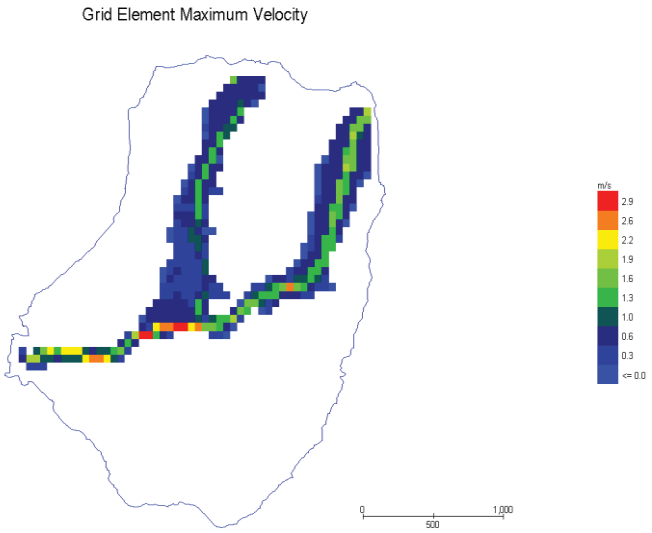

Figure 65 debris flow maximum velocity

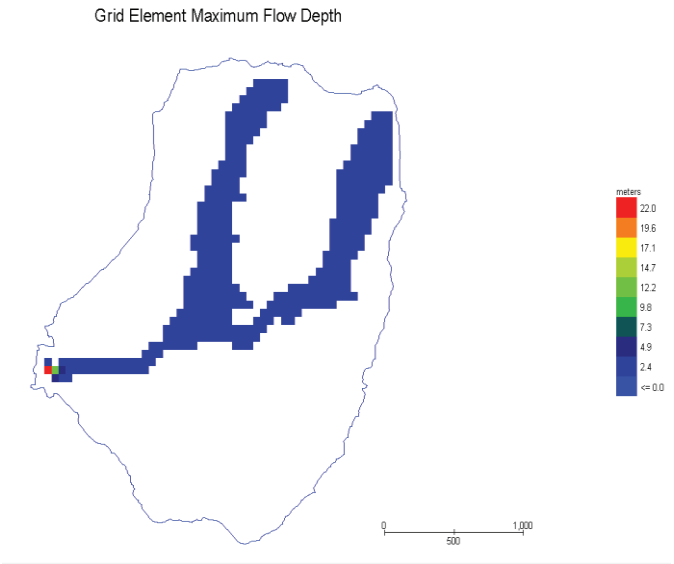

figure 66 debris flow maximum flow depth

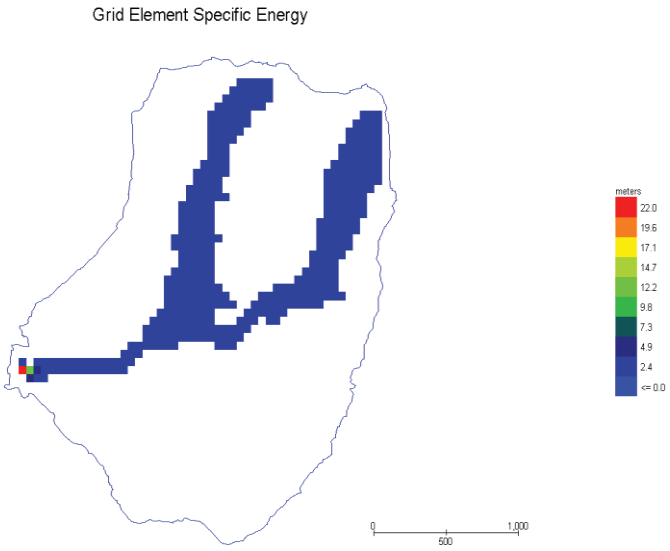

Figure 67 debris flow specific energy

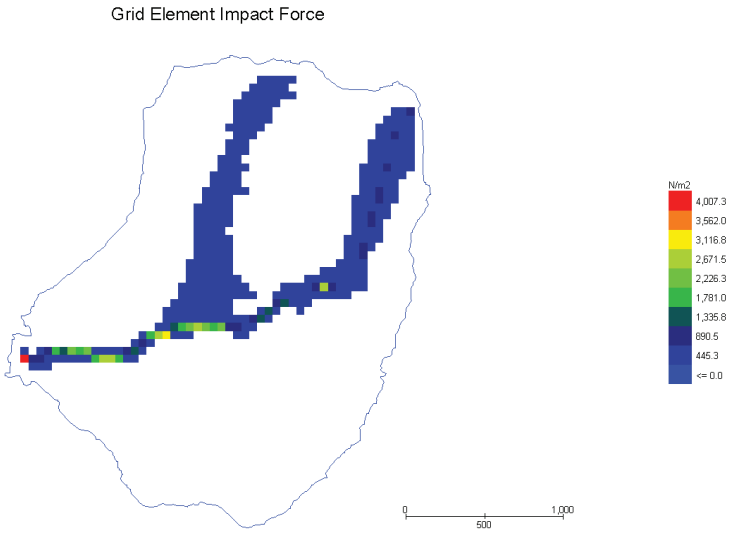

figure 68 debris flow impact force

C, for sediment concentration of 0.6, the velocity (see fig69), the depth (see fig70), the specific energy (see fig71) and the impact force (see fig72) are shown below

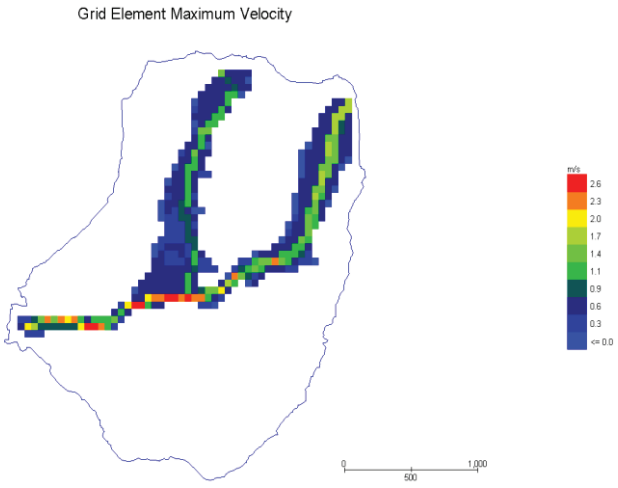

Figure 69 debris flow velocity

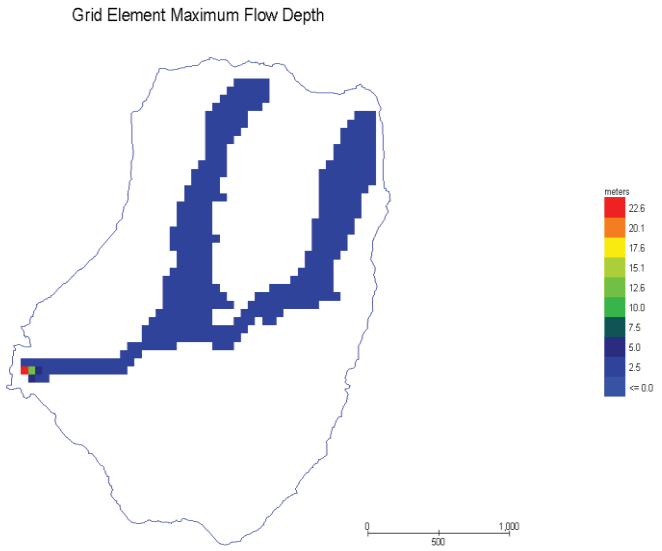

figure 70 debris flow depth

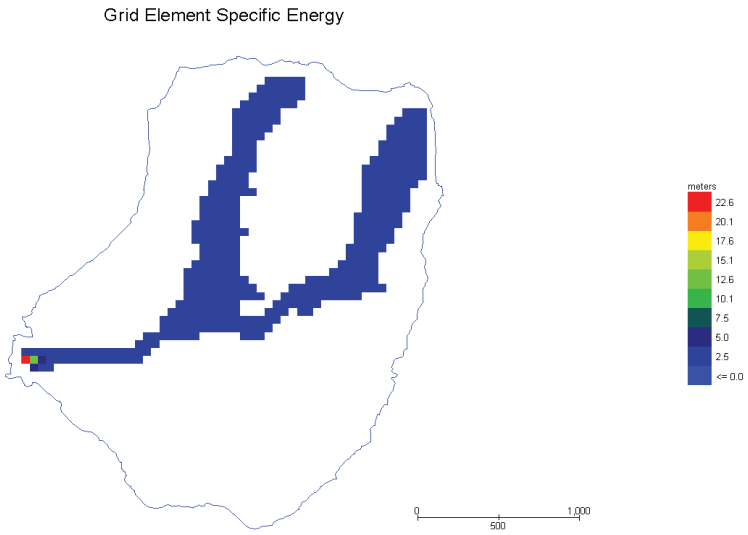

Figure 71 debris flow specific energy

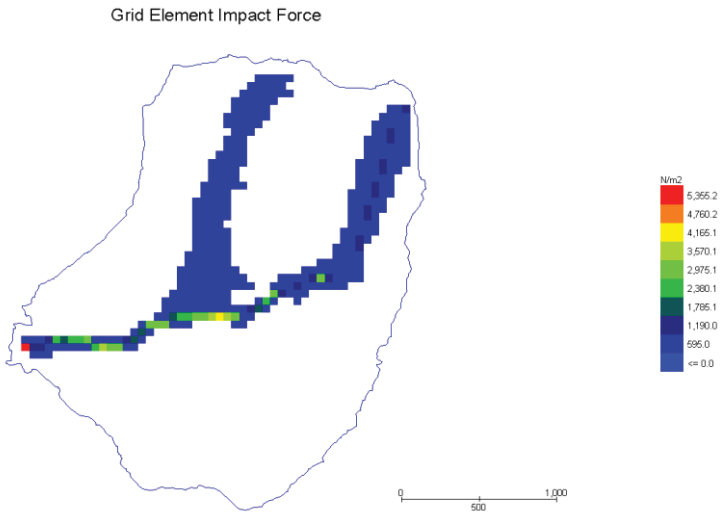

figure 72 debris flow impact force

D, for sediment concentration of 0.7, the velocity (see fig73), the depth (see fig74), the specific energy (see fig75) and the impact force (see fig76) are shown below

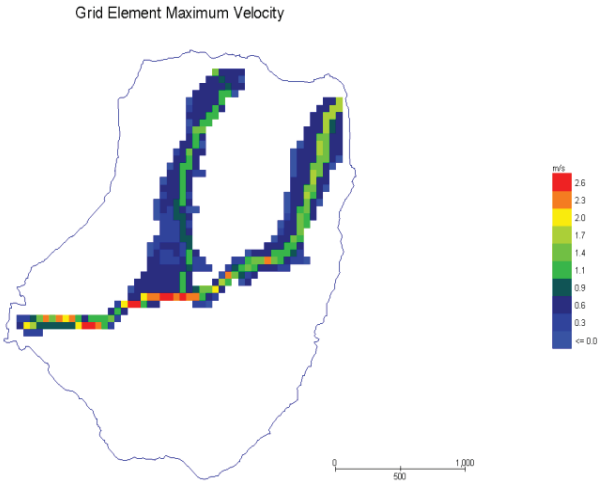

Figure 73 debris flow velocity

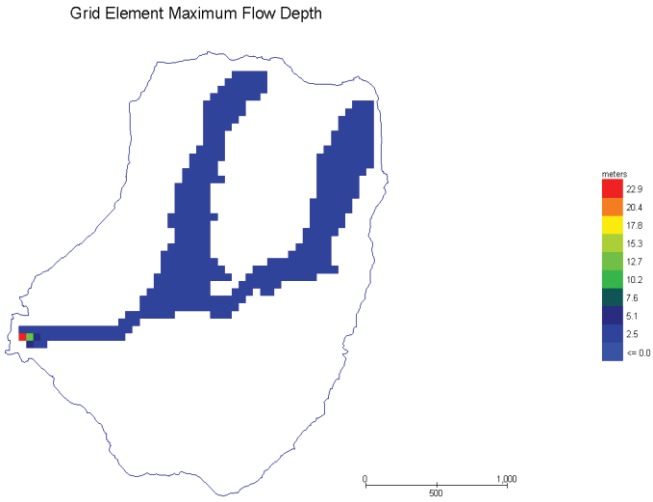

figure74 debris flow depth

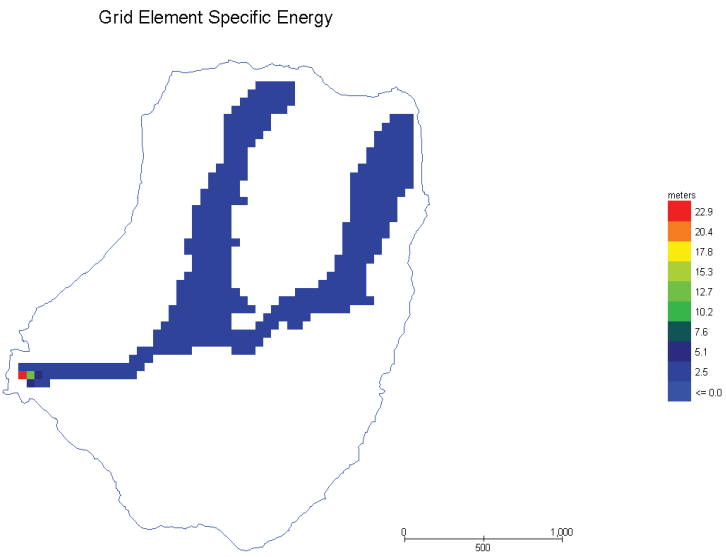

Figure 75 debris flow specific energy

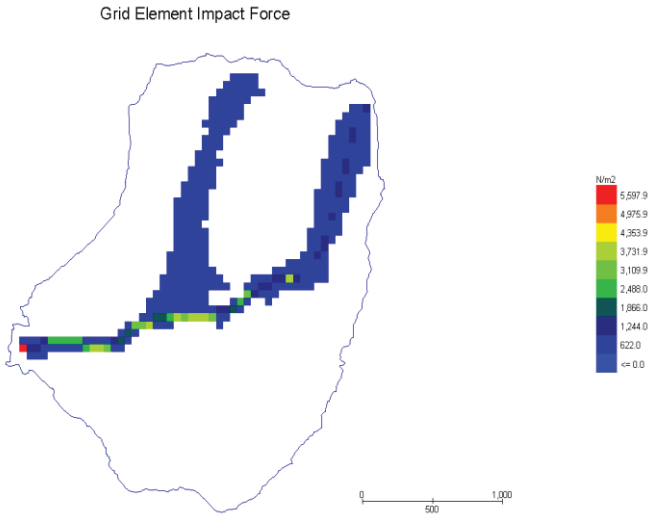

figure76 debris flow impact force

The results of the sensitivity analysis of the sediment concentration by volume is shown above (see table 14), it can be seen that an increase in the value of the concentration leads to an increase in the debris flow total volume, impact force which is a magnitude (intensity) factor. This is in agreement with the FLO-2D manual (2007) which state that the concentration is very important in describing the magnitude of an event. Increasing the concentration from 0.3 to 0.7 lead to an increase in the impact force from 3,554.5 N/m2 to 5,597.9 N/m2 respectively (see table 14, fig64 and fig76). However, the increase in concentration means increases the kinematic energy of the fluid matrix activities since the fluid will have gain more weight from the sediment particles. The impact force tends to be higher at the confluence of the catchment where the two main sources of debris flow in the catchment originate from as a result of

the combined effect at that point. The area of inundation also increase a little because they will be more sediment to be deposited along the channel, bank and at the debris flow fan.

With increase in concentration, the velocities at some point remain constant at 2.9m/s (see table 14), then drop to 2.8m/s when the concentration was 0.5. (fig 57) and remain constant again with further increase in concentration (see fig61, fig65, fig 69 and fig73).The reason why further increase in concentration, velocity generally decrease this is because the properties of the fluid matrix has change and become heavier with increasing concentration thereby decreasing the velocity. The debris flows velocities tend to be are higher mainly at the channel after the confluence (see fig61, fig65, fig69, and fig73) due to the narrowing of the channel at that point thereby increasing the fluid particle contact/collision leading to higher velocity. The debris flow depth and the specific energy vary slightly with increase in concentration (see table 14).

5.6.2 Sensitivity to viscosity parameters

Viscosity (poises) parameter is one of the sensitive parameters in debris flow propagation. FLO-2D routes debris flow as a fluid continuum by predicting viscous fluid motion as a function of sediment concentration. (FLO-2D manual, 2007). Debris flows are dominated by viscous stress and constitute a very different phenomenon than those processes of suspended sediment load and bedload in conventional sediment transport. Viscosity and yield stress varies with sediment concentration (FLO-2D manual, 2007). See more in chapter 4.3.4 of this thesis. However, due to lack of viscosity data and rheological analysis of the debris flow materials from the catchment, the empirical relationship (coefficient) derived and defined by laboratory analysis/experiment (O' Brien and Julian, 1998: see table 5) were used in this research and in caring out the sensitivity analysis.

All other parameter (yield stress, sediment specific gravity, "K" Laminar flow resistance) were held constant in including the sediment concentration (0.5) while testing the changes in viscosity parameters to area extent, velocity, depth, specific energy and the impact force of the debris flow respectively.

Table 15: Results of sensitivity analysis to viscosity parameters

	α = 0.00136 β =28.1	**α=0.00283** **β=23.0**	α=0.0538 β=15.5	α =0.0648 β=6.20
Total volume(m3)	161,355	**161,350**	161,349	161,349
Max velocity (m/s)	2.8	**2.8**	2.8	2.8
Average depth (m)	11.2	**11.2**	11.2	11.2
Average specific Energy (m)	11.2	**11.2**	11.2	11.2
Max impact force (N/m2)	4,609	**4,462**	4.549	4,757

A, for viscosity coefficient of α=0.0648 and exponent β=6.20, the velocity (see appendix 5 fig1), depth (see appendix 5 fig 2), the specific energy (see appendix 5 fig3) and the impact force (see appendix 5 fig 4). The reader

should note that results (figures) of sensitivity analysis to viscosity parameters and the yield stress parameters are shown on appendix 5 of this thesis.

B, for viscosity coefficient α=0.00283 and exponent β =23.0, the velocity (see appendix 5 fig5), the depth (see appendix 5 fig6), the specific energy (see appendix 5 fig 7) and the impact force (see appendix 5 fig 8).

C, for viscosity coefficient α=0.00136 and exponent β=28.4,
The velocity (see appendix 5 fig 9), the depth (see appendix5 fig 10), the specific energy (see appendix 5 fig11) and the impact force (see appendix 5 fig12).

D, for viscosity coefficient α=0.0538 and exponent β=14.5, the velocity (see appendix 5 fig 13), the depth (see appendix 5 fig 14), the specific energy (see appendix 5fig 15) and the impact force (see appendix 5 fig 16.) Also see table 15

Changing the viscosity coefficient and exponent while keeping the concentration constant (and other parameters) has shown little changes on the total volume of the debris flow (see table 15). The researcher observed that, there were no changes in the area extent of the debris, the flow depth (see table 15), velocity (see table 15) and specific energy (see table 15).The exact reasons for this are not known by the researcher, maybe because the sediment concentration was kept constant. In addition, the literature stated that the viscosity parameters vary with changes in concentration (FLO-2D manual, 2007). This was not tested in this research due to limited time and the focused of this research mainly at reconstructing the debris flow event of 2010.

However, there it was observed that increasing or decreasing the viscosity parameters caused some little changes in the impact force of the debris (see table 15). Although, the relationship of the viscosity parameters to the impact force was not known by the researcher. It may be interesting topic for research in the future as this research focused mainly at attempting to reconstruct the August 14th debris flow using mostly literature value (due to lack of adequate data/field measurement/laboratory analysis of geotechnical data).

5.6.3 Sensitivity to yield stress

Yield stress and Viscosity varies with sediment concentration (FLO-2D manual, 2007). See more in chapter 4.3.4 of this thesis. All other parameter (viscosity, sediment specific gravity, “K” Laminar flow resistance) were held constant in including the sediment concentration (0.5) while testing the changes in yield stress parameters to volume /area extent, velocity, depth, specific energy and the impact force of the debris flow respectively. The results are shown in table 16

Table 16: Result of sensitivity analysis to yield stress parameters

	α= 0.0345 β =20.1	**α= 0.0765** **β =16.9**	α =0.152 β =18.7	α =2.72 β=10.4
Total volume (m3)	161,350	**161,350**	161,349	161,354
Max velocity (m/s)	2.8	**2.8**	2.8	2.8
Average depth (m)	11.2	**11.2**	11.2	11.2
Average specific Energy (m)	11.2	**11.2**	11.2	11.2
Max impact force (N/m2)	4,444	**4,490**	4,533	4,565

A, for yield stress coefficient α=0.0765 and exponent β=16.9: the velocity (see appendix 5 fig17), the depth (see appendix 5 fig 18), the specific energy (see appendix 5 fig 19) and the impact force (see appendix 5 fig 20). Also see results on table 16.

B, for yield stress coefficient α =0.0345 and exponent β =20.1: the velocity (see appendix 5 fig21), the depth (see appendix 5 fig22), the specific energy (see appendix 5 fig23) and the impact force (see appendix 5 fig 24). The results are also shown on table 16.

C, for yield stress coefficient α =0.152 and exponent β =18.7: the velocity (see appendix 5 fig 25), the depth (see appendix 5 fig 26), the specific energy (see appendix 5 fig 27) and the impact force (see appendix 5 fig28). The results are also shown on table 16.

D, for yield stress coefficient α =2.72 and exponent β =10.4: the velocity (see appendix 5fig 29) the depth (see appendix 5 fig 30), the specific energy (see appendix 5 fig31) and the impact force (see appendix 5 fig 32). However, the results are also shown on table 16.

Similar explanation also holds for the yield stress parameters as see from the results on table 16 above. Increasing or decreasing the yield stress coefficient and exponent while keeping the concentration constant (and other parameters) , shows increase in the total volume of the debris flow (see table 16). The results also shows that there were no observed changes in the area extent of the debris, the debris flow depth (see table 16), velocity (see table 16), specific energy (see table 16).

The exact reasons for this are not known by the researcher, maybe because the sediment concentration was kept constant. In addition, the literature stated that the yield stress parameters vary with changes in concentration (FLO-2D manual, 2007). This was however, not tested in this research due to limited time and the focused of this research mainly at reconstructing the debris flow event. However, there it was observed that increasing or decreasing the yield stress parameters caused some noticeable changes in the impact force of the debris flow (see table 16).

However, the relationship of the yield stress parameters to the impact force was not known by the researcher. It may be interesting topic for research in the future as this research focused mainly at attempting to reconstruct the August

14th debris flow using mostly literature value (due to lack of adequate data/field measurement/laboratory analysis of geotechnical data).

5.6.4 Sensitivity to manning's n

Debris flow behavior is a function of the fluid matrix properties, channel geometry, slope and roughness (FLO-2D manual, 2007).

All other parameter (viscosity, yield stress, sediment specific gravity, "K" Laminar flow resistance) were held constant in including the sediment concentration (0.5) while testing the changes manning's n to volume/ areal extent, velocity, depth, specific energy and the impact force of the debris flow respectively. See results on table 17

Table 17: Results of the sensitivity analysis of the friction coefficient

	0.005	**0.04**	**0.15**	**0.250**
Total volume (m3)	161,352	**161,350**	161,357	161,376
Max velocity (m/s)	2.6	**1.8**	1.1	0.8
Average depth (m)	11.2	**11.1**	10.5	9.7
Average specific Energy (m)	11.2	**11.2**	10.5	9.7
Max impact force	4,058	**2,211**	1,136	799
Max area of inundation (m2)	955000	**950000**	937500	932500

A, for manning's n=0.005, the velocity (see fig77), depth (see fig78), specific energy (see fig79) impact force (see fig80)

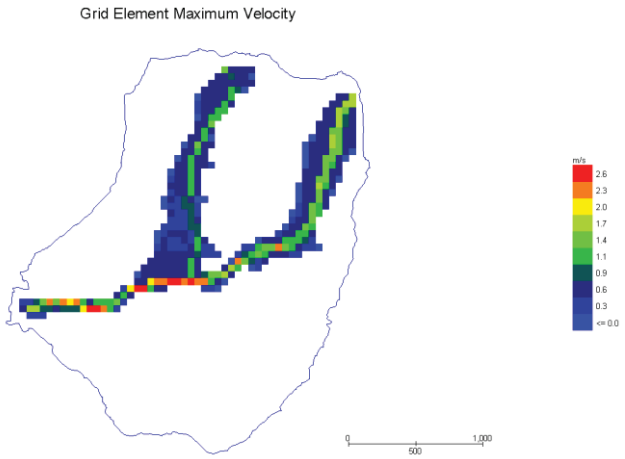

Figure77 debris flow maximum velocity

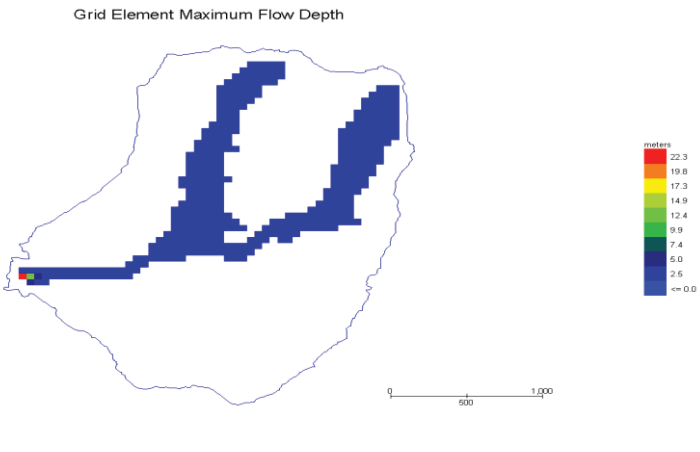

figure78 debris flow maximum flow depth

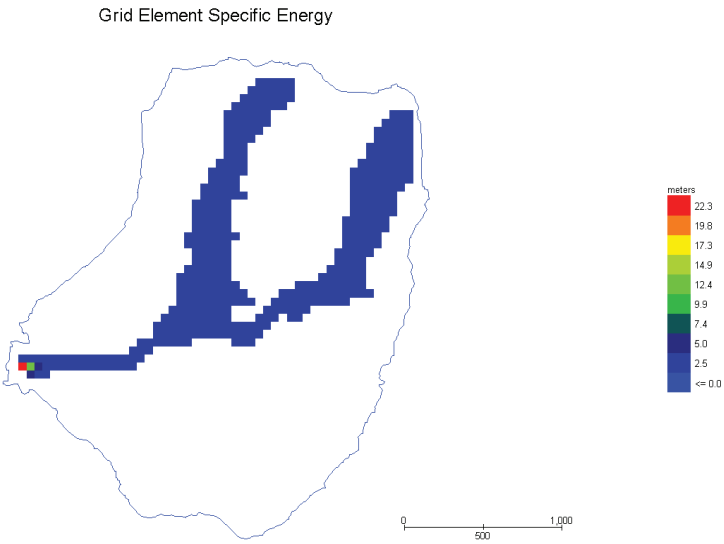

Figure 79 debris flow specific energy

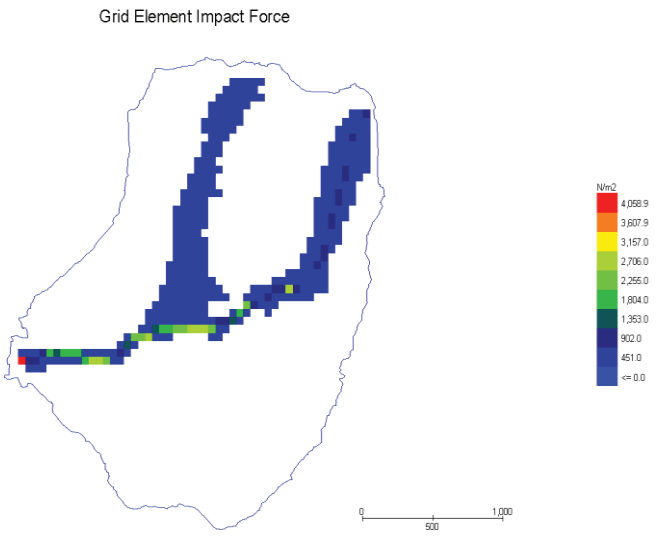

figure 80 debris flow impact force

B, for manning's n =0.04, the velocity (see fig81), depth (see fig82), specific energy (see fig83) impact force (see fig84) and the area of inundation are presented below:

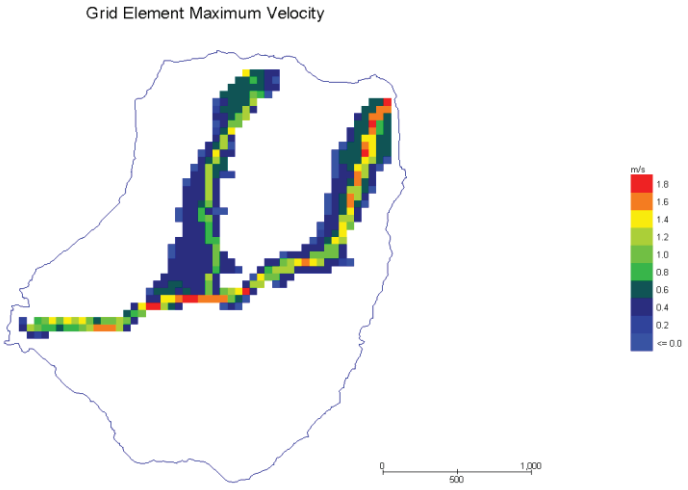

Figure 81 debris flow maximum velocity

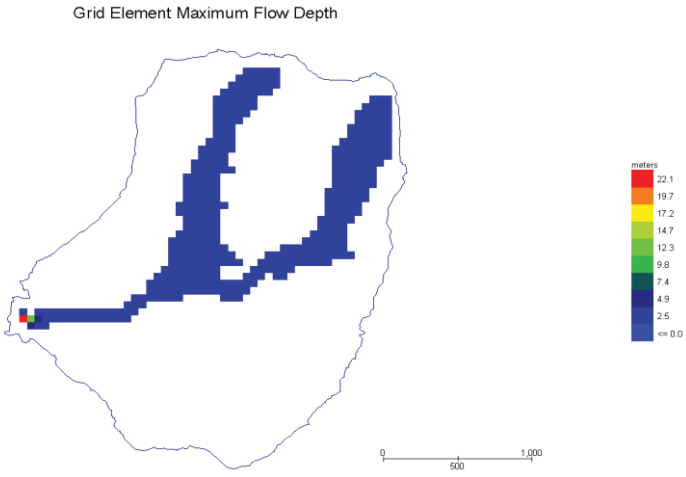

figure 82 debris flow maximum depth

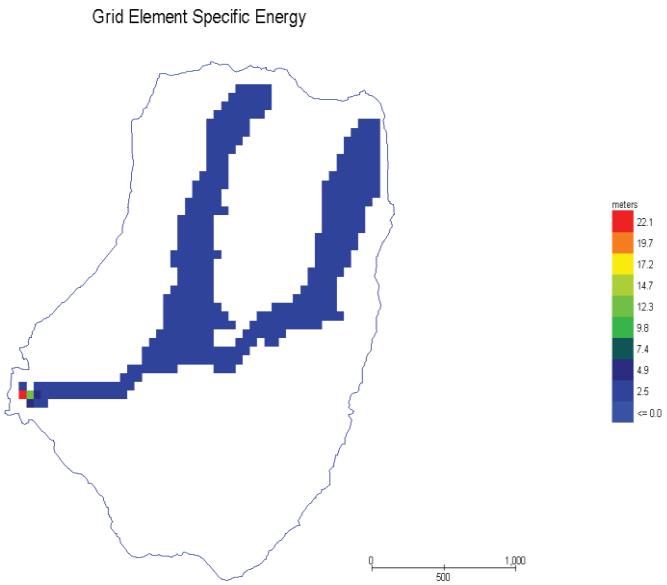

Figure 83 debris flow specific energy

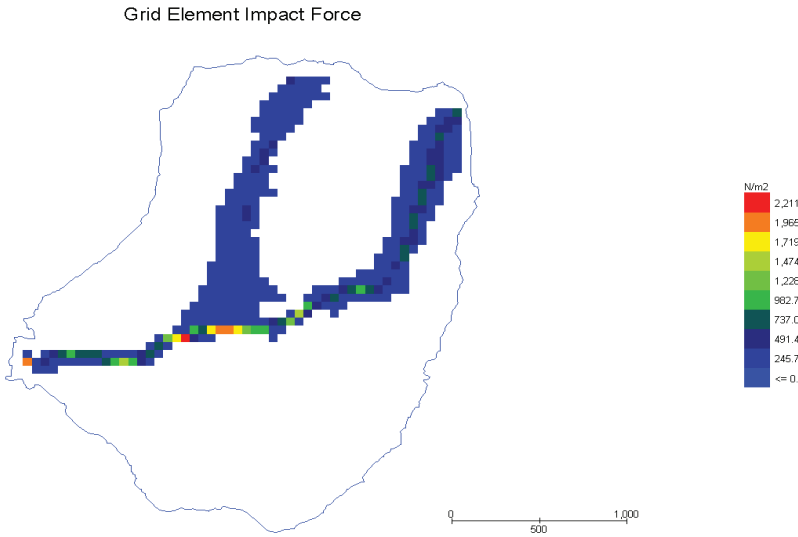

figure 84 debris flow impact force

C, for manning's n =0.15, the velocity (see fig85), depth (see fig86), specific energy (see fig87) impact force (see fig88) and the area of inundation are presented below

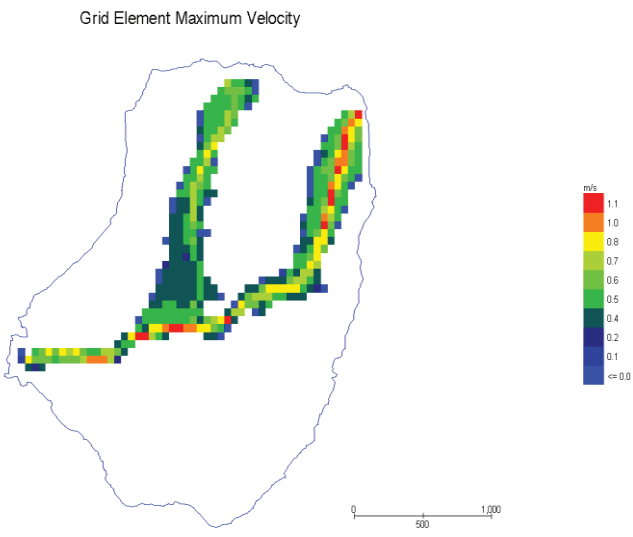

Figure 85 debris flow maximum velocity

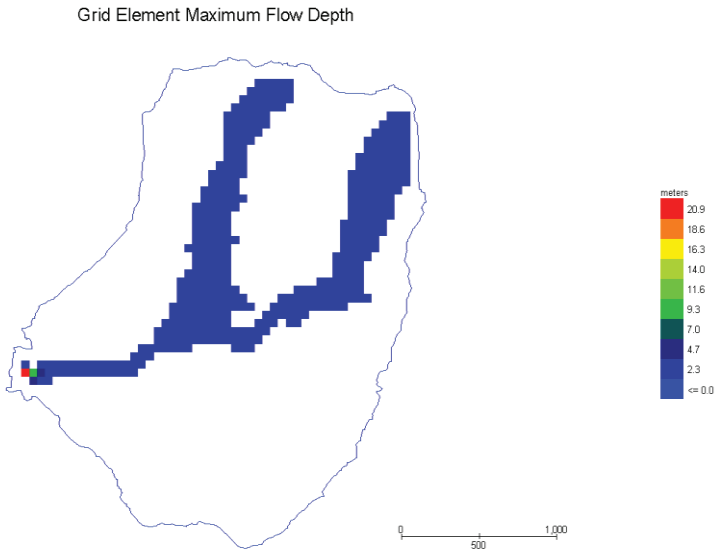

figure 86 debris flow maximum depth

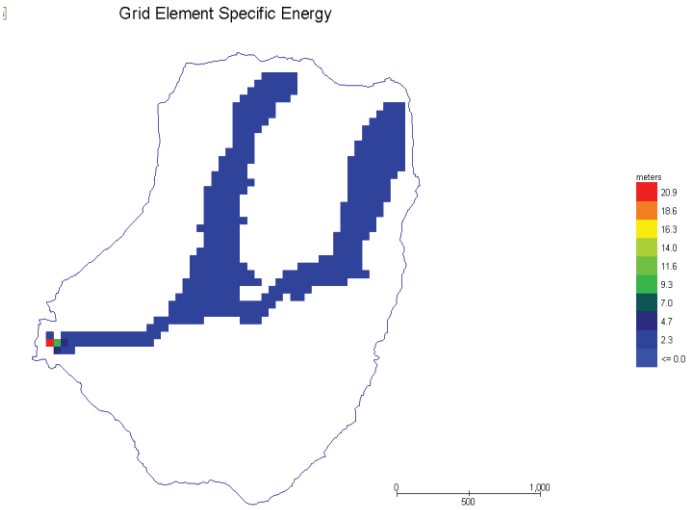

Figure87 debris flow specific energy

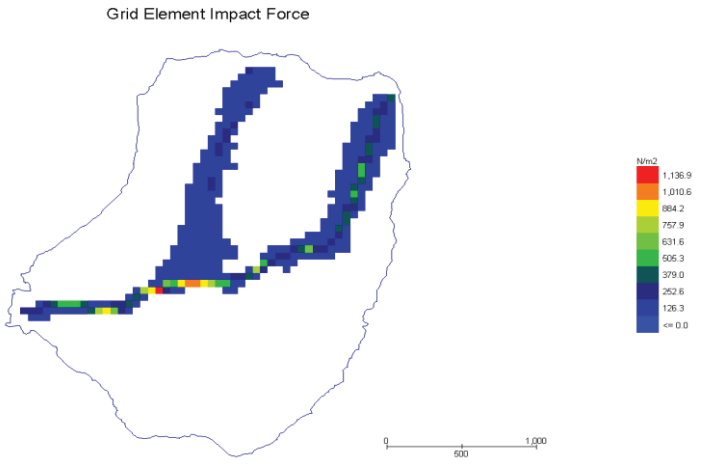

figure88 debris flow impact force

D, for manning's n =0.250, the velocity (see fig89), depth (see fig90), specific energy (see fig91) impact force (see fig92) and the area of inundation are presented below

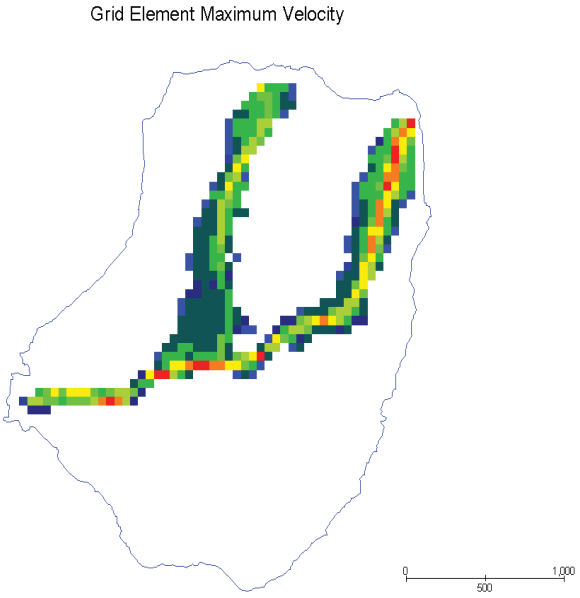

Figure 89 debris flow maximum velocity

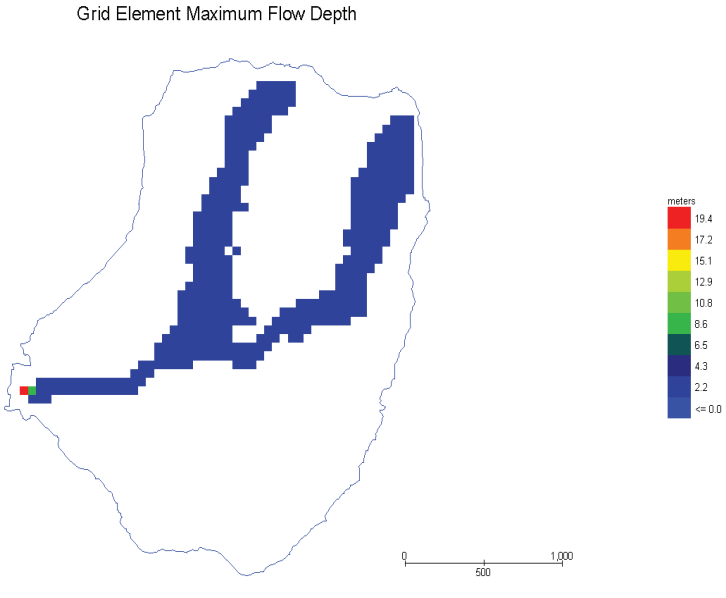

figure 90 debris flow maximum depth

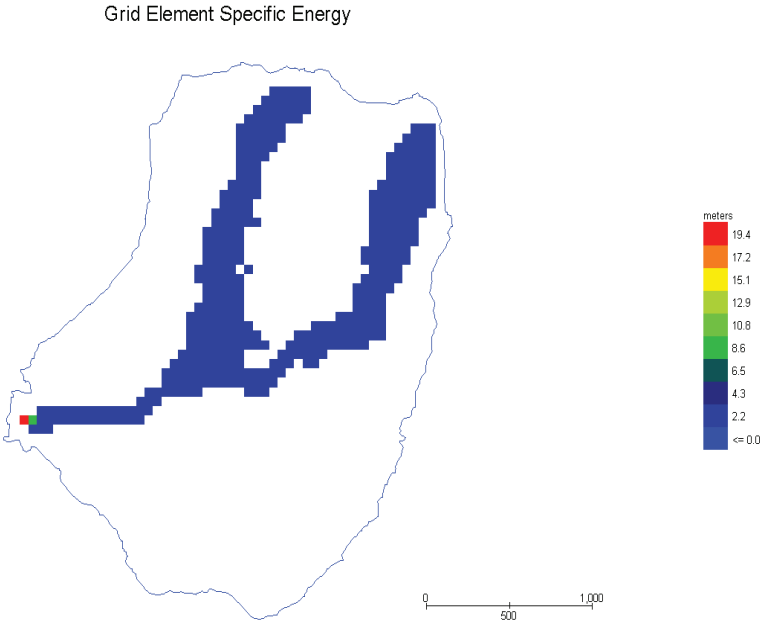

Figure 91 debris flow specific energy

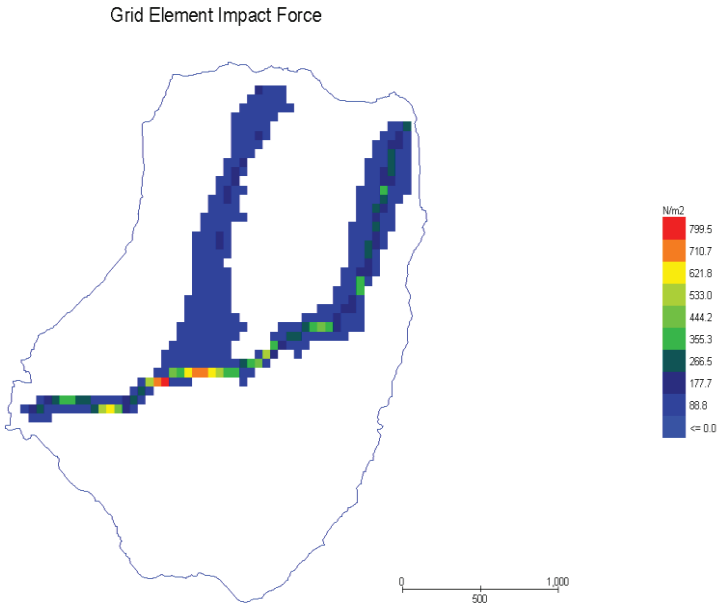

figure 92 debris flow impact force

The results in table 17 shows an increase in the manning's n (friction coefficient) cause decrease in the debris flow velocity see (fig77, fig81, fig85, fig89), decrease in depth of flow (fig78, fig82, fig86, fig90) and also a decrease in the impact force (a measured of hazard intensity) see fig80, fig84, fig88 and fig92. This is expected, due to the increase in the basal friction of the flow with increase in the friction coefficient. The total volume of debris deposit increased with increased in friction coefficient (see table 17) this may be because with low velocity, deposition take places.
The most sensitive parameter to the friction coefficient is the velocity of flow, followed by the impact force of the debris. The specific energy of the debris flow is also reduced with increased in the friction coefficient (see fig79, fig 83, fig87, fig 91 and table 17).

5.7 CALIBRATION

Calibration is an important part of modeling of debris flows or any other type of modeling trying to spatially replicate past events or predicts future ones. The aim of calibrating models is to adjust the parameters of the model so that the modeled results replicate real observed events and thus determine the range of values of the parameters.

The August 14th, 2010 debris flow event was calibrated with the parameters on table 13 and the bolded column on table 15, table 16 and table 17 by doing a back analysis of the 2010 event.
In carrying out the calibration, the sediment concentration of 0.5 was used because with higher concentration, the flow tends to become more of landslides (see fig 6). Also, at 0.5 concentrations, the velocity represents some kind of threshold (see table 14)

Due to lack of well documented modeling results (literature) and limited field measurement of the Hongchun debris flow event of 2010, a back analysis of the debris flow event, was carried out using the total debris flow volume of 400,000 m3 from interview (the only available information of the 2010 event). The calibrated volume from the FLO-2D model was 161,350 m3. This result represents 40.3% reconstruction of the August 14 debris flow event. The reader should note that, the low debris flow volume (161,350 m3) may be as a result of the limitation of FLO-2D model not including other important debris flow process like entrainment. Otherwise, the result may have been different.

However, compared with the Hongchun debris flow event of July 2011, the model reconstructed 80.7% of the total debris flow event (neglecting the effects of check-dams) see table 18. The reader should note that, the model results presented here in this research are preliminary results of the 2010 debris flow events in the Hongchun catchment. This is mainly because there have not been any other modelling results published about the Hongchun catchment to compare results with adequately.

Table 18: comparison of calibrated results to July 2011 event

	Volume (m3)	Calibrated volume (m3)	Reconstructed %
August 14th, 2010 event	400,000	161,350	40.3
July 21, 2011 event	200,000	161,350	80.7

In summary, I learnt that, the FLO-2D model is a capable tool for modelling debris flow irrespective of the numbers of initiation zone for any particular catchment. However, it does not incorporate entrainment in the process. This agrees with Abulohom et al (2001) who reported that there is no universal model.

6 DISUSSION, CONCLUSIONS AND RECOMMENDATION

6.1Discussion

6.1.1 Data collected and analyzed

Acquiring soil properties and rainfall data for modeling proved difficult. Firstly, the Ksat values were very high (an average of 396mm/h) and based on the assumption that the small ring used and the subsequent laboratory results were accurate. The soil sampling sizes (24 soil samples) were too small to give a true assessment. It can also be argued that the homogenous Ksat used in the modeling may not represent true catchment reality and the general conditions of the surface. However, the reversed argument may also be possible.

Another problem of concern was the loose nature of the soil and the very rugged nature of the catchment that made sampling very difficult and restricted to areas where they are accessibility. This also made it difficult to sample soil for direct shear test and other geo-technical parameter tests. The researcher cannot say for sure if, the transportation (or may be compaction) of the soil samples to the laboratory in Chengdu, China and the ITC, Laboratory in the Netherlands may have any effects on the laboratory determined results rather than field determinations (especially for the Ksat).

The porosity and the initial moisture content were moderately high. It may be inferred that the soil texture which is a function of the grain size distribution plays a very important role in the soil physical properties. The soil texture is fairly homogenous with pockets of clay mapped in few locations in the catchment. This may be as a result of the weathering process of the main granitic basement rock underlying the whole catchment.

Soil depth was not well determined and may not represent the true situation of the catchment. Although some concerted effort was made to make soil depth measurement at well exposed locations. However, the absence of road cuts, rugged nature of the catchment and the exposed bedrock made auggering difficult. In addition, effort was also made to understand the processes, it was difficult to ascertain even from the field observation the appropriate layer approach to use in the LISEM model. However, the Green and Ampt one layer was used although (trial and error),the suitability was not tested and verified.

The three days, hourly rainfall data (August 12-14th, 2010) see fig39 and table 8 collected from the Yinxiu rainfall station, was courtesy Prof Tang of the Chengdu University of Technology, China. All other efforts to collect a reasonable rainfall data say atleast two years rainfall data did not yield any result. The cumulative rainfall of 219.8 mm was used in LISEM rainfall runoff model while the discretized percentage of the cumulative rainfall was used in the FLO-2D model in line with FLO-2D model requirement and parameterization.

6.1.2 Runoff modeling and infiltration pattern

The results of the LISEM model shows that the three days rainfall intensities used in the modeling produced a very little runoff. Since this was the only available rainfall data, it really has to be optimized and this lead to the assumption that this little runoff (203mm) alone could not have led to the debris flow initiation in the catchment. Thus, led to the zero infiltration assumptions used in the FLO-2D model. This idea was supported by Van asch, Van Westen and

Quan luna in a joint personal communication to produce runoff which may have triggered the debris flows combined with antecedent rainfall. This means that, prior to the rainfall, the soil was already saturated by antecedent rainfall and combined with the little runoff triggered the debris flow in the catchment. However, this assumption is subject to further verifications and investigations but represent the preliminary conclusions of this research. The groundwater effect in the debris flow initiation was not considered in this research due to and may be a very good topic for future research.

Furthermore, the (Lisem result) values resulting from the sensitivity analysis of Ksat on the runoff are presented on table 12. It shows an inverse relationship with peak discharge, total volume and runoff output. Rainfall, interception and mass balance error remained constant. However, the more positive side of Ksat, there seems to be little influence. There seems to be a limiting threshold for the Ksat parameter. The lowering of Ksat follows after a study by Hessels et al (2003) who highlighted that field measurements of Ksat tends to be higher than those the model uses for calculations hence the emphasis on reducing Ksat. Ksat values affect the peak and shape of hydrograph as observed (see fig 52 and fig 53)

The LISEM model was also used to map the infiltration pattern see fig 54. This was done in order to see the spatial infiltration pattern across the catchment since the might reveal areas with high water intake and subsequently give an idea of areas that might be unstable (high chance of soil failure). The model reveals almost a uniform infiltration pattern for the catchment. This might be due to the uniform texture and geology of the catchment. However, it was observed from the Lisem cumulative infiltration result that , the infiltration tends to be a little more on the slopes and the upper parts of the catchment that were mapped geomorphologically as the source areas for the debris (see fig36 and fig37).

6.1.3 Landslides inventory

An intensive landslides mapping of the Hongchun catchement was undertaken with respect to the research question that states that, are the landslides bodies the potential source of debris responsible for the debris flow in the catchment?. However, this intensive mapping of landslides inventory was carried out in the catchment based on visual image interpretation/inspection. A total of 41 landslides were mapped in the catchment and their attribute determined, the scarp and the bodies of the landslides were also mapped see fig20, the degree of activity were also determined (see fig 21); whether it was active, dormant or re-activated landslides were mapped accordingly. Also, the landslides age were mapped and charcaterized as new and old landslides depending on how fresh the surfaces are. The new landslides were easily mapped in the catchment because of their fresh surfaces and fresh deposits of debris while the old ones have been overgrowned or have vegetation growing in them.

Based on the geomorphological mapping, field observation and image interpretations it may be concluded that the landslides bodies generates the debris that led to the debris flow in the catchment. The presence of large debris from these landslides are still seen everywhere in the catchment and this further confirms the research objectives that the landslides bodies are the potential source of the debris flow in the catchment.
However, hill slope failure, river/channel bank scour and channel bed sediment can also be potential sources of debris (FLO-2D manuals, 2007) for debris flow but was not the case of the Hongchun catchment as the field evidence supported. To further support the point that the landslides bodies were the potential source of debris, the historical information collected through interviews confirmed that, they have not been any record of debris flow

activities in the catchment prior to the co-seismic landslides induced by the May 12th, 2008 earthquake that hit he Sichuan province.

6.1.4 Field estimation of debris volume

The evaluation of the landslides volume was based on field observation of the deposit volume, detachment area, deposit height, deposit base, morphology and geometry. The landslides volumes were then classified based on threshold determine during reconnaissance survey of the catchment in a manner similar to Cardinali et al, 2002 (See details in chapter of 4.4.3).

The resulting total estimates of all the three categories of the landslides volume is 1,675,000 cubic meters. (See appendix 4)These give a very rough idea of the total volume of debris from the landslides in the catchment. The total estimated volume of the landslides volume from the field observation did not agree with the figure gotten from the field interview with Mr Wang, 2.25 million cubic meters of debris is still left in the catchment. This difference of 675,000 cubic meters may be due to differences in approach and the method used in the estimation of the landslides deposit volume. However, the details of Wang's approach are unknown.

Also, they might be a some underestimation or over-estimation of the volume by this approach. However, the approach used in this research was prompted by lack of good DEM after the earthquake but gave a rough idea of the volume of debris resulting from the earthquake induced landslides. In a data poor environment it may be very useful. Field estimations of landslides volume is not entirely a new concept, (Cardinali , et al., 2002) .

6.1.5 Interviews

In order to get the debris flow historical information of the catchment and to understand the risk perception of the community to the multi-hazard (earthquake, landslides, debris flow and flooding), interviews were conducted within the catchment and also among 15 randomly selected adults on the street. It was found out that the total debris left in the catchment after the May 12, earthquake, 2008 was estimated to be 3million cubic meters. This was one of the reasons that prompted the researcher's action in 6.1.4. The interview also revealed that on the 14th of August, 2010, 400,000 cubic meters of debris flow was recorded. On the 3rd of July, 2011 a debris flow event of 200, 000 cubic meters occurred after a rainfall of 130mm. This was also followed by another debris flow event of 50,000 cubic meters on the 21st of August, 2011 after a rainfall of 150mm. this implies that about 75% of the debris is still left in the catchment waiting to be mobilized.

The catchment has witnessed 3 debris flow event in two years. This means that the debris flow in the catchment may have a return period of 1 year (assumptions based on the interviews). The rainfall that has been triggering the debris flow is still within the normal rainfall for the region. Based on the present statistics of the assumed 1 year return period of the debris flows in the Hongchun catchment, based on the interviews, the geomorphological mapping of the catchment and the attempted quantification of the debris left in the catchment that, they may be more debris flow in the catchment in the coming periods even worse in the event of extreme weather event.

The earthquake of May 12, 2008 may have created disequilibrium (landslides/slope instabilities) in the catchment that led to the 3 million cubic meter of debris (from interview) generated from the landslides body see fig21. However, as

the catchment moves to attain the equilibrium, the catchment will keep finding more convenient ways of pushing out the debris (in the form of debris flow). This means that there will be more debris flow in the future in the catchment until the materials left in the catchment are completely removed.

The present of the checks dams (protective measures see fig23) and other embankments in the catchment as mapped (see fig25, and fig 26), may only reduce the debris flow volume but not stop the debris flow from occurring (this was confirmed from field mapping and interview). The effectiveness of the check dams in the overall debris flow management was not considered in this research but however, it might be a very good research topic in the future.

6.1.6 Debris flow modeling

The basic principles of debris flow modeling were broadly discussed in part of chapter 2.7and chapter 4.3.2, 4.3.3 respectively. Modeling debris flow as a complete phenomenon has been a difficult and challenging task (see chapter 2 of this thesis). However, some fundamental assumptions were made and used in modeling the Hongchun debris flow event which may, to a large or small extent, differ from the reality of the events viz:

First and foremost, it was assumed in the FLO-2D model that, the 10m resolution DEM (from contour interpolation) is accurate, plausible and depicts the channels/ topography of the Hongchun catchment very well. This may be far from true despite the removal of pits or sink holes from the DEM. If, the DEM is not accurately depicted by the DEM, the modeled flow may greatly be affected (Hussin, 2011). A LIDAR DEM can possibly give a more accurate depiction of the topography of the entire study area including the flat areas on the debris fan. LIDAR can acquire high density 3D terrain surfaces with higher accuracy for detailed representation of the study area Liu et al (2007). However, such a DEM was not available for this research work.

It is important to note that a DEM depicts the topography at a particular point in time. The actual topography may change over a period of time by deposition, erosion (soil), Landslides, earthquakes and erosion of subsequent debris flow or by human modifications to the channel, such as the construction of dikes along channel(Hussin, 2011). This research has tried to incorporate these changes.

However, the effect of checks dams in the upper and lower part of the catchment is very difficult to incorporate in the model. Assumed that this research has a question that says: Will the check dams hold when the debris flow occurs or will they be breached? The answer would have been: the check dams will hold when the debris flows occurs (from fieldwork and interviews: since they have pile foundation are designed to withstand an earthquake above 8.0 magnitudes on the Richter scale). But as to when breached? , Might be of future research interest. Since the FLO-2D model is capable of modeling impact force of debris flow, it might also be of future research interest to see how the stability of the check dams will be affected by the impact force of the debris flows. This was however not considered in this research.

6.1.7 Initiation zone

In this study, it was found that, the 2010 event initiated in two different areas contrary to Tang et al, 2011 who identified one initiation area. The models were chosen from these two main initiation zone based on susceptibility assessed from Geomorhological field mapping (see fig36 and fig37) and Tang (2011) , leaving out the areas determined to be less susceptible to the initiation of debris flows. FLO-2D model requires the identification of the susceptible areas.

A thorough susceptibility analysis of the slopes in the upper part of the catchment can give more accurate information on future initiation zones in the study area. Infinite slope model in the PCRaster environment would have been a very vital tool to explore the stability of the slope in the catchment but due to limited time, it was not used in this research. However, such a model would produce a detailed susceptibility map that can be used in the future as a basis for modeling debris flow or other mass movement in the catchment.

In addition, the prediction of future initiation zones and especially initiation volume, are extremely difficult to model. This thesis did not look into the uncertainty in initiation modeling but other studies (e.g.Kuriokose et al,(2010)) have shown that the initiation also has a very high degree of uncertainty. Especially the relationship between return periods of triggering events (rainfall duration and intensity) and initiation volume is still a largely unsolved problem , partly due to the unavailability of detailed spatial information on material properties (strength and depths of soil) and detailed rainfall data as reported by Hussin (2011). It should be noted that FLO-2D does not do entrainment. However, this is an important part of the debris flow process. The entrainment of material in the transport zone is extremely important to the production of the total deposit volume mostly on the debris flow fan. Thus, the entrainment volume is mostly larger than the actual initiation volume (Hussin, 2011).

6.1.8 Sensitivity analysis

In the to the sensitivity analysis , the effects of each parameter on the sensitivity of the total volume, velocity of the debris flow, the debris flow height, specific energy and the impact force depends on whether parameter value is being increased or decreased with respect to a standard value .

The parameter that shows the highest effect on the total volume is the concentration see table 14, followed by the coefficient of friction see table 17. The parameter that the show the highest effect on velocity of the debris flow is the friction coefficient see table 17. This followed by the increase in the sediment concentration. The viscosity and the yield stress parameters did not show any effects on the area extent of the debris flow.

The intensity parameter of the debris flow (impact force) is the most sensitive to concentration of the sediment. An increase in the value of the sediment concentration shows an increase in the debris flow impact force. However, a decrease in the friction coefficient shows an increase in the impact force. The viscosity and yield stress parameter did not show any significant (noticeable) effect on the impact force.

The viscosity and yield stress parameters has no effect on any of the parameter used in this research. However, FLO-2D manual, 2007 stated that these two parameters vary with sediment concentration. The debris flow height and the specific energy are mostly affected by the same parameter

6.1.9 Calibration

The application of calibration criteria in a back analysis of the debris flow events of the Hongchun catchment have shown how useful they are in replicating the debris flow similar to the august 14th, 2010 event in the Hongchun catchment. In this research, 40.3% of the 2010 event was reconstructed see table 18.

Furthermore, the use of literature values instead of field determined data also may also have short comings in the model results as this may be largely or under-estimated the catchment reality.

In addition, the assumptions used in the FLO-2D modeling (saturated conditions) of the Hongchun catchment may be far from true catchment situation. But however, the results of this research are preliminary results of the debris flow event of the Hongchun and therefore will be a very useful future guide for further research in the catchment.

It must also be mentioned that the calibration have been conducted under an environmental settings that may have been altered since the 2010 event. For instance, if the channel geometry were used in the calibration, it will not be identical to the 2010 geometry (a lot of changes would have taken place). Therefore, it cannot be expected that the debris flow will have the exact same area extent, flow depth, velocity impact force and run-out volumes (161,350 m3 : calibrated volume). The effect of channel widening might be obvious, where the model has a wider flow and deposit inside the channel (field observation).

6.2 Conclusions

With respect to the research objectives and the subsequent research questions asked (chapter 1) in order to understand the hydrological and hydraulic analysis of the post seismic Hongchun debris flow, inventorize the landslides as the potential source of debris in the catchment, estimated the volume of debris in the catchment based on field observation and attempt the reconstruction of the August 14th debris flow event in the Hongchun catchment. Data was collected (chapter 4) and analyzed before applying in the two models (chapter 5) to come out with the following preliminary conclusions;

Question 1: What are the hydrological parameters?

Answer 1: The hydrological parameters are the rainfall, the topography (including the geology and outcrops), the soil physical properties (Saturated hydraulic conductivity, porosity moisture content, Field capacity and bulk density), the soil texture, the landcover, the soil depth and the manning's n (surface roughness derived from the landcover classes: alkema, 2007.). The catchment has very high saturated hydraulic conductivity and moderate porosity. The soil depth was poorly determined and its influence remains uncertain and requires further investigation.

Question 2: Are the landslides bodies the potential source of debris flow?

The study found through the intensive field geomorphological mapping of the landslides (inventory), field observation and historical knowledge (through interviews) that the co-seismic landslides are the potential source of debris flows in the Hongchun catchment.

Question 3: Can the volume of debris material be estimated?

The volume of the debris materials was estimated to be 1,675,000 m^3 based on the geomorphological mapping and field observation of the catchment (compared to the 2.25 million cubic meters from interview). The evaluation of the landslides volume was based on field observation of the deposit volume, detachment area, deposit height, deposit base, morphology and geometry. The landslides volumes were then classified based on threshold determine during reconnaissance survey of the catchment in a manner similar to Cardinali et al, 2002. Furthermore, the approach used in this research was prompted by lack of good DEM after the earthquake but gave a rough idea of the volume of debris resulting from the earthquake induced landslides. In a data poor environment it may be very useful.

Question 4: Can the 2010 debris flow events be reconstructed?

40.3% of the August 14, 2010 debris flow event was reconstructed using FLO-2D model (see table 18) in a manner consistent within the limit of the data available and limit of the researcher expertise with the FLO-2D model. However, the zero infiltration (saturated soil condition) assumption used in the modelling may not be true catchment conditions during the debris flow event. Also, the literature values used in determining the viscosity parameters, yield stress parameters and the sediment concentration by volume used in the modelling may be far from catchment reality. However, the model was calibrated using a back analysis (see table 14) of the debris flow volume of 2010 event.

Finally, given the available tools, LISEM, FLO-2D, geomorphological mapping, field observation, interviews and data, 40.3% (161,350 m3) of the debris flow event of 14th August was reconstructed. However, these results are preliminary and are guide for future research.

6.2 Recommendations

A more detailed study of the Hongchun catchment is required. The findings of this report should be used as a preliminary guide for future research. Certainly, a good soil depth investigation is required along with detail infiltration pattern studies.

A comparison study of methods using the infinite slope model, along with other methods of determining the groundwater effect on slope stability should be explored in mapping out unstable areas where landslides might be initiated (potential areas).

Discharge data should be obtained to calibrate runoff model. In addition, it was apparent that the infiltration along the slopes may be significant, another item that warrants additional research.

Pre-landslides (disaster) DEM and post-landslides DEM subtraction technique and other methods be used in determining the volume of materials (debris) in the catchment. This is because the estimation of the debris material from the landslides based on geomorphological field mapping may grossly underestimate or over-estimate the volume of debris. However, it gives a good first approximation and rough idea of the imminent Hazard in the catchment.

A higher accuracy DSM, perhaps LIDAR DEM, should be used in modeling and also to validate the findings of the study regarding flow paths and inundations, caused by DTM inaccuracies.

Assumptions of model parameter values from literature should be done with due caution as most of those laboratory and or literature determined value may not be representative for the area under study.

A comparative study of the catchment using other Debris flow software should be done in other to validate the FLO-2D model results. This is mainly due to lack of adequate data for the calibration /validation of the results.

Further research need to be done to determine the volume of materials entrained during the debris flow events.

LIST OF REFERENCES

Abulohom, M. S., Shah, S. M. S., & Ghumman, A. R. (2001). Development of a Rainfall-Runoff model, its calibration and validation. *Water Resources Management, 15*, 149-163.

Aleotti, P. (2004). A Warning System for Rainfall-induced Shallow failures. *Engineering Geology, 73. (3-4)*, 247-265.

Alkema, D. (2007). Simulating floods on the application of a 2D-hydraulic model for flood hazard and risk assessment. *Enschede,International Institute for Geo-information Science and earth observation(ITC).*

Broomhead, E. N. (1996). Slope Stability Models. EV5VCT94. Final Report Part 1, Summary Report. *European Community, CEC Environment Programme.*

Brunsden, D. (1999). Some Geomorphological Considerations for the Future Developments of Landslides Models. *geomorphology, 30*, 13-24.

Cardinali , M., Reichenbach, P., Guzzetti, F., Ardizzone, F., Antonini, G., Galli, M., et al. (2002). A geomorhological approach to the estimation of landslides hazards and risks in Umbria, Central Italy. *nat Hazards and Earth System Science, 2*, 57-72.

CCI and AD. (2003). Debris flow Origin. *http://adaptation.nrcan.gc.ca/posters/images/bc_05_02_e.gif. Accessed on:2011,05, September.*

Cesca, M., & D'Agostino, V. (2006). Comparison between FLO-2D and RAMMS in debris flow Modeling: a case study in the Dolomites. *International Conference on Monitoring simulation, prevention and remediation of Dense and Debris flow II, 60*, 161-168.

Chigira, W. M., Furuya, W. T., & Kamai, T. (2003). Geological Causes and Geomorphological precursors of the Tsaoling Landsildes Triggered by the 1999 Chi-Chi earthquake, Taiwan. *Engineering Geology, 68*, 259-273.

Christen, M., Kowalski, J., & Bartelt, P. (2010c). RAMMS: Numerical Simulation of Dense snow-avalanches in three dimensional terrain. *Cold Regions Science and Technology, 63(1-2)*(1-14).

Crosta, G. B., & Frattini, P. (2003). Distributed Modelling of Shallow Landslides Triggered by Intense Rainfall. *Nat Hazards and Earth Syatem Science, 3*, 81-93.

Cui, p., Zhu, Y. Y., Han, Y. S., Chen, X. Q., & Zhuang, J. (2009). The 12 May Wenchuan-Induced Landslides:Distribution and Preliminary Risk Evaluation. *Landslides, 6*, 209-223.

Dai, F. C., Lee, C. F., & Ngai, Y. Y. (2002). Landslide risk assessment and management: an overview. *Engineering Geology, 64(1)*, 65-87.

DeRose, R., Trustrum, N. A., & Blaschke, P. M. (1991). Gemorphic change implied by regolith-slope relationships on steepland hillslopes, Taranaki, New Zealand. *CATENA, 18 (5)*, 489-514.

Ellen, S. D. (1988). Description and Mechanics of soil slip/Debris flow stroms. In: S.D Ellen and G.F.Wieczorek (Editors). Landslides, Floods and Marine Effects of the Storm of January 3-5, 1982, in the San Franscisco Bay Region, Califronia, USGS, Washington.

FLO-2D manual. (2007). Webpage: www.flo.2d.com/information/description.htm. accessed on 2011, 1st, August. FLO-2D Software Inc. Nutrioso.

Glade, T., Micheal, C., & peters , S. (2000). Applying Probability Determination to Refine Landslide-Triggering Rainfall Thresholds Using an Emperical Antecedent Rainfall Model. *Pure and Applied Geophysics, 157*, 1059-1079.

Hessel, R., Jetten, V., Liu, B., Zhang, Y., & Stole, J. (2003). Calibration of the LISEM model for a small Loess plateau catchment. *CATENA, 54*, 235-254.

Huang, R. Q., & Li, W. L. (2008). Analysis of the Geo-hazards Triggered by the 12 May 2008 Wenchuan Earthquake, China. *Bull Eng Geol Environ, 68*(363-371).

Hungr, O., Evans, S. G., Bovis, M. J., & Hutchinson, J. N. (2001). A review of the classification of landslides of the flow type. *Environment and Engineering Geoscience, 7(3)*, 221-238.

Hussin, H. Y. (2011). Probabilistic Run out Modeling of a Debris in Barcelonnette, France. *Msc. Thesis, University of Twemte (ITC Faculty, Enschede)*, 60.

Inverion, R. M. (1997). The Physics of Debris Flow. Reviews of Geophysics. *35(3)*, 245-296.

Jacob, M. (2005). Debris flow hazard analysis. In M.Jacob and O. Hungr (Eds), Debris flow hazard and related phenomena. 411-443.Chicester: Springer-Praxis.

Jetten, V. (2002). LISEM user manual. The netherlands, Utrecht Centre for Environmental and Landscape Dynamics, Utrecht University.

Karssenberg, D. (2002). Building dynamic Spatial Environmental models. *PhD Thesis, Utrecht University, Utrecht*(222).

Keefer, D. K. (1984). Landslides Caused by earthquakes. *Geological Society of America Bulletin, 95*, 406-421.

Khazai, B., & Sitar, N. (2004). Evaluation of Factors Controlling earthquake-Induced Landslides caused by Chi-Chi earthquake and Comparison with the Northbridge and Loma Prieta evnets. *Engineering Geology, 71*, 79-95.

Kinosita, T. (1983). Runoff and flood characteristics in small humid tropical regions in hydrology of humid tropical regions with particular refference to the hydrological effects of Agricultural and forestry practice. *Hamburg Symposium, August 1983, Hamburg, IAHS Publ.no 140*.

Kowalski, J. (2008). Two-phase Modeling of debris flows. PhD Thesis. *Swiss Federal Institute of Technology, Zurich*.

Kuriakose, S. L., Van Beek , L. P. H., & Van Westen, C. J. (2010). Comparison of physically Based models for debris initiation- A case study in the Tikovil River of the Western Ghats of Kerala, India. computers and Geosciences (Under review). .

Lan , H., Wu, F., Zhou, C., & Wang, L. (2003). Spatial Hazard Analysis and Prediction on Rainfall-Induced Landslide using GIS. *Chinese Science Bulletin, 48*, 703-709.

Lin , Q., Liu , S., & LIu, C. (2006). Impacts of the Chi-Chi Earthquake on subsequent Rain-Induced landslides in Central Taiwan. *Engineering Geology, 86*, 87-101.

Liu , X., Zhang, Z., Peterson, J., & Chandra, S. (2007). The effect of LIDAR dat density on DEM accuracy proceedings of the international congress on modelling and simulation 'MODISM07', 10-13 December (pp.1363-1369). *Christchurch, New Zealand*.

Malet, J. P., Laigleb, D., Remaitrea, A., & Marquaire, O. (2004). Triggering conditions and mobility of debris flow associated to complex earthflows. *geomorphology, Article in Press*.

Moradkhami, H., & Sorooshian, S. (2009). General Review of Rainfall-Runoff Modeling:Model Calibration,Data Assimilation and Uncertaintity Analysis. *IN SOROOSHIAN, N.S ,HSU, K-L, COPPOLA, E, TOMASSETTI, B, VERDECCHIA, M AND VISCONTI, G (Eds) Hydrological Modeling and the Water Cycle, Berlin, Springer*.

Naldini, D. (2004). Debris flow Modelling with PCRaster, the event of June, 1996 in the Apuan Alps Cardoso Basin. *Thesis, ITC,Enschede*, 39.

O'Brien, J. S., Julien, P. Y., & Fullerton, W. T. (1993). Two-dimensional water flood and Mudflow simulation. *Journal of Hydraulic Engineering, 119(2)*, 244-261.

Odeh, I. O. A., Chittleborough, D. J., & McBratney, A. D. (1991). Elucidation of soil-landform inter-relationships by canonical ordination analysis. *Geoderma, 49 (1-2)*, 1-32.

Oyebande, L. (1998). Forests, Climate and Hydrology-Regional Impacts, The United Nations University, Tokyo.

Pack, R. T., Tarboton, D. G., & Goodwin, C. N. (1998). The SINMAP Approach to Terrain Stability Mapping. *8th Congress of the International Association of Engineering Geology. Vancouver, British Columbia, Canada*.

Petrascheck, A., & Kienholz, H. (2003). Hazard Assessmemt and hazard Mapping of Mountain Risk-examples of Switzerlands in : Debris flows Hazard Mitigation: Mechanics, Prediction and Assessment. *3rd International DFHM conference, Davos, Switzerlands, September 10-12, Rotterdam, Millpress*, 25-38.

Pranchansri, S. (2007). Analysis of Soil and Land cover parameters for Flood hazard assessment; A case study of the Nam chum Watershed, Phetchabun, Thailand. *Earth System Analysis, Enschede, International Institute for Geo-information Science and Earth Observation (ITC)*.

Quan Luna, B. (2007). Assessment and Modeling of two Lahars caused by 'Hurricane Stan' at Atitlan, Guatemala, October, 2005. *Msc. Thesis, University of Oslo, Oslo*.

Remaitre, A., & Malet, J. P. (2010). The effectiveness of torrent check dams to control channel instability: examples of debris flow events in clay shales. In C.C. Garcia & M.A. Lenzi (Eds.), check dams, morphological adjustments and erosion control in torrential streams. 211-237. New York: Nova Science Publishers Inc.

Styczen, M. E., & Morgan, R. P. C. (1995). Engineering Properties of Vegetation. In R.P.C Morgan and R.J Rickson (Editors). Slope Stabilization Control: A Bioengineering Approach.E & FN Spon, London.

Takahashi, T. (1981). Debris flow. Annual reviews of Fluid Mechanics. *13*, 57-77.

Tan, W., & Hen , Q. (1992). Study on Regional Critical Rainfall Induced Debris flow in Sichuan Province. *Journal of Catastrology, 7*, 37-42 (in chinese).

Tang, C., Zhu, J., Qi, X., & Ding, J. (2011). Landslides Induced by the Wenchuan earthquake and the subsequent rainfall event. A case study of in the Beichuan area of China. *Engineering Geology*, 12.

Van Asch, T. W. J., Buma, J., & Van Beek, L. P. H. (1999). A Review on Some hydrological triggering systems in Landslides. *Geomorphology, 30*(25-32).

Van Beek, L. P. H. (2002). Assessment of the influence of changes in landuse and Climate on Landslide Activity in Mediterranean. PhD Thesis, Utrecht University, Utrecht., 363.

Van Westen, C. J. (2010). Multi-hazard risk assessment: RiskCity, distance education. Enschede, The Netherlands: ITC.

Varnes, D. J. (1978). Slope movement types and processes. In Special Report 176: Landslides: Analysis and control (Eds: Schuster, R.L and Krizek, R.J), Transportation and Road research board, National Academy of Science, Washington D.C. 11-33.

APPENDIX 1

The outlined steps below were followed in the laboratory in order to determine the soil physical properties mentioned in chapter 4.5.1.

1. Take sample in the field
2. Put nylon filter on the sample
3. Weigh field sample (W1)
4. Put sample for 24 hour in water to saturate it, however, it was observed during the saturation of the soil samples that within 5 minutes, the water was already seen to start appearing on the surface. This may be due to the loosed nature of the soil and the stoniness observed in the field. This make the soil very porous and with a very high permeability.
5. Weigh saturated sample (W2)
6. Put saturated sample in the test set-up
7. Create constant head. The constant head of 1cm was maintain throughout the laboratory analysis this was because it allows the effective monitoring of the water movement through the soil samples, giving the nature of the soil described earlier. Higher constant head tends to increase, the flow of the water through the soil, maybe as the pressure of the water increase with height.
8. Measure the constant head dH
9. Measure the amount of percolated water per constant time, e.g. 5 min or 10 min. the percolated water was observed carefully and recorded after every 5 minutes.
10. Stop when reading becomes constant
11. Put rings on rack for 24hour to let water leak out
12 .Remove caps and Weigh sample (W3)
13. put the rings in an oven at 105 degree centigrade for 24 hour (in a tray)
14 Weigh sample (W4)
15 Remove soil and clean the rings
16 Weigh ring (W5)

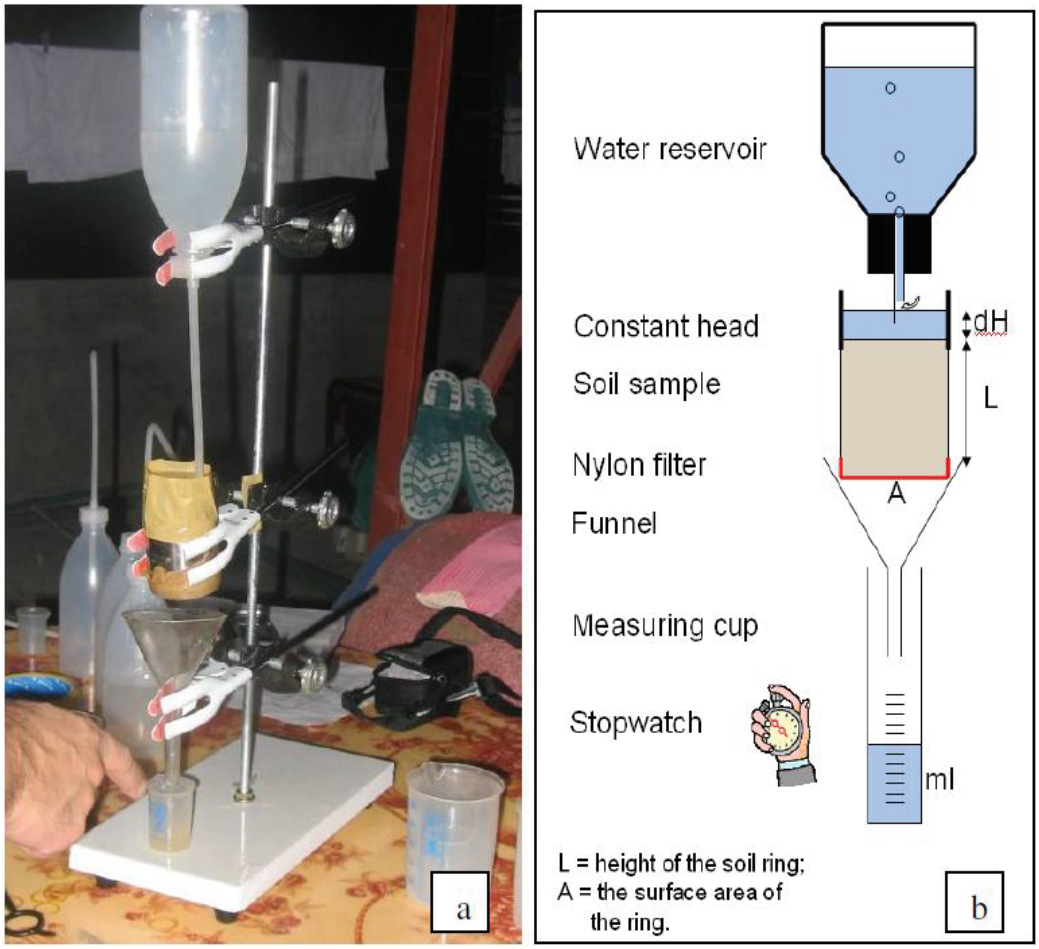

Fig xa laboratory set-up for Ksat

In order to calculate the various parameters mentioned in chapter 4.5.1, the following procedures are followed.

To calculate the various parameters:

Calculate volume of the ring (L x A) in ml (= 100 cm^3 = 100 ml).

(To convert differences in weight due to changes in soil water content, consider that 1 gram of water = 1 ml of water)

Porosity: Pore space (volume) divided by total sample volume.

Pore volume = (W2-W5) – (W4-W5) (express result in ml).

Porosity = 100% x Pore volume / Ring volume

Field moisture content: Amount of water in the soil at the moment of sampling.

Field moisture volume = (W1-W5) – (W4-W5) (ml).

Field moisture content = 100% x Field moisture volume / Ring volume

Field capacity: Amount of water in the soil after the soil has been drained by gravity forces (≈ soil dependent).

Field capacity volume = (W3-W5) – (W4-W5) (ml).

Field capacity = 100% x Field capacity volume / Ring volume

Bulk density = (W4-W5) / Ring volume

APPENDIX 2

Table 4.5 showing 10 days of discharge measurement

Day 1		**Remarks: little rain drop at night prior to measurement**				
d (m)	W (m)	A=1/2*d*w(m^2)	Distance (m)	Time (s)	Velocity=D/S (m/s)	Discharge=A*V (M^3/s)
0.51	4.40	1.122	2.35	2.93	0.8021	0.8999
0.52	4.40	1.144	2.35	2.94	0.7993	0.9144
Day 2		**Remarks: no rain**				
0.50	4.44	1.110	2.35	2.83	0.8304	0.9217
0.49	4.43	1.090	2.35	2.73	0.8608	0.9383
Day 3		**Remarks: little rain drop during measurement**				
0.49	4.45	1.090	2.35	2.67	0.8801	0.9594
0.49	4.45	1.090	2.35	2.70	0.8704	0.9487
Day 4		**Remarks: no rain**				
0.50	4.44	1.110	2.35	2.80	0.8393	0.9316
0.50	4.44	1.110	2.35	2.83	0.8304	0.9217
Day 5		**Remarks: no rain**				
0.50	4.45	1.113	2.35	2.81	0.8363	0.9283
0.50	4.44	1.110	2.35	2.79	0.8423	0.9349
Day 6		**Remarks: no rain**				
0.51	4.43	1.123	2.35	2.82	0.8333	0.9250
0.50	4.44	1.110	2.35	2.81	0.8363	0.9283
Day 7		**Remarks: no rain**				
0.50	4.44	1.110	2.35	2.80	0.8393	0.9316
0.50	4.43	1.110	2.35	2.78	0.8453	0.9383
Day 8		**Remarks: no rain**				
0.50	4.44	1.110	2.35	2.80	0.8393	0.9316
0.50	4.43	1.110	2.35	2.80	0.8393	0.9316
Day 9		**Remarks: no rain**				
0.51	4.43	1.110	2.35	2.83	0.8304	0.9217
0.50	4.44	1.110	2.35	2.81	0.8363	0.9283
Day 10		**Remarks: no rain**				
0.51	4.44	1.122	2.35	2.82	0.8333	0.9350
0.51	4.44	1.122	2.35	2.81	0.8363	0.9383

APPENDIX 3

LISEM input maps

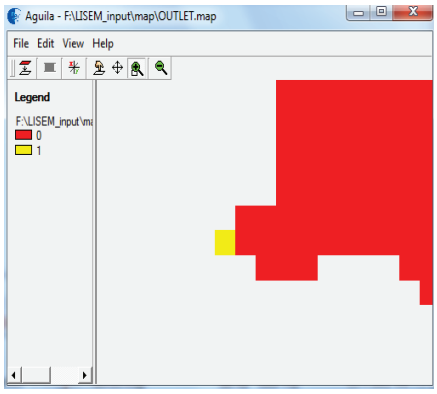

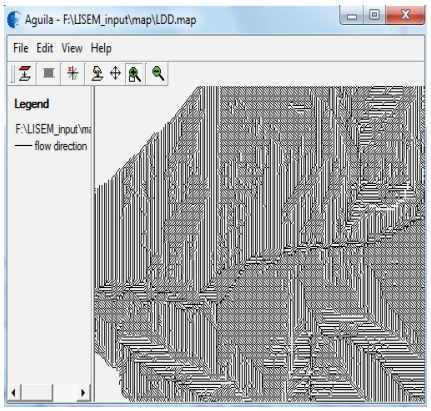

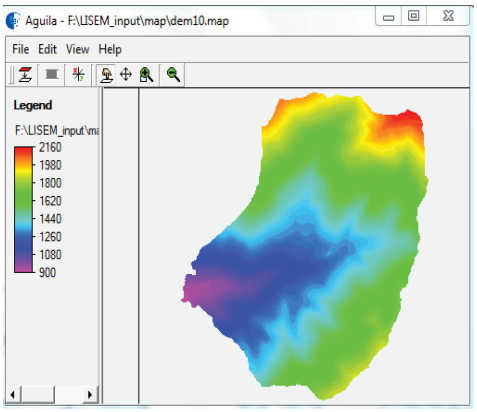

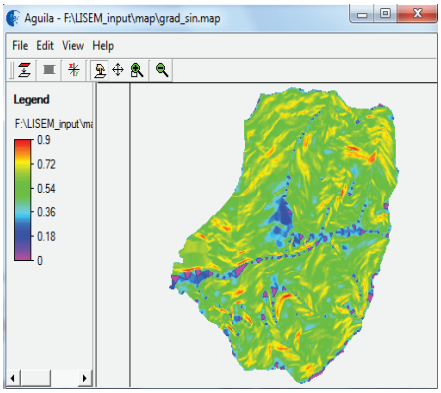

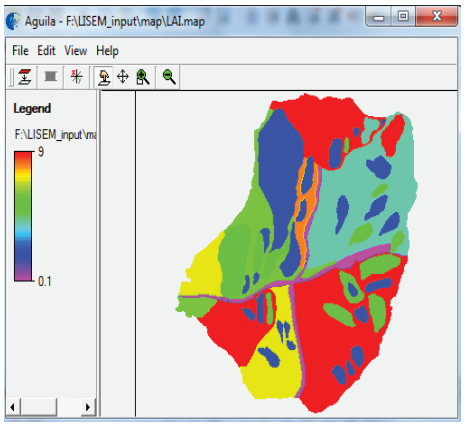

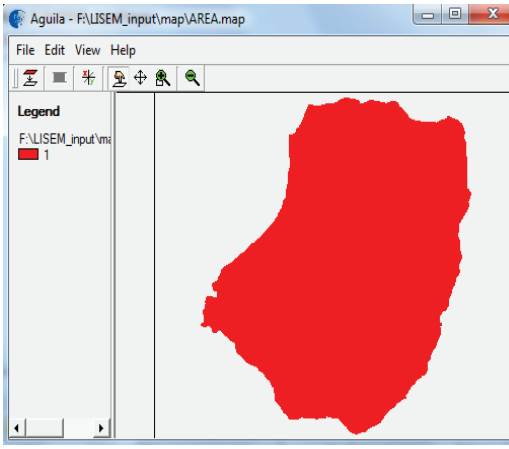

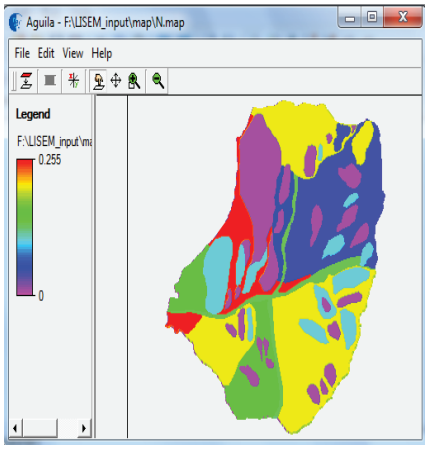

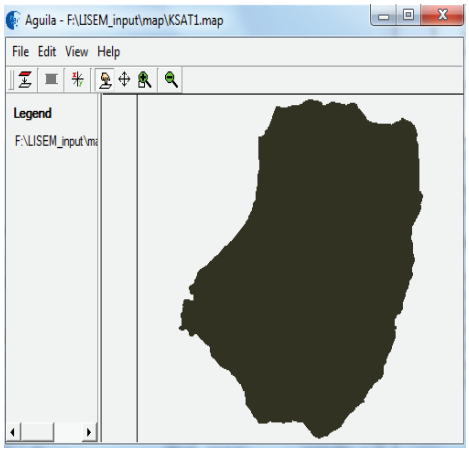

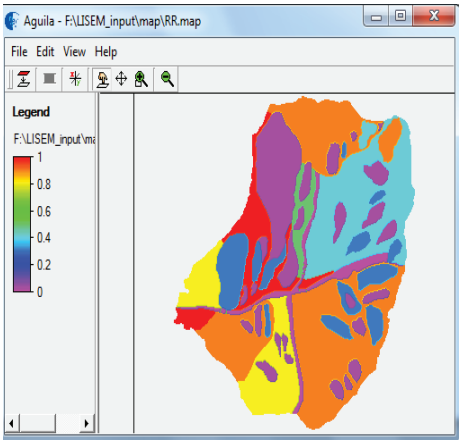

APPENDIX 4

Landslides inventory/ estimated values

Table "Hongchun" - ILWIS

File Edit Columns Records View Help

	Type	Part	Body_size	Age	Activity	estimated vo
pnt 1	Landslide	Body	Thick	New	Active	120000.00
pnt 2	Landslide	Body	Thin	New	Active	7000.00
pnt 3	Landslide	Body	Thick	Old	Dormant	60000.00
pnt 4	Landslide	Body	Medium	New	Active	40000.00
pnt 5	Landslide	Scarp	Thick	New	Active	70000.00
pnt 6	Landslide	Body	Thin	New	Active	8000.00
pnt 7	Landslide	Body	Medium	New	Active	30000.00
pnt 8	Landslide	Body	Thick	Old	Dormant	55000.00
pnt 9	Landslide	Body	Thick	New	Active	80000.00
pnt 10	Landslide	Body	Thick	New	Active	100000.00
pnt 11	Landslide	Body	Thick	New	Active	70000.00
pnt 12	Landslide	Body	Medium	Old	Dormant	35000.00
pnt 13	Landslide	Body	Medium	New	Active	50000.00
pnt 14	Landslide	Body	Thick	New	Active	60000.00
pnt 15	Landslide	Body	Thin	New	Active	9000.00
pnt 16	Landslide	Body	Thin	New	Active	8000.00
pnt 17	Landslide	Body	Thin	New	Active	8000.00
pnt 18	Landslide	Body	Thin	New	Active	9000.00
pnt 19	Landslide	Body	Thin	New	Active	8000.00
pnt 20	Landslide	Body	Thin	New	Active	5000.00
pnt 21	Landslide	Body	Thick	New	Active	70000.00
pnt 22	Landslide	Body	Thick	New	Active	80000.00
pnt 23	Landslide	Scarp	Thin	New	Active	9000.00
pnt 24	Landslide	Body	Thin	New	Active	8000.00
pnt 25	Landslide	Body	Medium	New	Active	50000.00
pnt 26	Landslide	Body	Medium	New	Active	40000.00
pnt 27	Landslide	Body	Medium	New	Active	45000.00

Column "Body_size"

Appendix 5

Sensitivity analysis

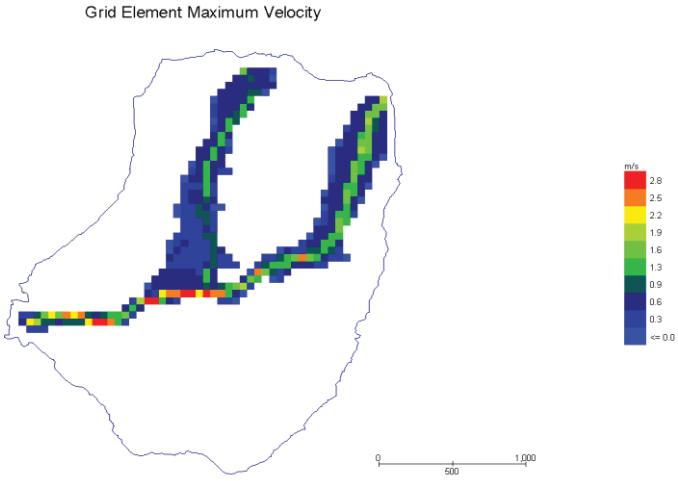

Figure1 debris flow maximum velocity

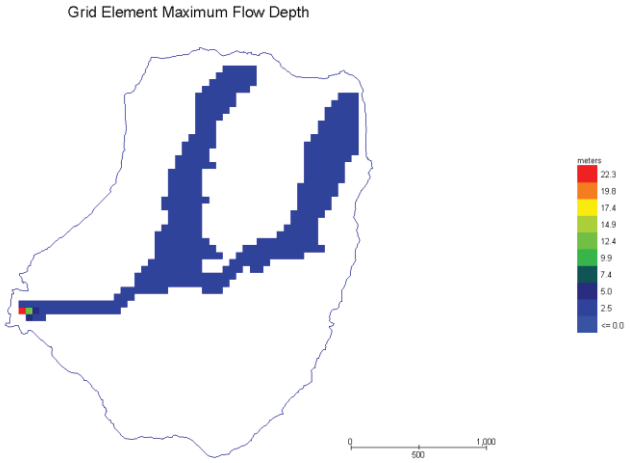

figure 2 debris flow depth

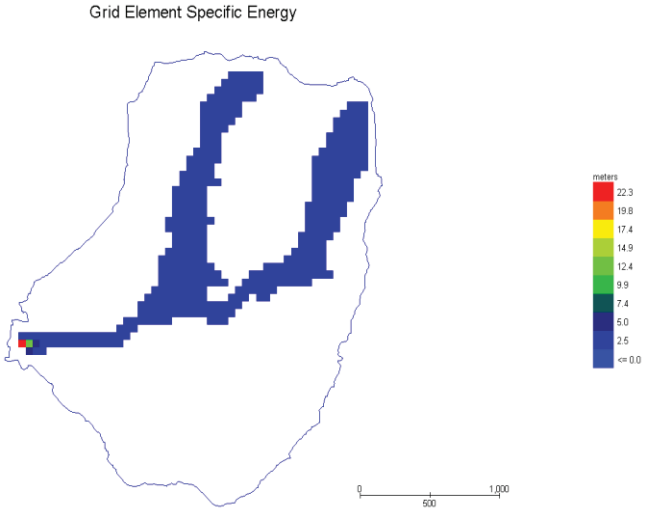

Figure3 debris flow specific energy

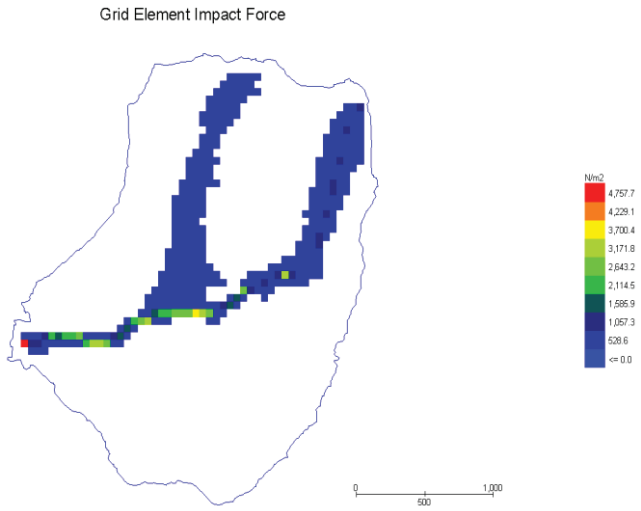

figure 4 debris flow impact force

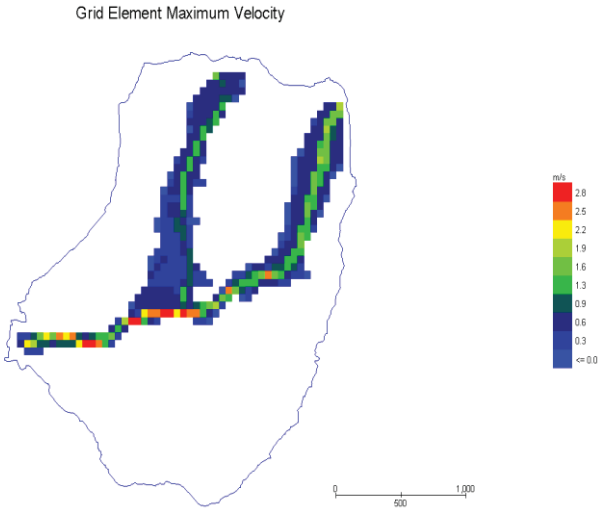

Figure 5 debris flow maximum velocity

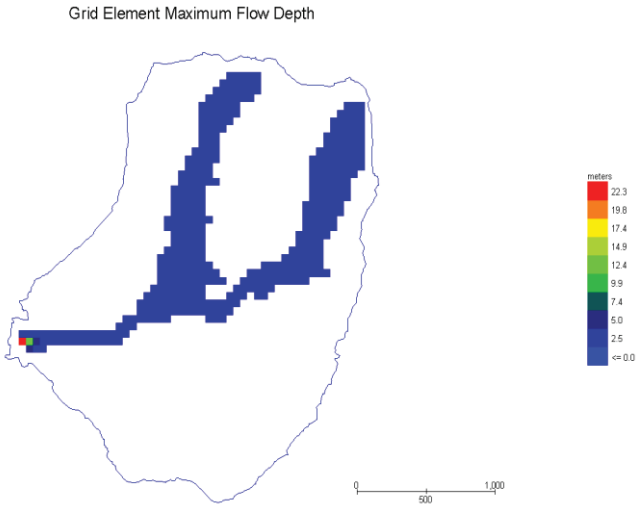

figure 6 debris flow maximum flow depth

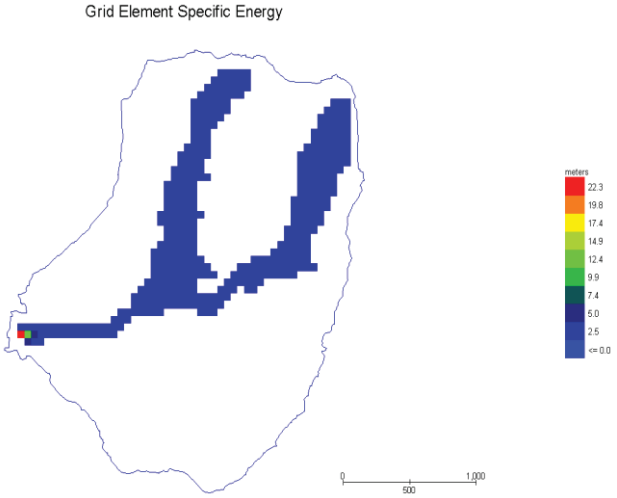

Figure 7 debris flow specific energy

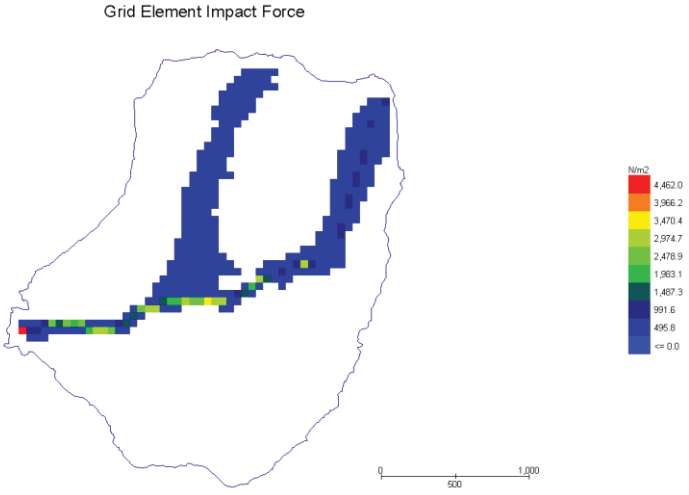

figure 8 debris flow impact force

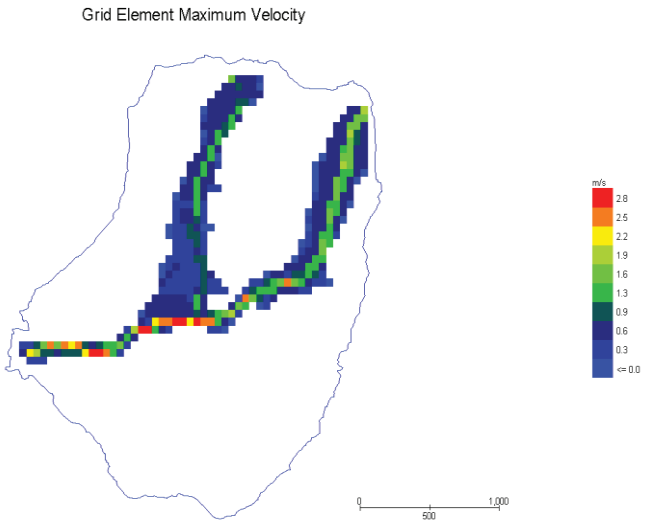

Figure 9 debris flow maximum velocity

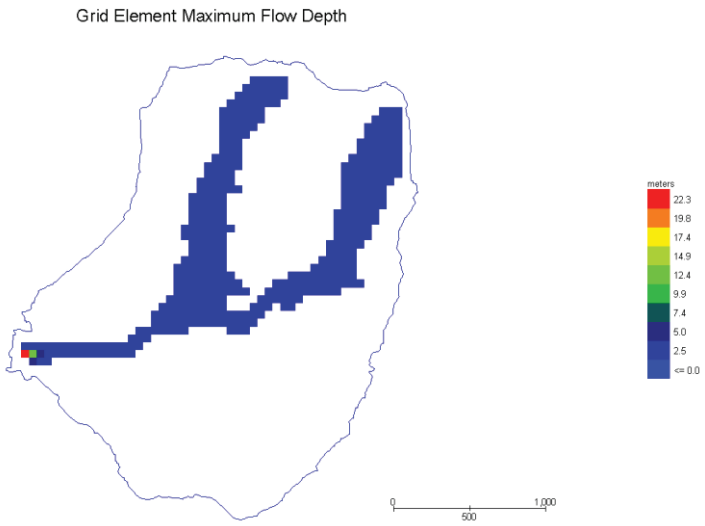

figure 10 debris flow depth

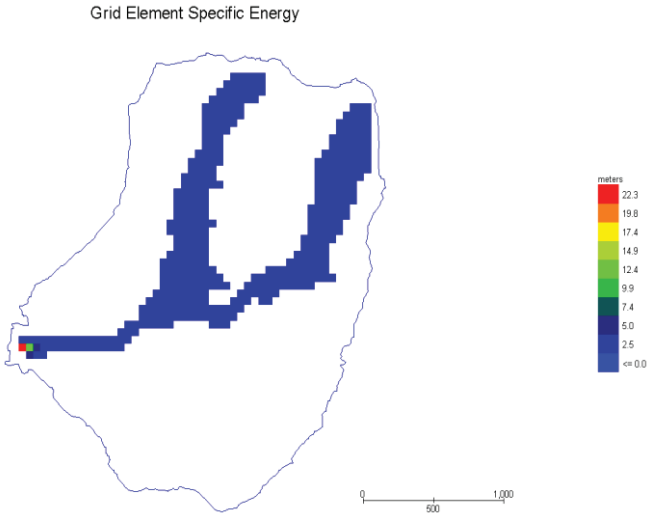

Figure 11 debris flow specific energy

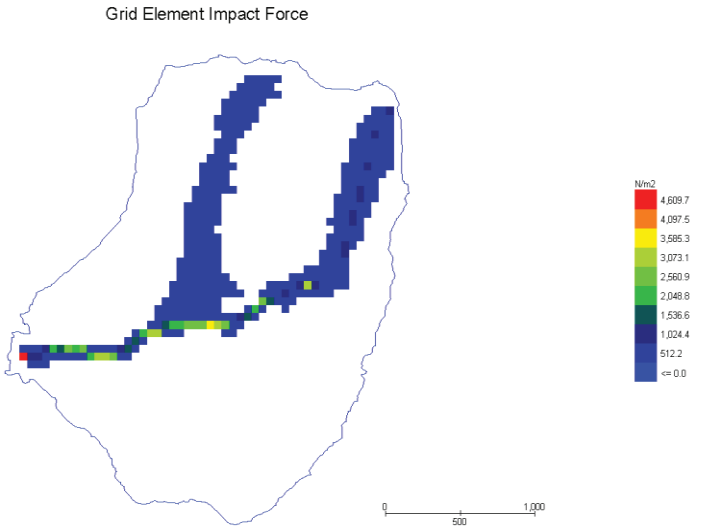

figure 12 debris flow impact force

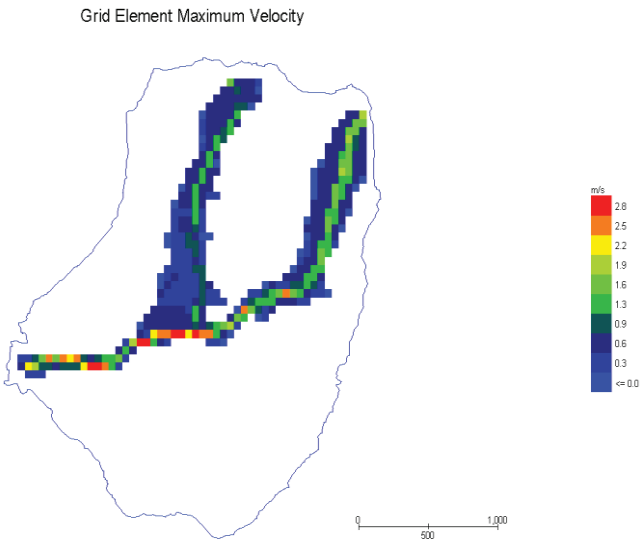

Figure 13 debris flow maximum velocity

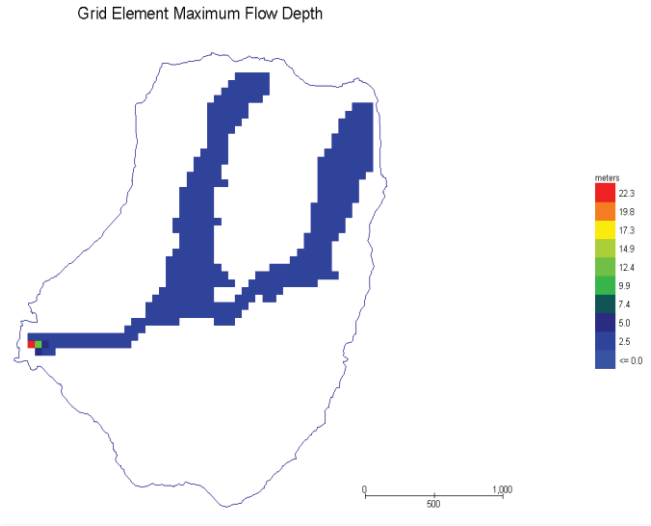

figure 14 debris flow depth

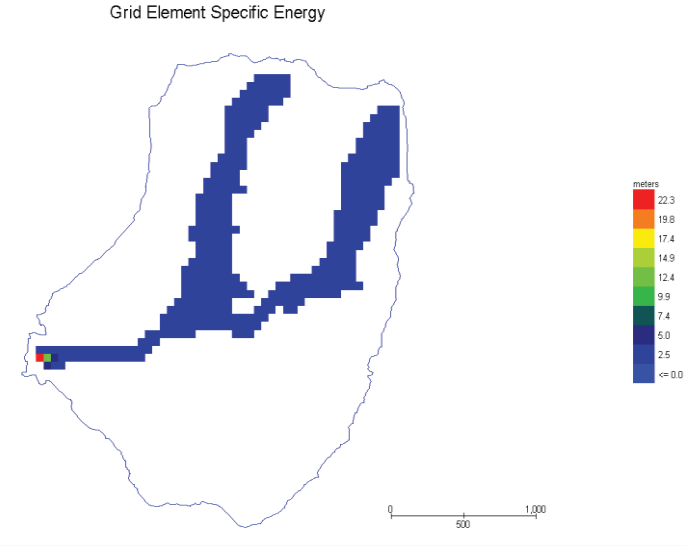

Figure 15 debris flow specific energy

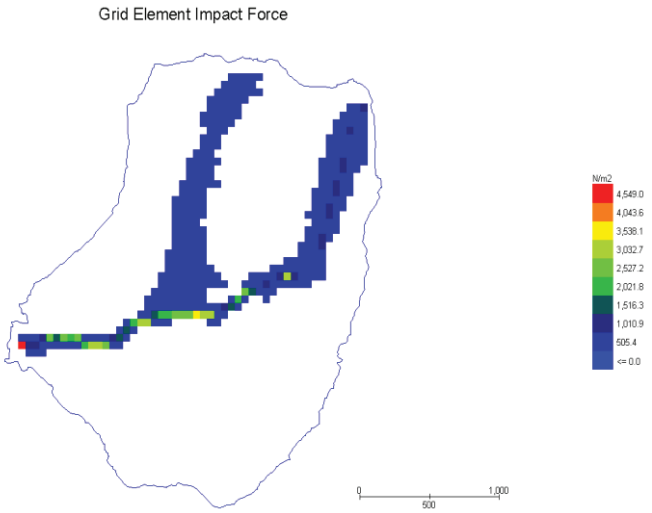

figure 16 debris flow impact force

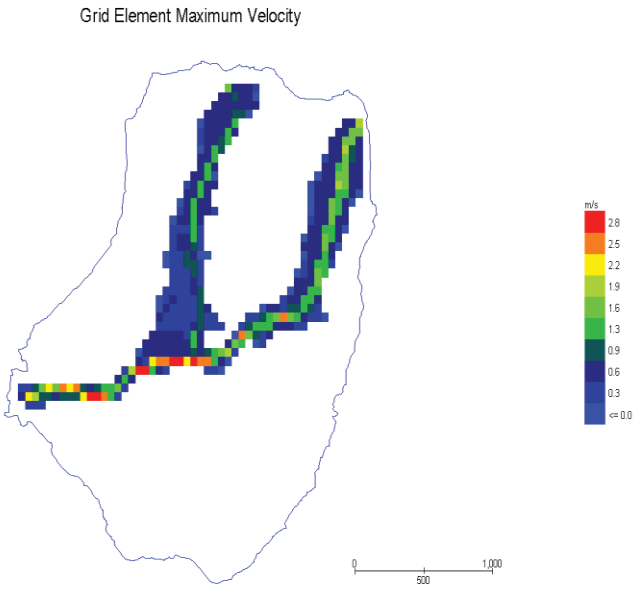

Figure 17 debris flow maximum velocity

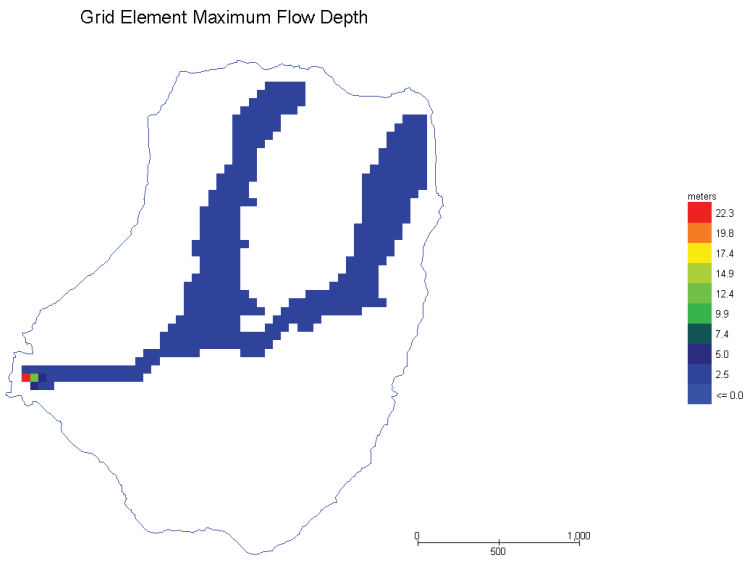

figure 18 debris flow maximum depth

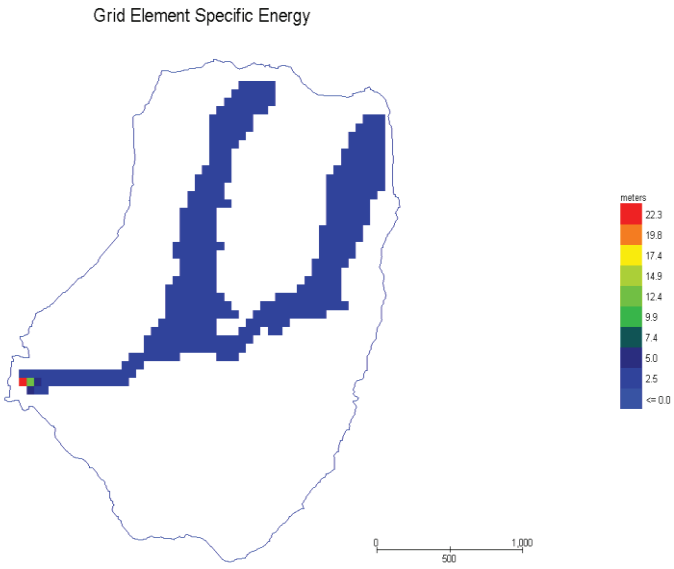

Figure 19 debris flow specific energy

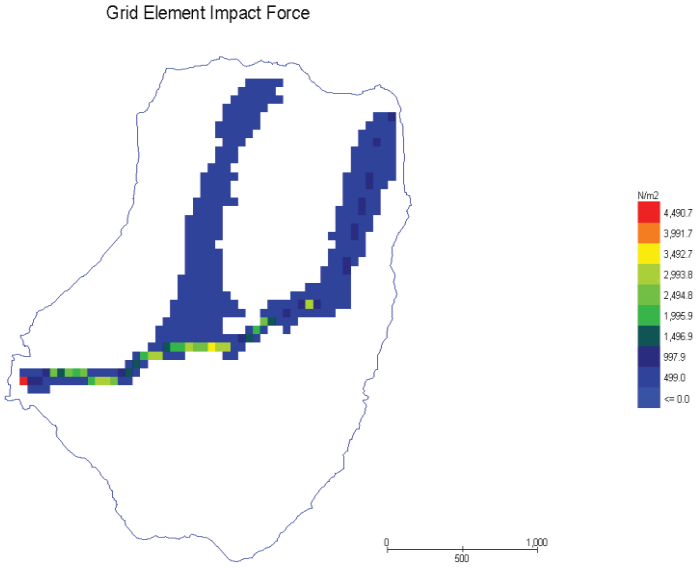

figure 20 debris impact force

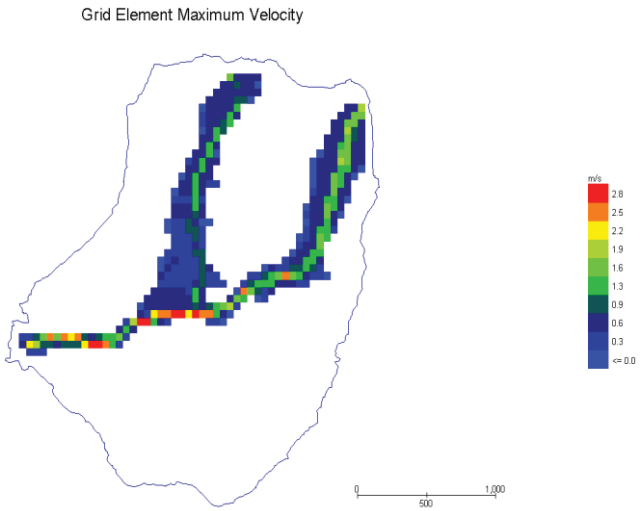

Figure 21 debris flow velocity

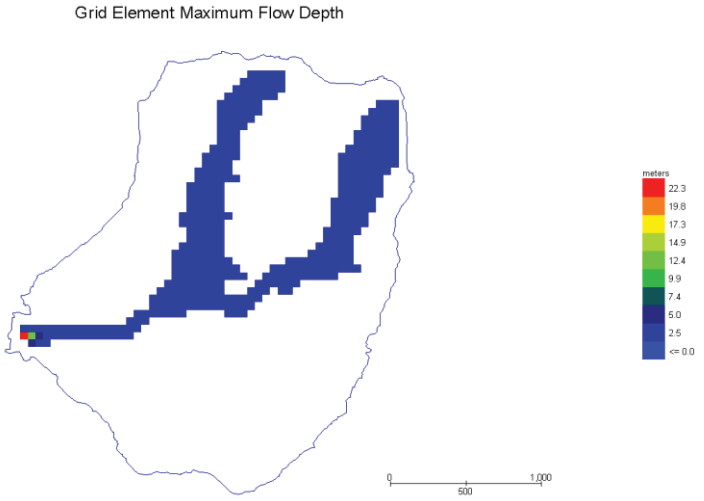

figure 22 debris flow maximum depth

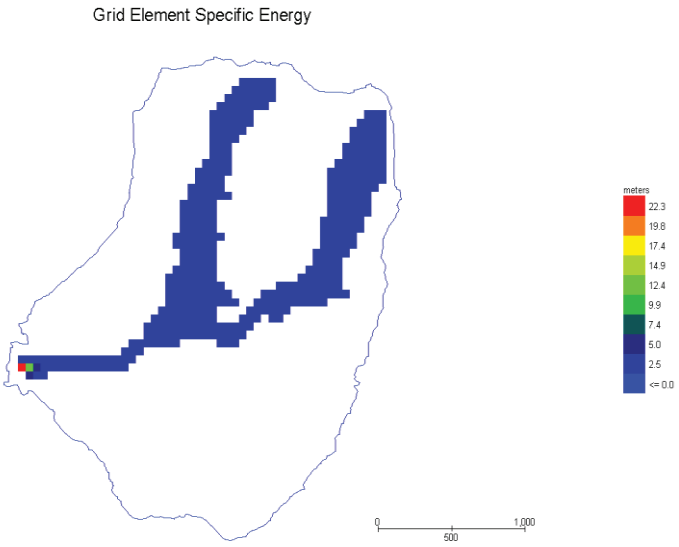

Figure 23 debris flow specific energy

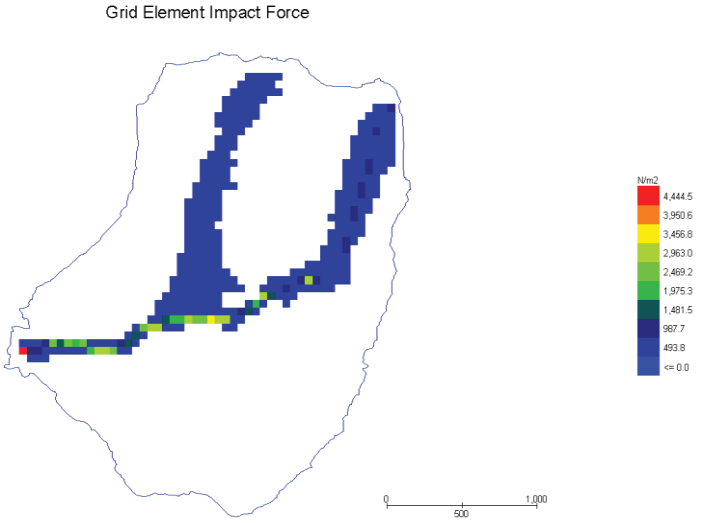

figure 24 debris flow impact force

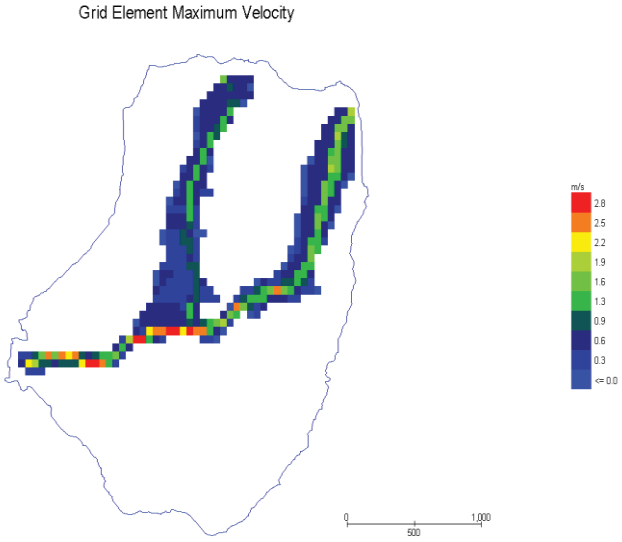

Figure 25 debris flow maximum velocity

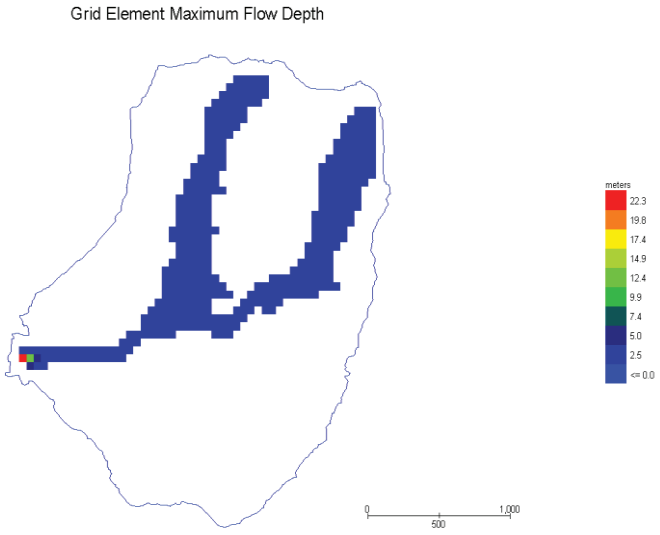

figure 26 debris flow maximum depth

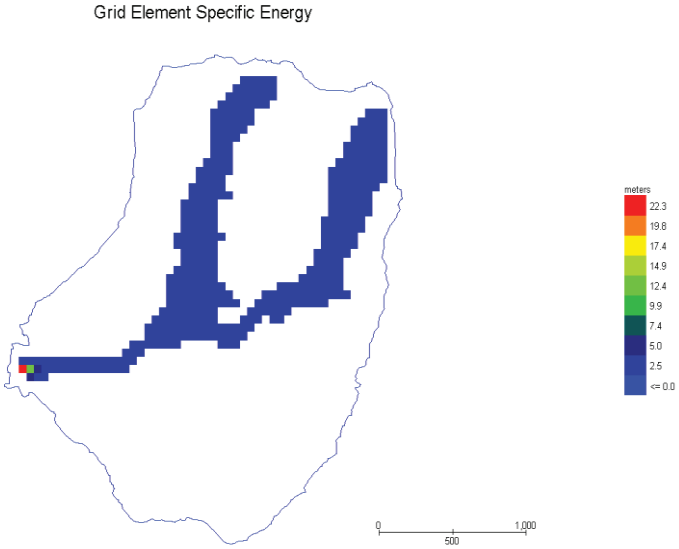

Figure 27 debris flow specific energy

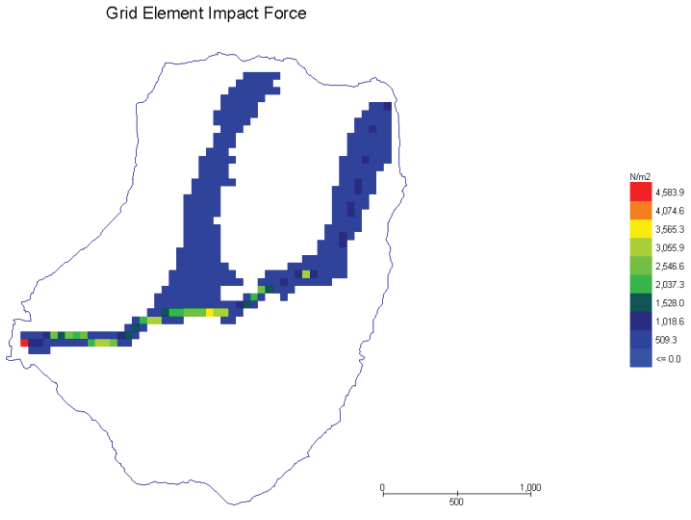

figure 28 debris flow impact force

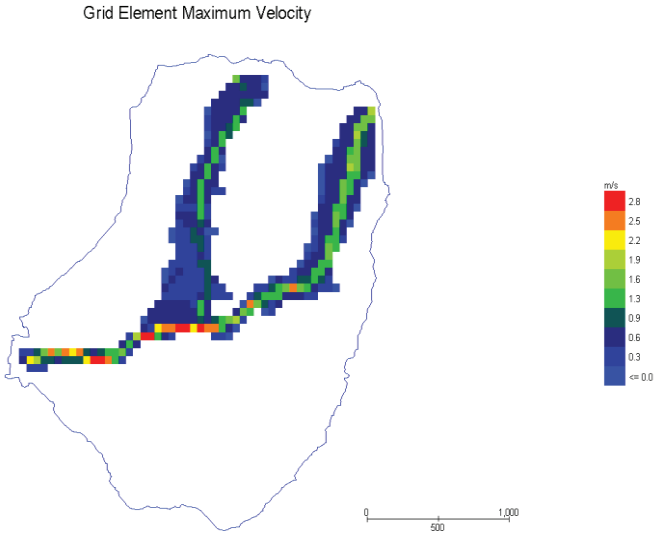

Figure 29 debris flow maximum velocity

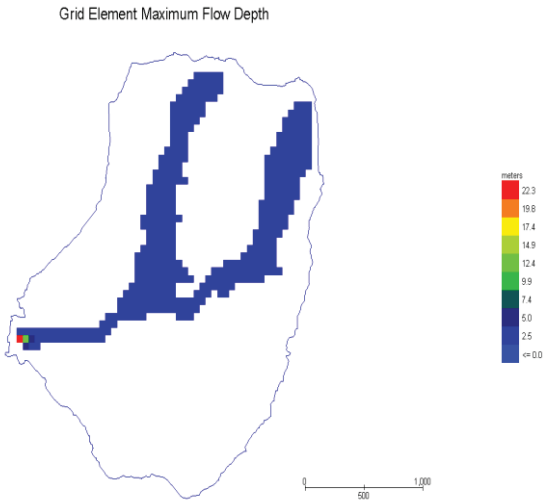

figure 30 debris flow maximum flow depth

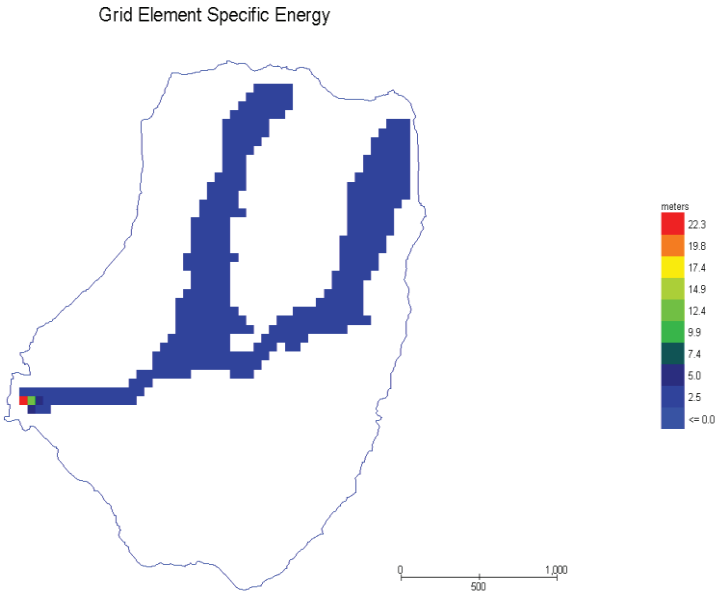

Figure 31 debris flow specific energy

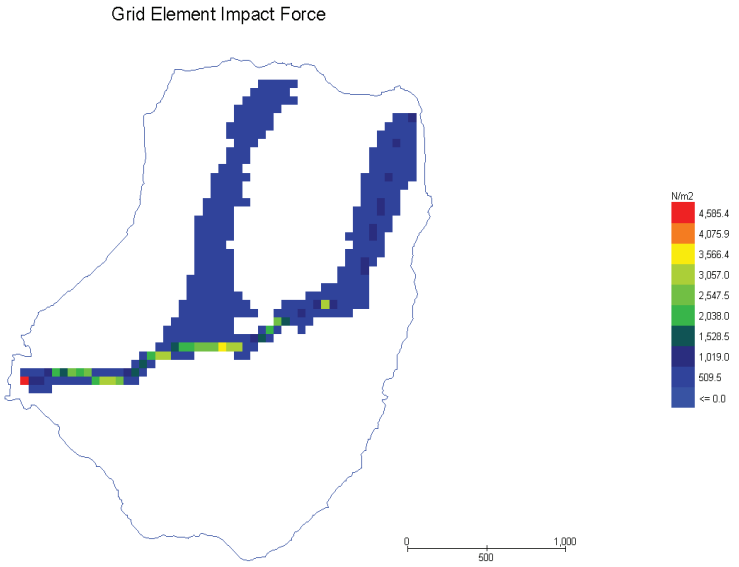

figure 32 debris flow impact force